

AD A 070253

AFFDL-TR-79-3003

LEVEL 1

2

**EVALUATION OF F-111 WEAPON BAY  
AERO-ACOUSTIC AND WEAPON SEPARATION  
IMPROVEMENT TECHNIQUES**

*RODNEY L. CLARK  
AERODYNAMICS AND AIRFRAME BRANCH  
AEROMECHANICS DIVISION*

FEBRUARY 1979

DDC FILE COPY

TECHNICAL REPORT AFFDL-TR-79-3003  
Final Report for Period May 1976 -- August 1978

Approved for public release; distribution unlimited.

AIR FORCE FLIGHT DYNAMICS LABORATORY  
AIR FORCE WRIGHT AERONAUTICAL LABORATORIES  
AIR FORCE SYSTEMS COMMAND  
WRIGHT-PATTERSON AIR FORCE BASE, OHIO 45433

DDC  
RECEIVED  
JUN 22 1979  
D

18

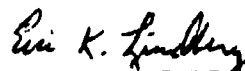
# NOTICE

When Government drawings, specifications, or other data are used for any purpose other than in connection with a definitely related Government procurement operation, the United States Government thereby incurs no responsibility nor any obligation whatsoever, and the fact that the government may have formulated, furnished, or in any way supplied the said drawings, specifications, or other data, is not to be regarded by implication or otherwise as in any manner licensing the holder or any other person or corporation, or conveying any rights or permission to manufacture, use, or sell any patented invention that may in any way be related thereto.

This technical report has been reviewed and is approved for publication.

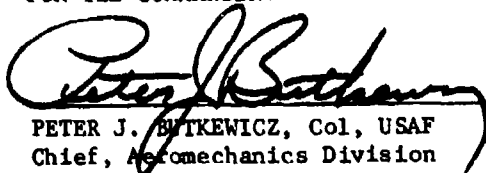


RODNEY L. CLARK  
Project Engineer  
Aerodynamics and Airframe Branch  
Aeromechanics Division



ERIC K. LINDBERG, Maj., USAF  
Chief, Aerodynamics & Airframe Br  
Aeromechanics Division

FOR THE COMMANDER:



PETER J. BUTKEWICZ, Col, USAF  
Chief, Aeromechanics Division

"If your address has changed, if you wish to be removed from our mailing list, or if the addressee is no longer employed by your organization please notify: AFFDL/FXM, W-P AFB, OH 45433 to help us maintain a current mailing list".

Copies of this report should not be returned unless return is required by security considerations, contractual obligations, or notice on a specific document.

UNCLASSIFIED

SECURITY CLASSIFICATION OF THIS PAGE (When Data Entered)

REPORT DOCUMENTATION PAGE		READ INSTRUCTIONS BEFORE COMPLETING FORM
1. REPORT NUMBER	2. GOVT ACCESSION NO.	3. RECIPIENT'S CATALOG NUMBER
14 15 AFDDL-TR-79-3003		
4. TITLE (and Subtitle)		5. TYPE OF REPORT & PERIOD COVERED
6 Evaluation of F-111 Weapon Bay Aero-Acoustic and Weapon Separation Improvement Techniques		9 Final Technical Report 1 May 1976 - 1 Aug 1978
7. AUTHOR(s)	8. CONTRACT OR GRANT NUMBER(s)	
10 Rodney L. Clark	16 2404 17 10	
9. PERFORMING ORGANIZATION NAME AND ADDRESS		10. PROGRAM ELEMENT, PROJECT, TASK AREA & WORK UNIT NUMBERS
Air Force Flight Dynamics Laboratory (FXM) AF Wright Aeronautical Laboratories, AFSC Wright-Patterson Air Force Base, Ohio 45433		Program Element 62201F, Project 2404, Task 240410, Work Unit 24041012
11. CONTROLLING OFFICE NAME AND ADDRESS		11. REPORT DATE
Air Force Flight Dynamics Laboratory (FX) AF Wright Aeronautical Laboratories, AFSC Wright-Patterson Air Force Base, Ohio 45433		February 1979
14. MONITORING AGENCY NAME & ADDRESS (if different from Controlling Office)		12. NUMBER OF PAGES
12 149 p		150
		15. SECURITY CLASS. (of this report)
		Unclassified
		15a. DECLASSIFICATION/DOWNGRADING SCHEDULE
16. DISTRIBUTION STATEMENT (of this Report)		
Approved for public release; distribution unlimited.		
17. DISTRIBUTION STATEMENT (of the abstract entered in Block 20, if different from Report)		
18. SUPPLEMENTARY NOTES		
19. KEY WORDS (Continue on reverse side if necessary and identify by block number)		
Weapons bay                      Cavity flow Weapons separation              Cavity resonance Weapon compatibility            Cavity buffet Internal carriage                Cavity acoustics Aero-acoustics                   Cavity turbulence		
20. ABSTRACT (Continue on reverse side if necessary and identify by block number)		
Several aero-acoustic suppression devices have been evaluated which were considered feasible for installation on an F-111 aircraft for flight test evaluation. The most promising modification consists of a saw tooth spoiler mounted at the leading edge of the weapon bay. This device would be erected to a 90 degree position during the bay doors opening sequence. The spoiler is folded flush with the fuselage during all other flight conditions. Wind tunnel tests have shown that this spoiler improves the aero-acoustic environment		

DD FORM 1 JAN 73 1473

EDITION OF 1 NOV 65 IS OBSOLETE

UNCLASSIFIED

SECURITY CLASSIFICATION OF THIS PAGE (When Data Entered)

012 070 *over*

UNCLASSIFIED

SECURITY CLASSIFICATION OF THIS PAGE(When Data Entered)

20 (cont'd)

within the open weapon bay and improves the weapon separation characteristics over the Mach range of .95 to 1.3 investigated during the drop test phase.

UNCLASSIFIED

SECURITY CLASSIFICATION OF THIS PAGE(When Data Entered)

## FOREWORD

This report was prepared by the Aeromechanics and Airframe Branch, Aeromechanics Division, Air Force Flight Dynamics Laboratory, Wright-Patterson Air Force Base, Ohio. The effort reported was conducted as a joint Air Force Weapons Laboratory (AFWL) and Air Force Flight Dynamics Laboratory (AFFDL) program. The objective of the program was to identify and evaluate potential modifications to the F-111 weapon system which would reduce the carriage loads imposed upon the B-43 weapon just prior to release from the internal weapons bay of this aircraft. The effects of the modifications on weapon separation characteristics were also evaluated using both the B-43 and B-57 weapons. Mr. John W. Doran was the AFWL Project Engineer and participated actively in all phases of this program.

This report presents the results of work performed under Work Unit 24041012 during the period from May 1976 to August 1978.

The author wishes to acknowledge the technical assistance provided by Mr. Grady Barton of General Dynamics/FW; and Messrs Sam W. Brown and Dale K. Smith of ARO, Inc.

Accession For	
NTIS GRA&I	<input checked="checked" type="checkbox"/>
DDC TAB	<input type="checkbox"/>
Unannounced	<input type="checkbox"/>
Justification	
Distribution/	
Availability Codes	
Dist	Avail and/or special
A	

DDC  
RECEIVED  
JUN 22 1979  
D

## TABLE OF CONTENTS

SECTION		PAGE
I	INTRODUCTION AND BACKGROUND	1
II	PRELIMINARY DESIGN STUDY OF CANDIDATE SUPPRESSION DEVICES	4
III	DESCRIPTION OF MODEL AND TEST PROGRAM	13
IV	DISCUSSION OF RESULTS	37
V	CONCLUSIONS	134
	REFERENCES	135

# LIST OF ILLUSTRATIONS

FIGURE		PAGE
1	F-111 Wind Tunnel Model Installed in AEDC Propulsion Wind Tunnel -16T	2
2	Bay Turbulence Suppression Concepts I, II, and III	6
3	Bay Turbulence Suppression Concepts IV, V, and VII	7
4	Bay Turbulence Suppression Concept VI	8
5	Bay Turbulence Suppression Concept VIII	9
6	Bay Turbulence Suppression Concept IX	10
7a	1/15 Scale F-111 Model Configuration	14
7b	Weapon Bay Drawing	15
8	Location of Instrumentation	16
9	B-43 Model Weapon (1/15 Scale)	20
10	B-57 Model Weapon (1/15 Scale)	21
11	B-43 Weapon in Bay	22
12	B-57 Weapon in Bay	23
13	Model Store Ejection System	24
14	Suppressor A - Saw Tooth Spoiler Concept V	26
15	Suppressor B - Vortex Generators Concept VI	27
16	Suppressor C - Rear Facing Step Concept VIII	28
17	Suppressor D Rear Ramp Deflector Concept IX	29
18	Installation of Suppressor A (Saw Tooth)	30
19	Installation of Suppressor B (Vortex Generators)	31
20	Installation of Suppressor C (Rear Facing Step)	32
21	Installation of Suppressor D (Rear Ramp Deflector)	33
22	Combination of Suppressors A and D	34
23a	Comparison of Bay Loadings at Mach .95, Centerline Distribution	38

23b	Comparison of Bay Loadings at Mach .95, Left Wall Distribution	39
24a	Comparison of Bay Loadings at Mach 1.3, Centerline Distribution	41
24b	Comparison of Bay Loadings at Mach 1.3, Left Wall Distribution	42
25	Comparison of Suppressor Effectiveness Left Wall Mid-Bay Location	44
26	Comparison of Forward Mounted Suppressor Devices Combines with Rear Ramp Deflector, Left Wall Mid-Bay Location	45
27a	Detailed Comparison of Suppressor Characteristics of Most Effective Devices at Mach .85, Centerline Distribution	46
27b	Left Wall Distribution	47
28a	Detailed Comparison of Suppressor Characteristics of Most Effective Devices at Mach 1.3, Centerline Distri- bution	48
28b	Left Wall Distribution	49
29a	Bay Environment with and without Suppressor A and a Single B-57 Weapon in the Bay, Centerline Distribution	51
29b	Left Wall Distribution	52
30	Bay Environment at Mach 1.3 with and without Suppressor A and a Single B-57 Weapon, Left Wall Distribution	53
31	Pitch Attitude of B-43 Store During Separation with and without Suppressor at Mach .95	55
32a	Baseline F-111/B-43 Weapon Separation Trajectory at Mach .95 and 1000 ft. Altitude	56
32b	F-111/B-43 Separation Characteristics with Suppressor A, Mach .95 and 1000 ft Altitude	57
33a	Baseline B-43 Separation Trajectory at Mach 1.2 and 1000 ft Altitude	59
33b	Trajectory with Suppressor A	60
34a	Baseline B-43 Separation Trajectory at Mach 1.3 and 10,000 ft Altitude	61



34b	Trajectory with Suppressor A	62
35a	Baseline B-43 Separation Trajectory with Angle of Attack of 5 Degrees	63
35b	Trajectory at 5 Degrees Alpha with Suppressor A	64
36	Separation Trajectory with Best Combination of Suppressors, A and D	66
37	Model with Internal Bay Mounted Gun, ECM Pod, and Modified Suppressor A	67
38a	B-43 Separation Trajectory with Bay Mounted Gun Pod	68
38b	Trajectory with Gun Pod and Modified Suppressor A	69
39a	B-43 Separation Trajectory with Bay Mounted Gun Pod Plus ECM Pod	70
39b	Trajectory with Gun Plus ECM Pod and Modified Suppressor A	71
40a	B-57 Separation Trajectory at Mach .95	73
40b	B-57 Trajectory with Suppressor A at Mach .95	74
41a	B-57 Separation Trajectory at Mach 1.2	75
41b	Trajectory with Suppressor A at Mach 1.2	76
42a	Comparison of Baseline, Single B-43 Bay Environment as Measured in the 16T and 4T Tunnels, Centerline Distribution	78
42b	Left Wall Distribution	79
43a	Comparison of Baseline, Single B-43 Bay Environment at Mach 1.3 as Measured in the 16T and 4T Tunnels, Centerline Distribution	80
43b	Left Wall Distribution	81
44	Phase II Suppressor Configurations	83
45	Comparison of Suppressors at Mach .95, Left Wall Distribution	84
46	Comparison of Suppressors at Mach 1.3, Left Wall Distribution	85

47	Angle of Attack Effects on Bay Environment at Mach .95, Left Wall Distribution	87
48	Angle of Attack Effects on Bay Environment at Mach 1.3, Left Wall Distribution	88
49	Angle of Attack Effects with Suppressor A Installed at Mach .95, Left Wall Distribution	89
50	Angle of Attack Effects with Suppressor A Installed at Mach 1.3, Left Wall Distribution	90
51	Angle of Attack Effects with Suppressor AIII Installed at Mach .95, Left Wall Distribution	91
52	Angles of Attack Effects with Suppressor AIII Installed at Mach 1.3, Left Wall Distribution	92
53	Baseline Sideslip Data at Mach .95, Left Wall Distribution	94
54	Baseline Sideslip Data at Mach 1.3, Left Wall Distribution	95
55	Sideslip Effects on Bay Environment at Mach .8 with Suppressor A Installed, Left Wall Distribution	96
56	Sideslip Effects on Bay Environment at Mach .95 with Suppressor A Installed, Left Wall Distribution	97
57	Sideslip Effects on Bay Environment at Mach 1.3 with Suppressor A Installed, Left Wall Distribution	98
58	Sideslip Effects on Bay Environment at Mach .95 with Suppressor AIII Installed, Left Wall Distribution	99
59	Sideslip Effects on Bay Environment at Mach 1.3 with Suppressor AIII Installed, Left Wall Distribution	100
60	Model Frontal View in 16T Showing Inlet and Inlet Rake Details	103
61	Model Viewed from Below Showing Physical Relationship of Suppression Device A to Inlets and Bay Doors	104
62a	Inlet Pressure Recovery Contours for Baseline Configuration, Beta = 0 degrees	105
62b	Inlet Pressure Recovery Contours for Baseline Configuration, Beta = 2 degrees	106

63	Inlet Pressure Recovery Contours with Suppressors A Installed	107
64	Inlet Pressure Recovery Contours with Suppressor AI Installed	108
65	Inlet Pressure Recovery Contours with Suppressor AII Installed	109
66	Inlet Pressure Recovery Contours with Suppressor AIII Installed	110
67a	Inlet Pressure Recovery Measured with Rake Located in Lower Corner of Left Inlet, Beta = 0 degrees	112
67b	Inlet Pressure Recovery in Lower Corner of Inlet, Beta = 2 degrees	113
68a	Static Pressure Distributions Along Centerline of Baseline Configuration at Mach .95 Obtained in AEDC PWT 4T and 16T Wind Tunnels	114
68b	Comparison of Static Pressure Distributions on Left Wall, Mach .95	115
69a	Comparison of Static Pressure Distributions Along Centerline with Suppressor A Installed, Mach .95	116
69b	Comparison of Static Pressure Distributions on Left Wall with Suppressor A Installed, Mach .95	117
70a	Effect of Sideslip on Basic Configuration Static Pressure Distribution at Mach .95, Centerline	118
70b	Effect of Sideslip on Left Wall Static Pressure Distributions at Mach .95	119
71a	Effect of Sideslip on Static Pressure Distribution with Suppressor A Installed at Mach .95, Centerline	120
71b	Effect of Sideslip on Left Wall Static Pressure Distribution Suppressor A Installed at Mach .95	121
72a	Effect of Sideslip on Centerline Static Pressure Distribution with Suppressor A Installed at Mach 1.3	122
72b	Effect of Sideslip on Left Wall Static Pressure Distribution with Suppressor A Installed at Mach 1.3	124

73a	Comparison of Suppressor Effects on Static Pressure Distributions at Mach .95, Centerline	125
73b	Comparison of Suppressor Effects on Static Pressure Distributions at Mach .95, Left Wall	126
74a	Comparison of Suppressor Effects on Static Pressure Distributions at Mach 1.3, Centerline	127
74b	Comparison of Suppressor Effects on Static Pressure Distributions at Mach 1.3, Left Wall	128
75	Comparison of Bay Environment Achieved with Suppressor A to Target Environment at Mach 1.2 and 1000 ft Altitude	130
76	Comparison of Bay Environment Achieved with Suppressor A to Target Environment at Mach 1.3 and 4000 ft Altitude	132
77	Effect of Modified Suppressor A on Bay Environment with Gun Installed	133

#### LIST OF TABLES

##### TABLE

1	Candidate Devices	5
2	Contractor Qualitative Ranking of Separation Characteristics	11
3	Fluctuating Pressure Transducer Non-Dimensional Locations	17
4	Steady State Pressure Orifice Non-Dimensional Locations	18
5	Drop Test Conditions	36
6	Weapon Ejection Parameters	36

# LIST OF SYMBOLS

$C_p$	Static Pressure Coefficient, $(P-P_\infty)/Q$
H	Stimulated altitude of store drop, ft.
L	Length of model weapons bay, 12.1 in.
$M_\infty$	Free stream Mach number
P	Local static pressure, psf.
$P_{RMS}$ , $P_{rms}$	Root mean square dynamic pressure, psf.
$P_\infty$	Free stream total pressure, psf.
$P_T$	Free stream total pressure, psf.
Q	Free stream dynamic pressure, psf.
REX	Reynolds number per foot $\times 10^{-6}$
X	Distance from weapon bay forward lip, positive aft, in.
$X'$	Store cg displacement in the wind axis $X_w$ direction, relative to the drop position, full-scale (ft), positive forward
Y	Lateral distance from centerline of weapons bay, positive to pilots left, in.
$Y'$	Store cg displacement in the wind axis $Y_w$ direction, relative to the drop position, full-scale (ft), positive for cg movement to the pilot's right when looking along the $X_w$ -axis
Z	Vertical distance from lower model surface, positive up into bay, in.
$Z'$	Store cg displacement in the wind axis $Z_w$ direction, relative to the drop position, full-scale (ft), positive for cg movement down
t	Store trajectory time, full scale, sec.
cg	Center of gravity
FS	Fuselage station

## LIST OF SYMBOLS (CONT'D)

### Coordinate System for Drop Test (Wind-Axis System)

$X_W$	Parallel to the wind tunnel centerline, positive upstream
$Y_W$	Perpendicular to the $X_W$ axis in the horizontal plan of the wind tunnel, positive to the right when looking upstream
$Z_W$	Perpendicular to the $X_W$ and $Y_W$ axes in the vertical plane of the wind tunnel, positive down
ALFA, ALF-M, and $\alpha$	Alpha, angle of attack (fuselage body angle), deg.
$\beta$	Beta, sideslip angle, positive nose left, deg.
$\nu$	Nu, pitch angle of store (angle between the projection of the store longitudinal axis in the $X_W - Z_W$ plane and the $X_W$ axis), positive nose up, deg.
$\eta$	Eta, yaw angle of store (angle between the store longitudinal axis and its projection in the $X_W - Z_W$ plane), positive nose right
THETA	Pitch attitude of store, $\nu$ minus $\alpha$ , deg.

## SECTION I

### INTRODUCTION AND BACKGROUND

Flight experience with aircraft equipped with internal weapons bays has shown that high speed flow over an open bay can produce a turbulent environment within the bay that can damage the weapon(s) or aircraft structure. Various studies have been conducted to define this environment and means to improve or suppress the aero-acoustic energy of this turbulent flow.

This investigation, conducted jointly by the AF Flight Dynamics and the AF Weapons Laboratories, has been directed toward the F-111/FB-111 family of aircraft. Specifically, the objective of this effort was to identify and experimentally verify means of suppressing the internal weapon bay aero-acoustic environment associated with the B-43 weapon carried in the F-111 bay. This weapon has had structural failures of the parachute tail-can to weapon body attachment which have resulted in establishment of weapon bay delivery limits for this weapon significantly below the capabilities of the F-111 and FB-111 aircraft.

A candidate suppression device has been identified and wind tunnel tested which shows significant potential for retrofit to the F-111 family of aircraft. This device, a saw tooth spoiler, was derived from a similar device evaluated during an earlier AFFDL/AFWL in-house research program (Reference 1). The spoiler successfully suppresses the internal weapons bay aero-acoustic environment while improving the bay separation characteristics of the B-43 weapon for all conditions tested. Similar improvements were also observed with the smaller B-57 weapon. Figure 1

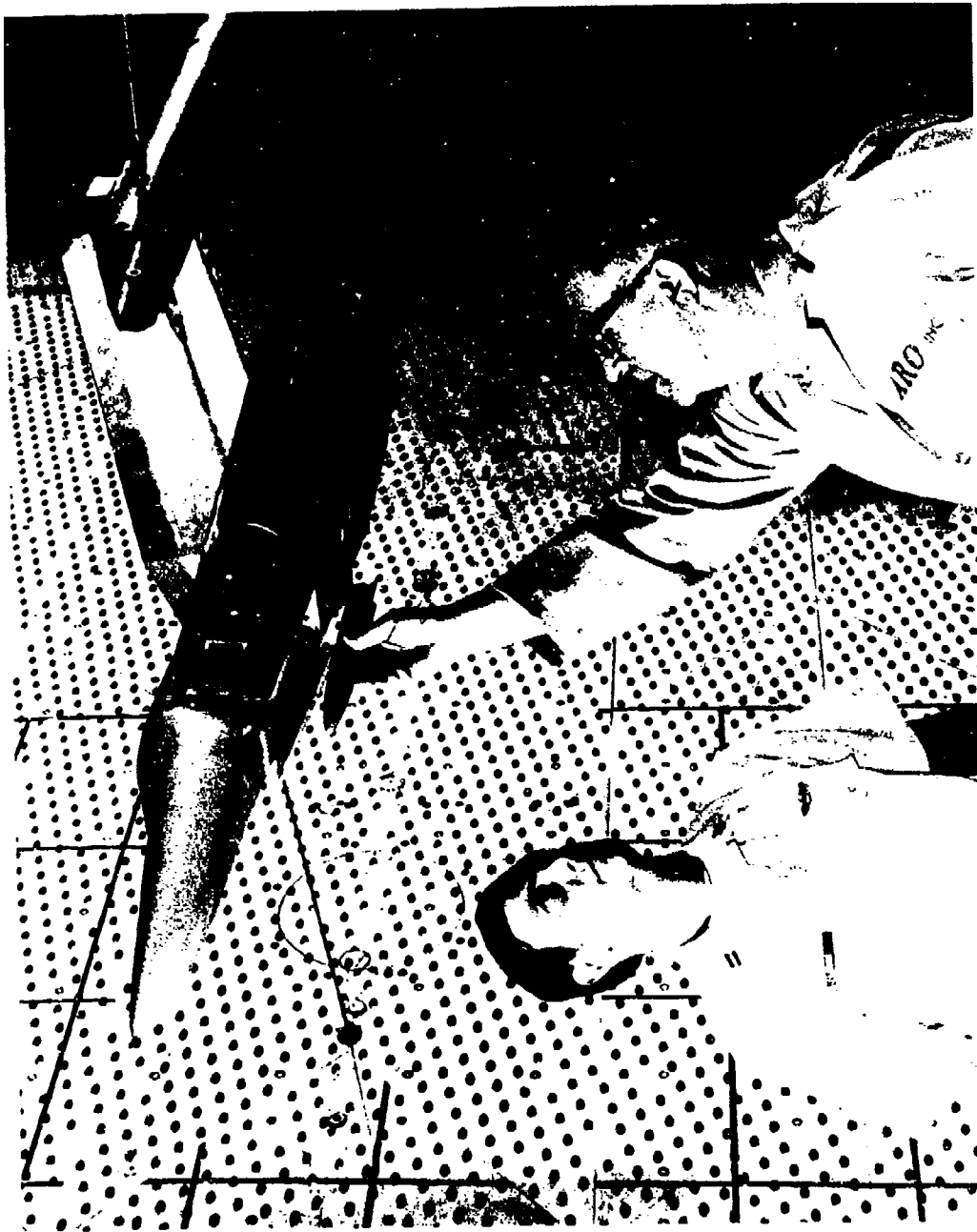


Figure 1. F-111 Wind Tunnel Model Installed in  
AEDC Propulsion Wind Tunnel - 16T



shows the wind tunnel model installed in the AEDC 16T wind tunnel with the model scale saw tooth spoiler mounted at the bay leading edge.

The first phase of this program consisted of a preliminary design study performed by General Dynamics-Fort Worth Division conducted under contract F04606-D-0114 sponsored by the AFWL (Reference 2). The contractor evaluated the feasibility of modifications to the F-111 aircraft required to incorporate each of nine candidate suppression devices and identified the most promising based upon preliminary estimates of the effects of these devices on the aircraft and weapon separation characteristics. More details of this phase are presented in Section II.

SECTION II  
PRELIMINARY DESIGN STUDY OF  
CANDIDATE SUPPRESSION DEVICES

This section briefly discusses the design study performed under contract by General Dynamics-Fort Worth Division (Reference 2). This study assessed the feasibility of incorporating each of nine candidate devices designed to suppress the turbulent environment in the internal weapon bay of the F-111 aircraft. These devices were evaluated from the structural, aerodynamic, stability and control, and weapon separation view points. Two of the devices were selected for more detailed analysis. Table 1 identifies the nine concepts. Figures 2 through 6 show the aircraft installation drawings for these concepts.

All nine concepts were considered feasible for installation on an F-111 aircraft for flight test evaluation. No significant structural, aerodynamic, or handling quality problems were identified. All of the devices were qualitatively evaluated relative to the effect of each on weapon separation characteristics. Table 2 lists the nine devices in order of preference based upon the contractor's assessment of the separation characteristics of each. The contractor was concerned that the devices installed at or near the leading edge of the bay could have undesirable effects on the weapon separation characteristics.

The saw tooth spoiler (Device V) and the slanted rear ramp deflector (Device IX) were selected for more detailed analysis. Airloads were estimated, and structural and actuator loads computed for each of these.

TABLE 1 CANDIDATE DEVICES

<u>Concept Number</u>	<u>Description</u>
I	Perforated Spoiler - 25 percent porosity
II	Perforated Spoiler - 14 percent porosity
III	Perforated Spoiler - 50 percent porosity
IV	Saw Tooth Spoiler - height = 1.3 boundary layer height
V	Saw Tooth Spoiler - height = 1.0 boundary layer height
VI	Fixed Vortex Generators
VII	Notched Spoiler - height = 1.0 boundary layer height
VIII	Island Deflector Step - Vortex generator
IX	Slanted Rear Ramp Deflector

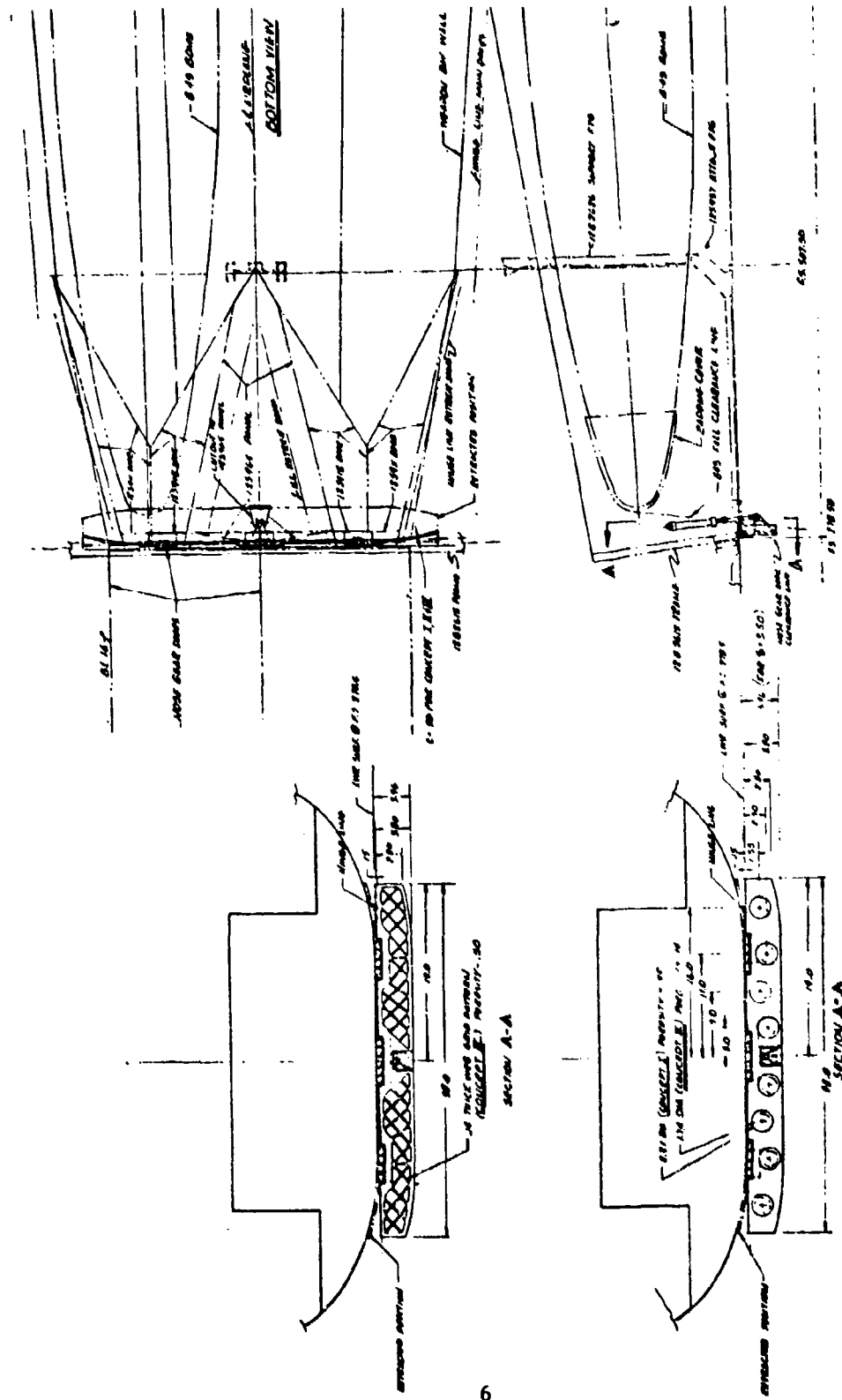
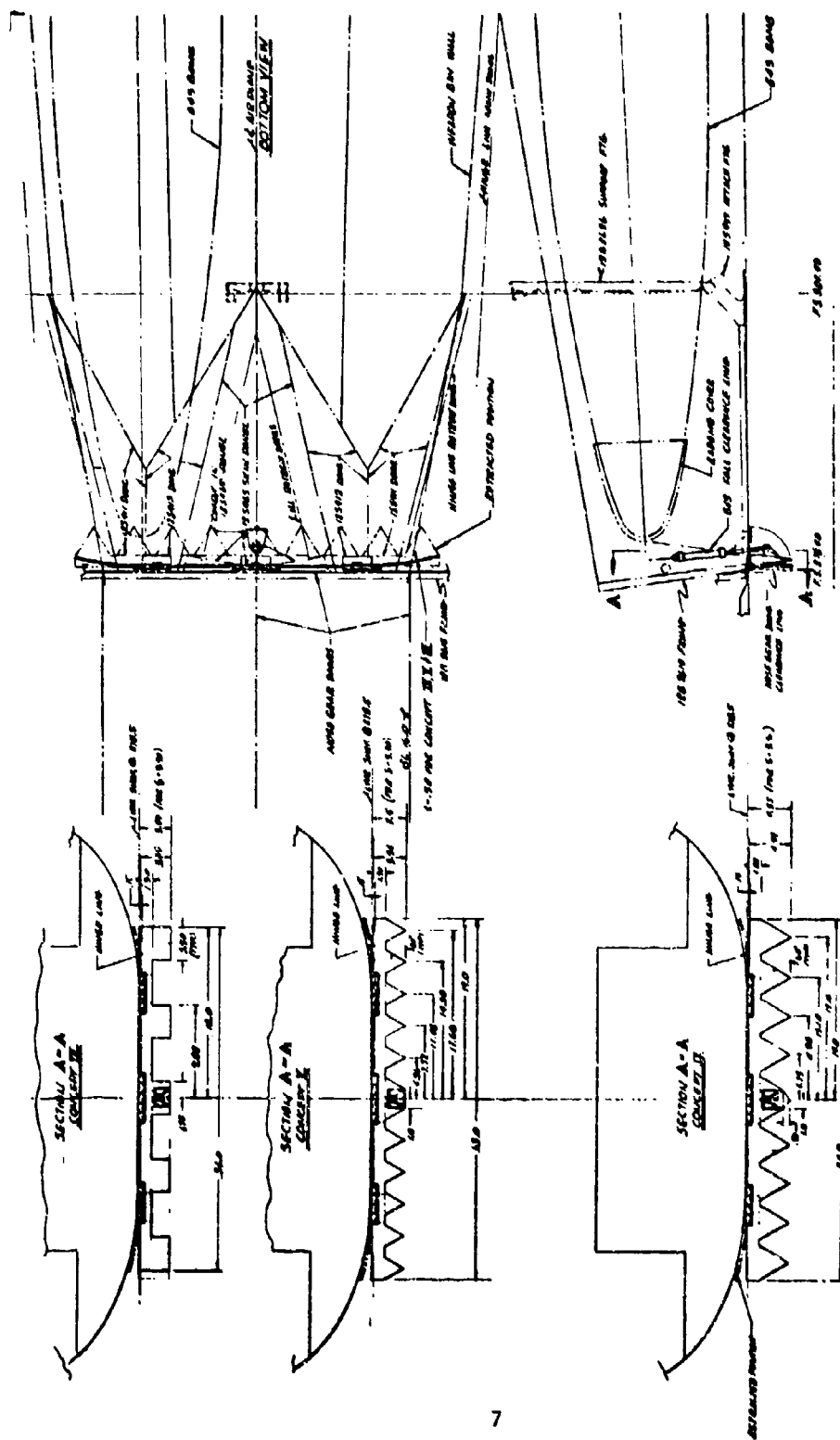


Figure 2. Bay Turbulence Suppression Concepts I, II, and III



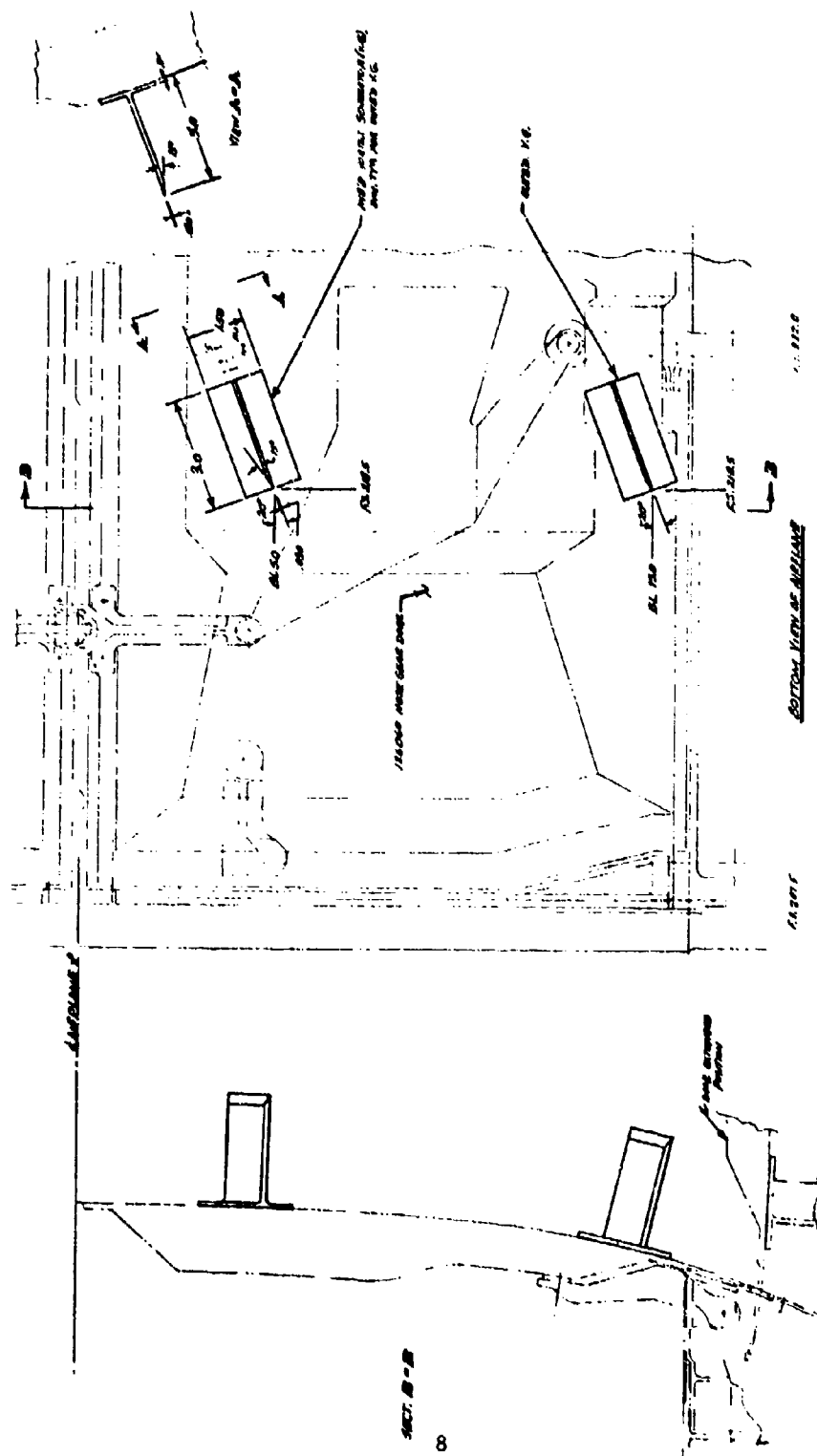


Figure 4. Bay Turbulence Suppression Concept VI



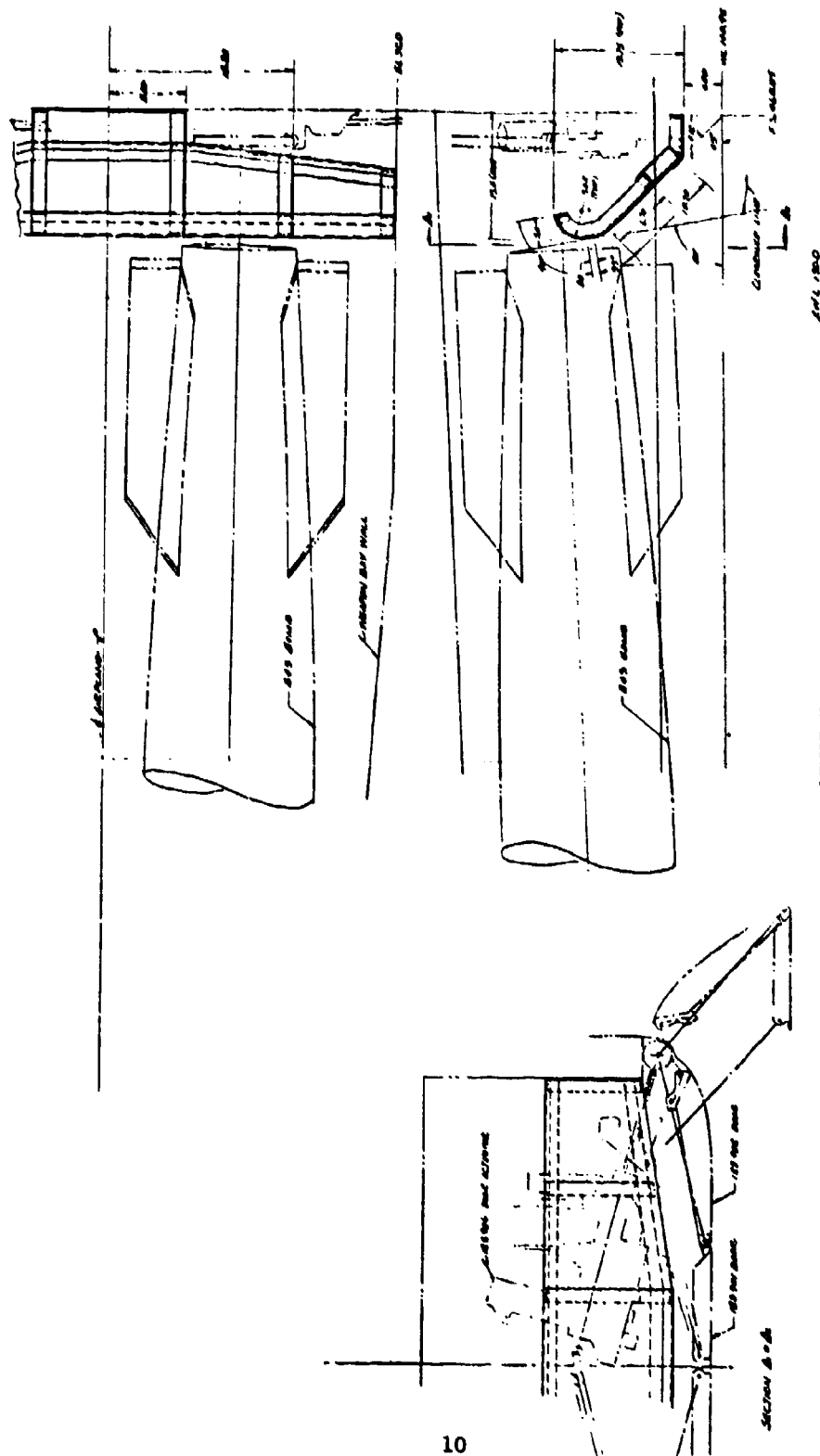


Figure 6. Bay Turbulence Suppression Concept IX



TABLE 2  
CONTRACTOR QUALITATIVE RANKING OF  
SEPARATION CHARACTERISTICS

<u>Order of Preference</u>	<u>Concept Number</u>
1	IX
2	VI
3	V
4	IV
5	VII
6	III
7	I
8	II
9	VIII

Based upon these loads, a preliminary stress analysis was performed, materials were selected, and thicknesses determined for the full scale parts.

Based upon the contractor's recommendations and previous test experience with a saw tooth spoiler (Reference 1), four devices were selected for evaluation during a wind tunnel test program. The devices selected were Concepts V, VI, VIII, and IX. Section III contains details of the two phased test program and the model parts.

## SECTION III

### DESCRIPTION OF MODEL AND TEST PROGRAM

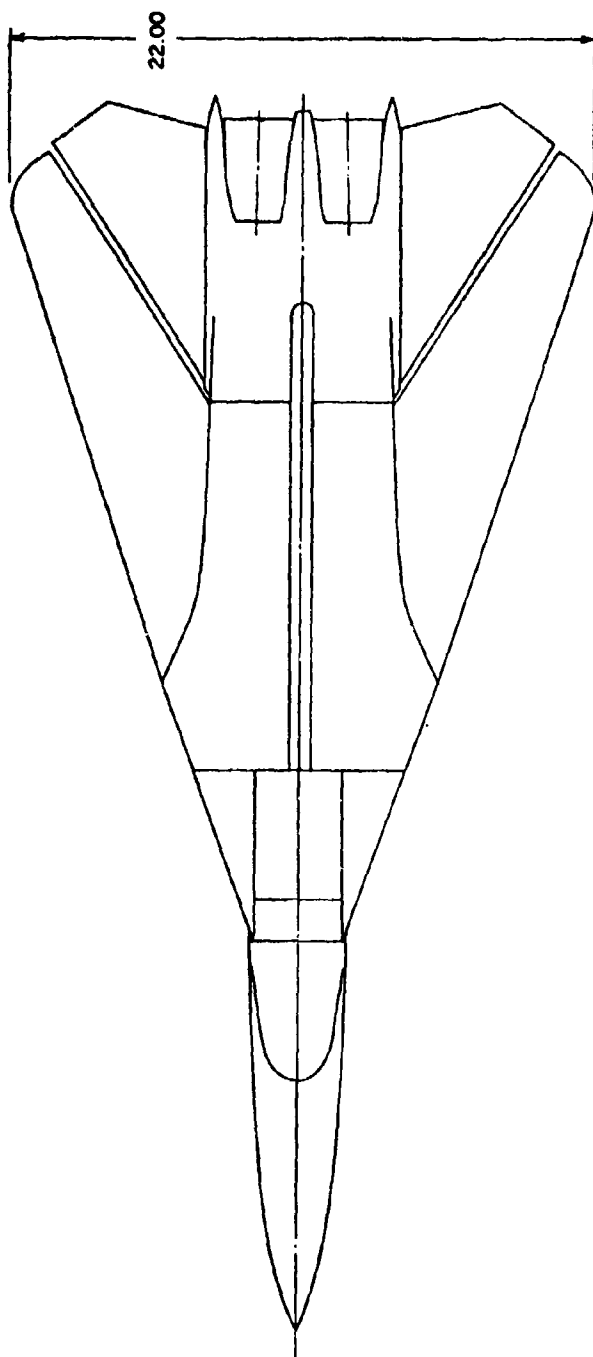
3.0 The test program consisted of two phases. The first, conducted in the Arnold Engineering and Development Center Propulsion Wind Tunnel, Transonic (16T), evaluated the effectiveness of the four candidate suppression devices and the effect of the most effective device on weapon separations from the bay. The second phase was conducted in the AEDC Aerodynamic Wind Tunnel (4T). This phase was conducted to investigate the sensitivity of the most effective suppression device from Phase 1 to changes in geometry and to angle of attack and sideslip variations. See Reference 3 for detailed descriptions of the above test facilities.

#### 3.1 Model Description

The model used for both test phases was a 1/15 scale F-111 model originally manufactured for store drop tests from the bay and wing stations. The model geometry is shown in Figure 7. The wings were positioned throughout this program in the full sweep position as shown in Figure 7a. The weapon bay in the model (Fig. 7b) was 12.1 inches in length. The model installation in the PWT 16T tunnel is shown in Figure 1.

##### 3.1.1 Model Instrumentation

The model bay instrumentation locations can be seen in Figure 8. Fifteen (15) Kulite solid state pressure transducers were installed and Table 3 lists the location of each in non-dimensional units, referenced to the bay length ( $L$ ) = 12.1 inches. One transducer was installed in the nose of the model. Three thermocouples were installed as shown in Figure 8.



DIMENSIONS IN INCHES

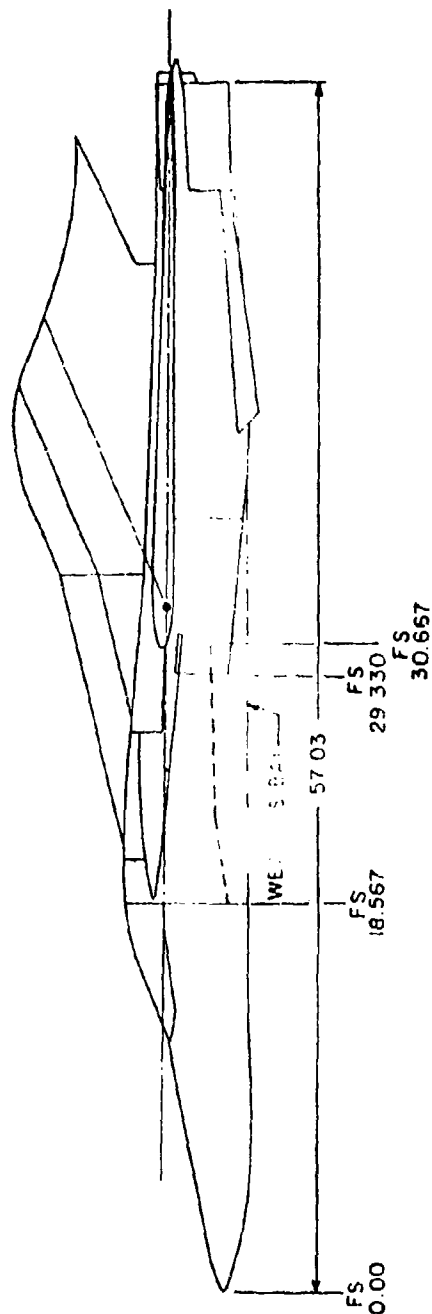
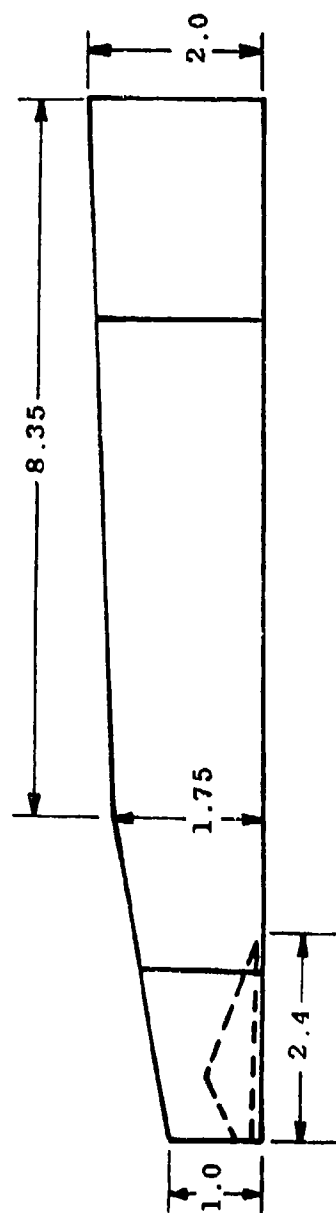
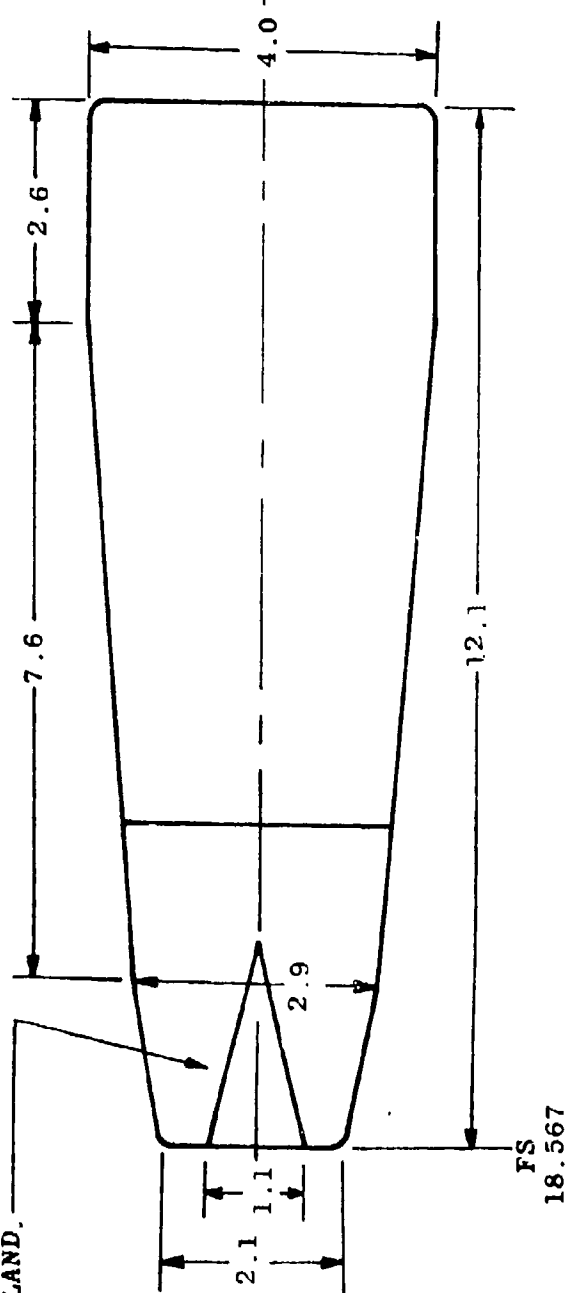


Figure 7a. 1/15 Scale F-111 Model Configuration



WEAPONS BAY  
ISLAND.



DIMENSIONS IN INCHES

Figure 7b. Weapon Bay Drawing

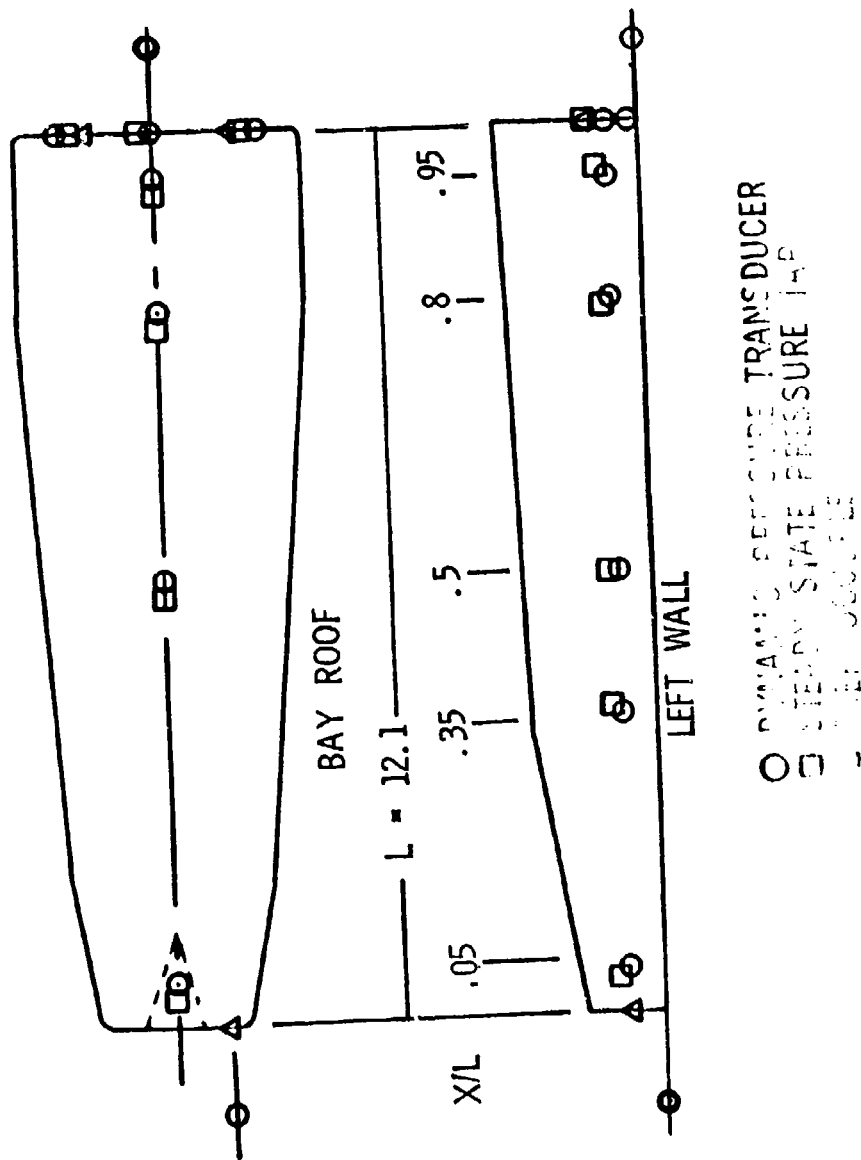


Figure 8. Location of Instrumentation

TABLE 3

## FLUCTUATING PRESSURE TRANSDUCER NON-DIMENSIONAL LOCATIONS

Orifice No.	X/L	Y/L	Z/L
RMS1	(Fuselage Nose)	0	-
RMS15	-0.10	0.06(L)	0
RMS2	0.05	0	-
RMS3	0.50	0	-
RMS4	0.80	0	-
RMS5	0.95	0	-
RMS6	1.00	0	0
RMS7	1.10	0	0.05
RMS13	1.00	0.10(Lt)	0.05
RMS14	1.00	-0.10(Rt)	0.05
RMS8	0.05	Left side	↓
RMS9	0.35	Wall	
RMS10	0.50	↓	
RMS11	0.80	↓	
RMS12	0.95	↓	

Static pressure taps were installed at the locations listed in Table 4. The left engine inlet was also instrumented with an array of twelve total pressure taps installed in three rakes located at the inlet face.

TABLE 4  
Steady State Pressure Orifice Non-Dimensional  
Locations

Orifice No.	X/L	Y/L	Z/L
PS15	-0.10	0.052 (Left)	0
PS2	0.033	0	-
PS3	0.483	0	-
PS4	0.783	0	-
PS5	0.933	0	-
PS6	1.00	-0.01(Rt)	0
PS16	1.00	0	0.05
PS17	1.00	0	0.066
PS7	1.10	0	0
PS13	1.00	0.09(Lt)	0.05
PS14	1.00	-0.09(Rt)	0.05

Left Side Wall

PS8	0.04	-	0.058
PS9	0.342	-	0.058
PS10	0.492	-	0.058
PS11	0.792	-	0.058
PS12	0.942	-	0.058



### 3.1.2 Drop Models and Store Ejection System

Two store models were designed for the drop test phase. The primary weapon was the B-43. A much smaller B-57 weapon was included to determine if the suppression devices affected the small store in any adverse or different way than the B-43 was affected. These stores were designed using the "heavy" scaling technique described in Reference 4. Figures 9 and 10 present the geometry details of these store models and Figures 11 and 12 show these weapons installed in the model bay. The black dots indicate the location of the Kulite pressure transducers relative to the stores. Only the roof (centerline) and left sidewall transducers are shown.

Figure 13 contains details of the model store ejection system. The ejection force is provided by a nitrogen pressure system acting on a piston. The ejection velocity required is obtained by adjusting the pressure level. The pitch rate applied to the model is determined by the geometry of the ejector foot relative to the store center of gravity. The proper values of these variables were determined prior to the test by the contractor during calibration drops using specially fabricated calibration bodies representing each store. The ejection sequence is initiated by supplying an electrical current to the "burn bolt." The fusible section of the bolt is melted, releasing the retaining spring which, in turn, retracts the two slide feet which hold the store in the bay. The piston/ejector foot then propels the model store out of the bay. High speed cameras record the ejection sequence.

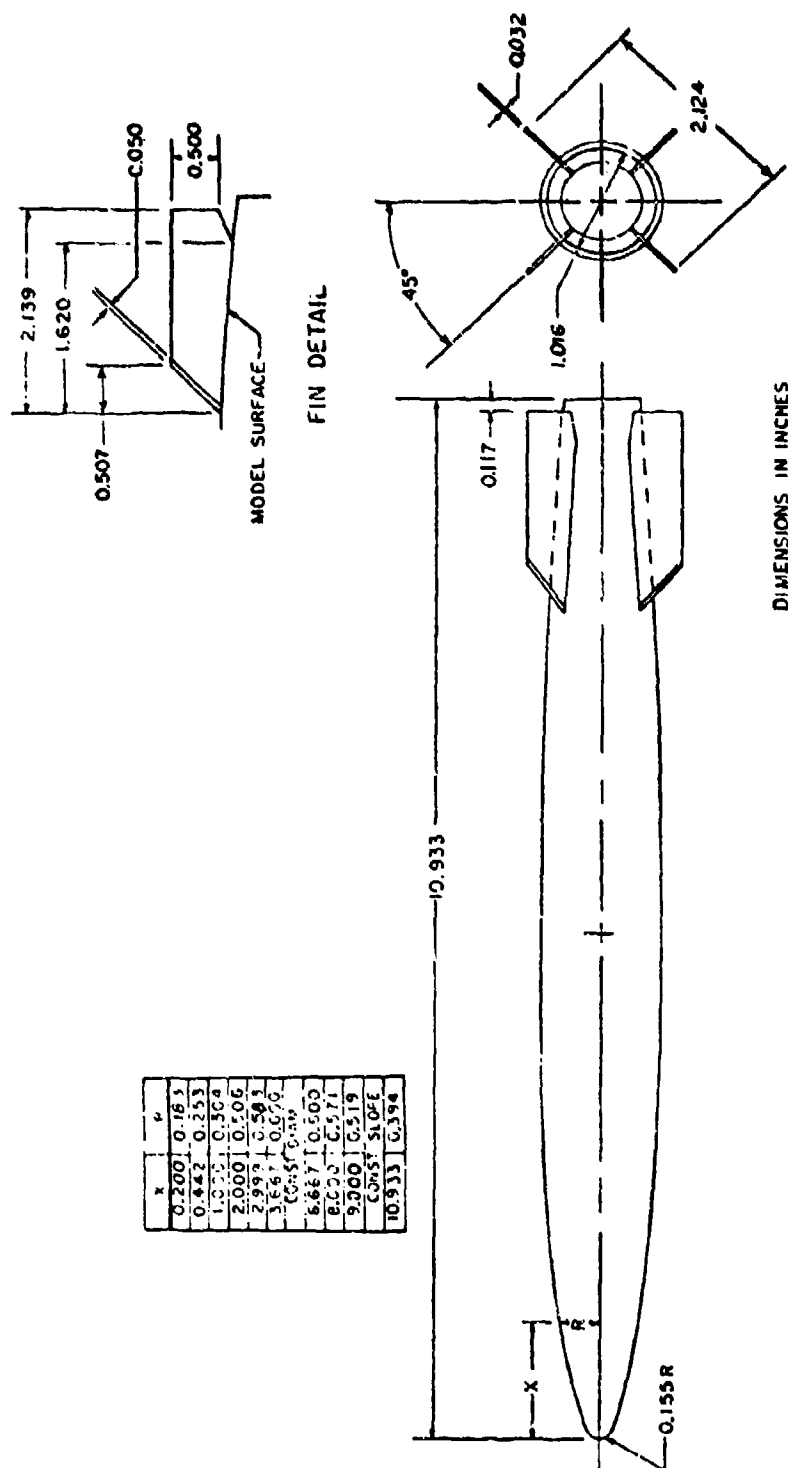
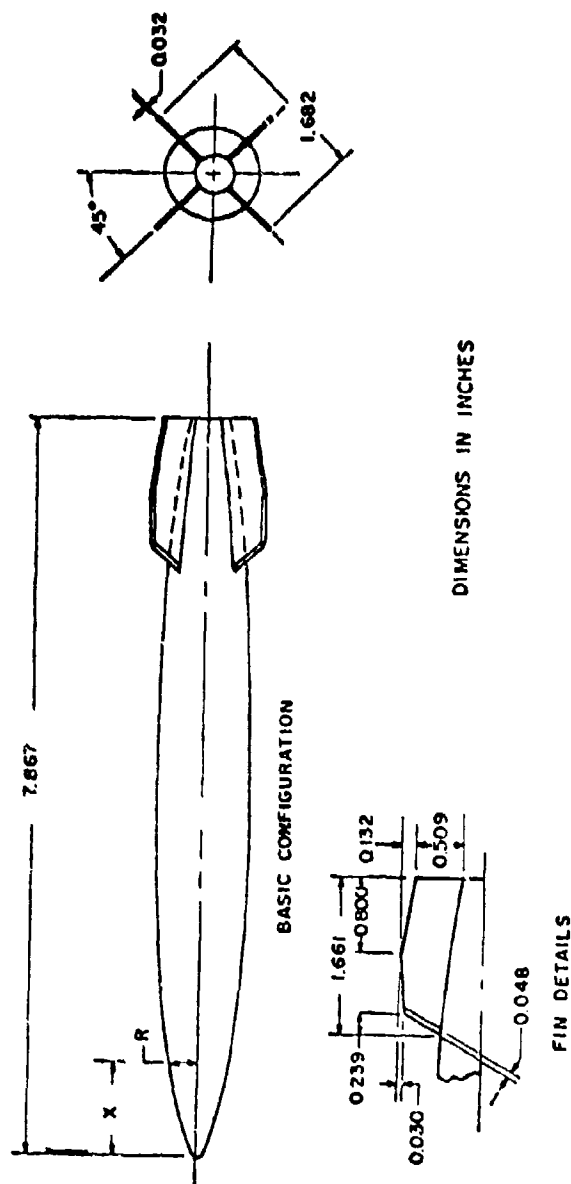


Figure 9. B-43 Model Weapon (1/15 Scale)

X in	R in
0	0
0.033	0.057
0.067	0.081
0.200	0.140
0.333	0.181
0.500	0.222
0.657	0.256
0.800	0.281
0.933	0.303
1.267	0.354
1.333	0.363
1.667	0.405
2.000	0.441
2.400	0.469
2.933	0.485
3.333	0.490
3.533	0.492
3.667	0.492
4.000	0.489
4.400	0.481
5.067	0.465
5.733	0.438
6.400	0.392
6.667	0.367
7.067	0.322
7.333	0.286
7.600	0.246
7.667	0.200



DIMENSIONS IN INCHES

FIN DETAILS

Figure 10. B-57 Model Weapon (1/15 Scale)

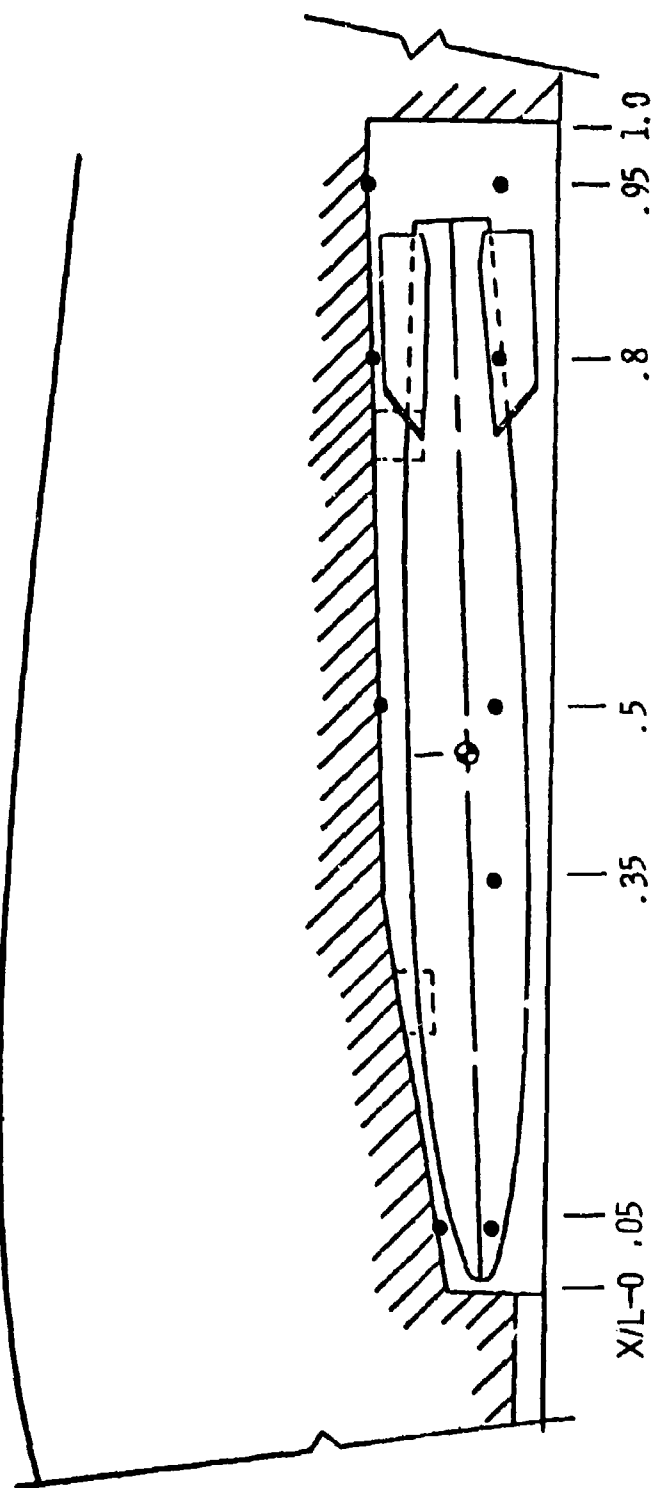


Figure 11. B-43 Weapon in Bay

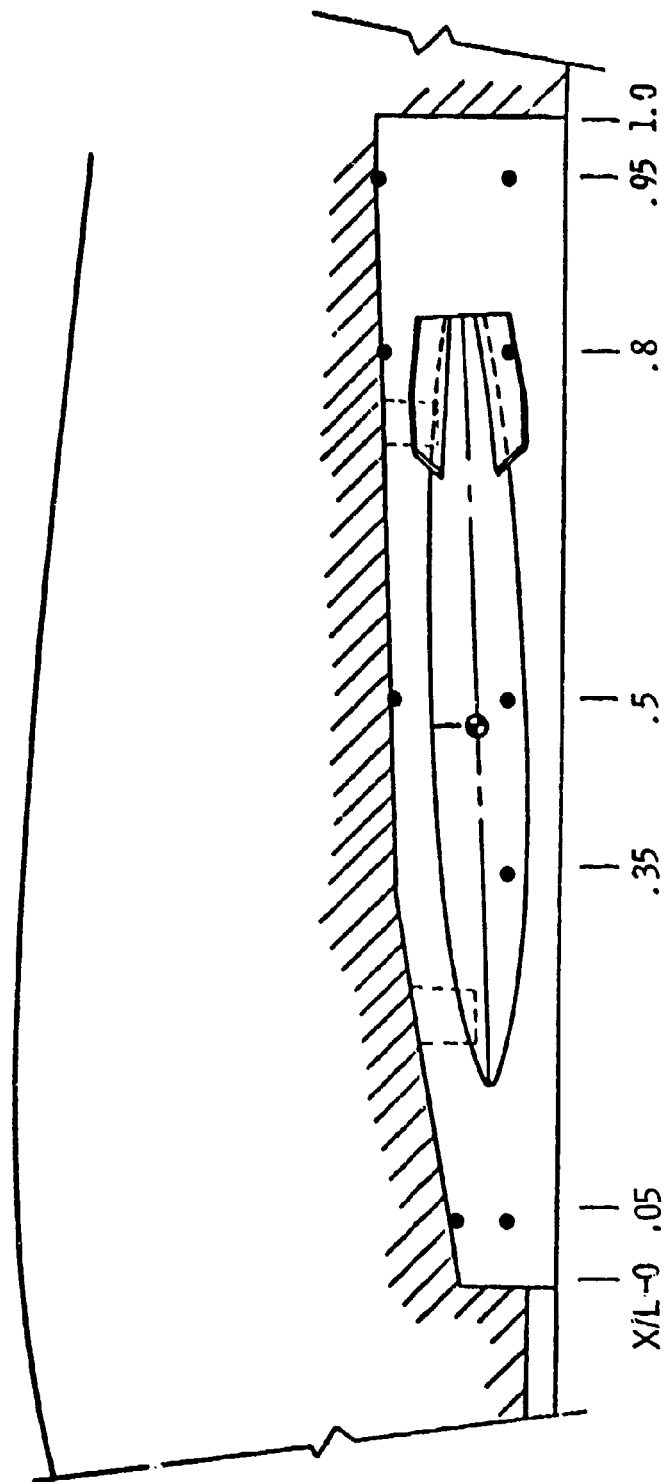


Figure 12. B-57 Weapon in Bay

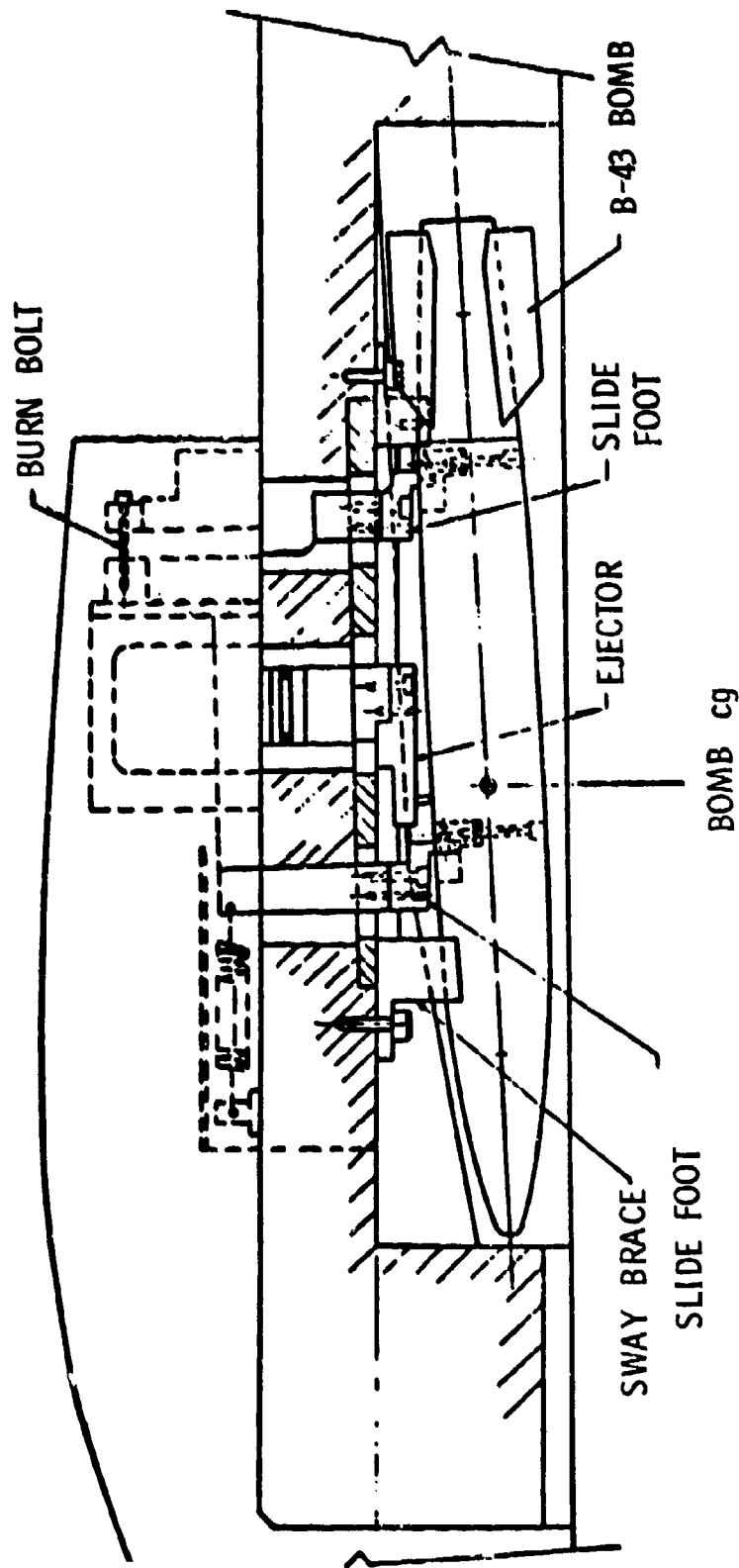


Figure 13. Model Store Ejection System

The model separation trajectory and the equivalent full scale trajectory are then determined in accordance with the procedures described in Reference 4. These procedures consist of frame by frame plotting of the location of the nose and tail positions of the model store overlaid on a grid photographically obtained and calibrated prior to the actual drops with no airflow through the test section.

### 3.1.3 Model Suppression Devices

The four model suppression devices evaluated during the first test phase are depicted in Figures 14 through 17. These are scaled directly from the full scale devices identified in these figures from Section II. This geometric scaling results in devices which are aerodynamically smaller than if scaled to the local boundary layer height. The local boundary layer height at the bay forward lip is 3.5 inches full scale. Geometric scaling of this height using the 1/15 scale factor results in a dimension of .23 inches. The actual model boundary layer at this location was calculated to be between .313 and .331 inches for the wind tunnel test conditions. Therefore, the height of Suppression Device A is approximately 70 percent of the local boundary layer. Figures 18 through 21 show the devices installed on the model in the wind tunnel. Figure 22 shows the combination of A and D.

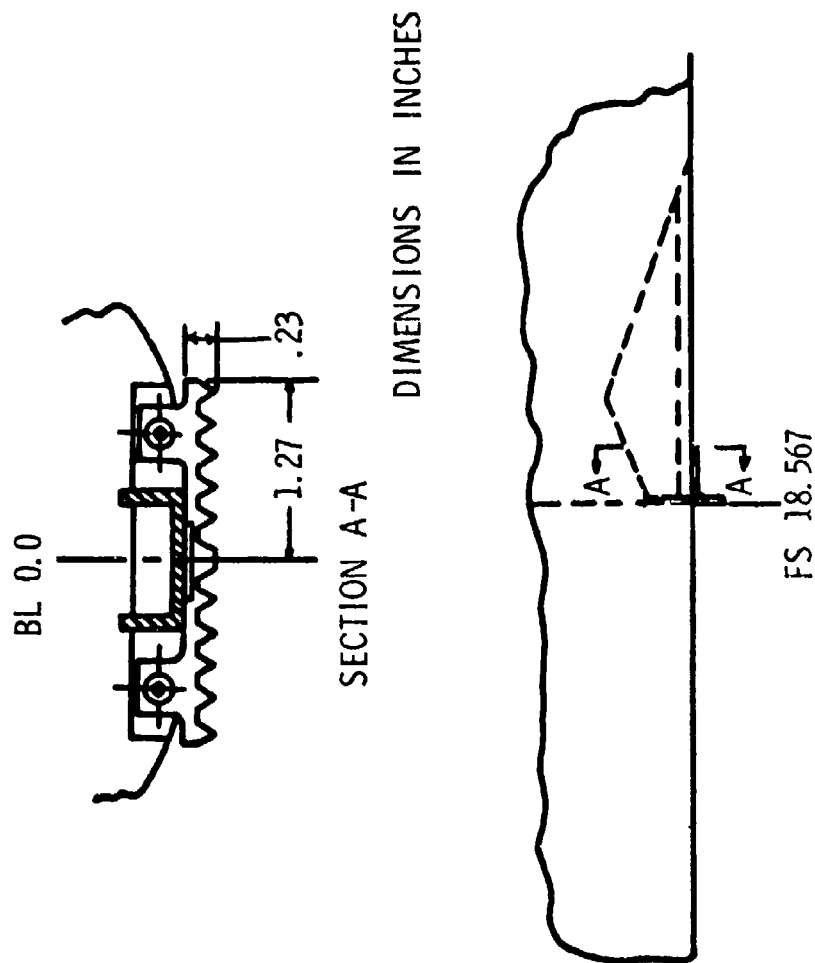


Figure 14. Suppressor A - Saw Tooth Spoiler  
Concept V





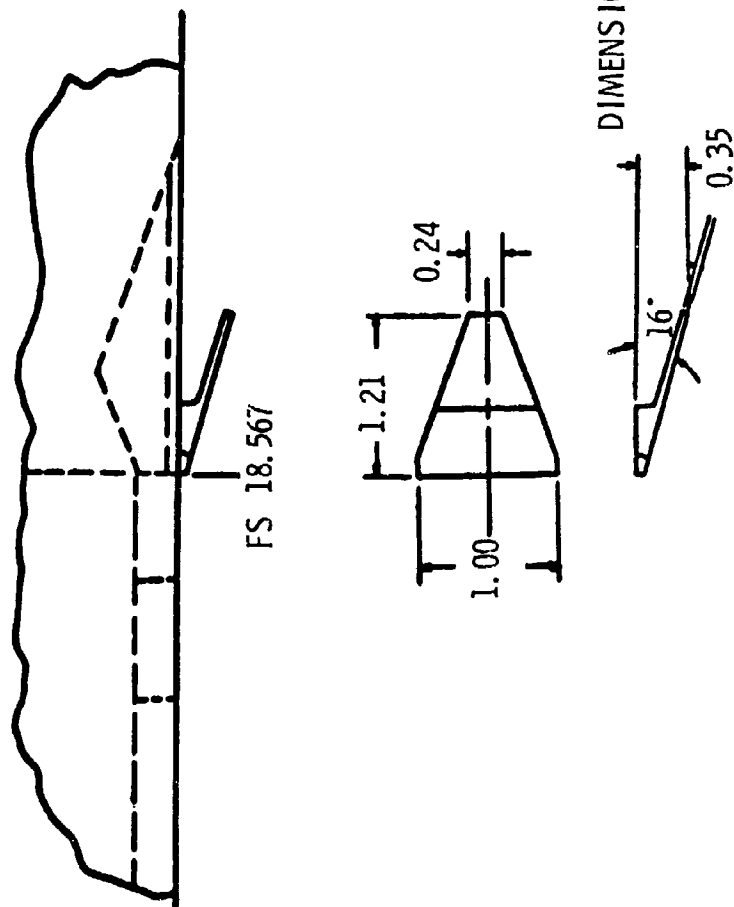


Figure 16. Suppressor C - Rear Facing Step; Concept VIII

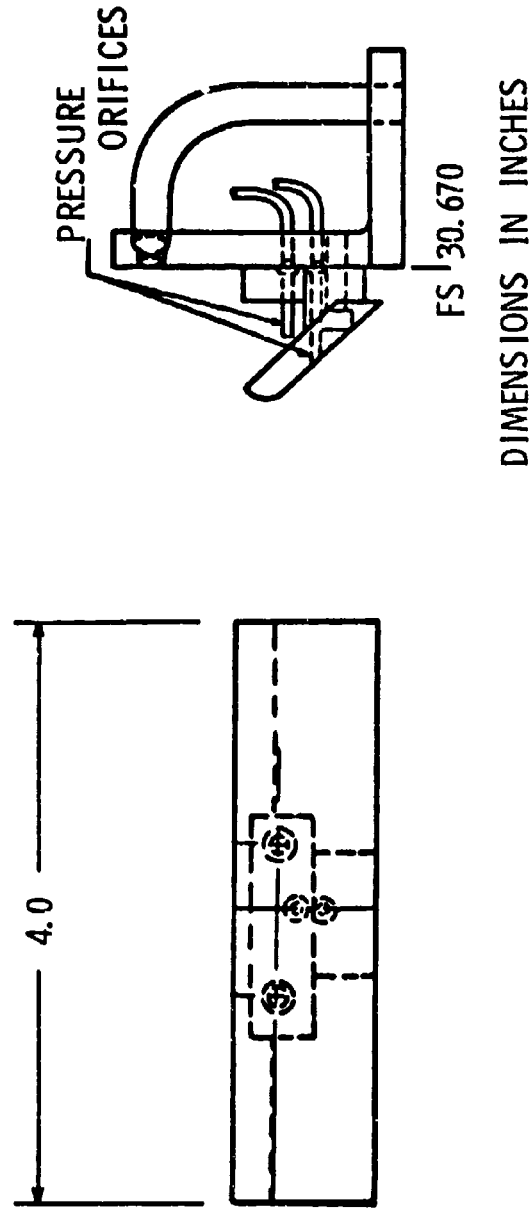


Figure 17. Suppressor D Rear Ramp Deflector; Concept IX

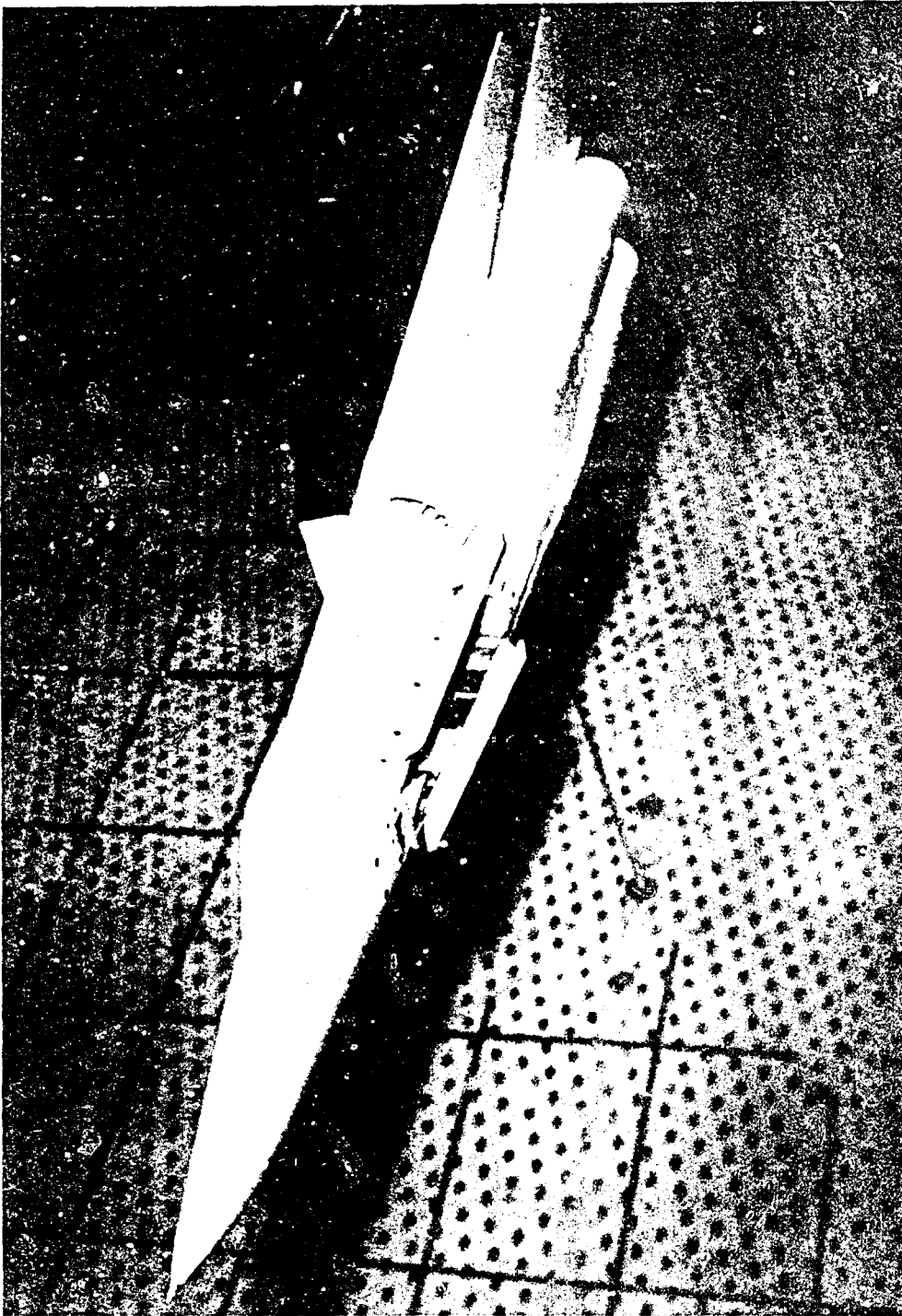


Figure 18. Installation of Suppressor A (Saw Tooth)

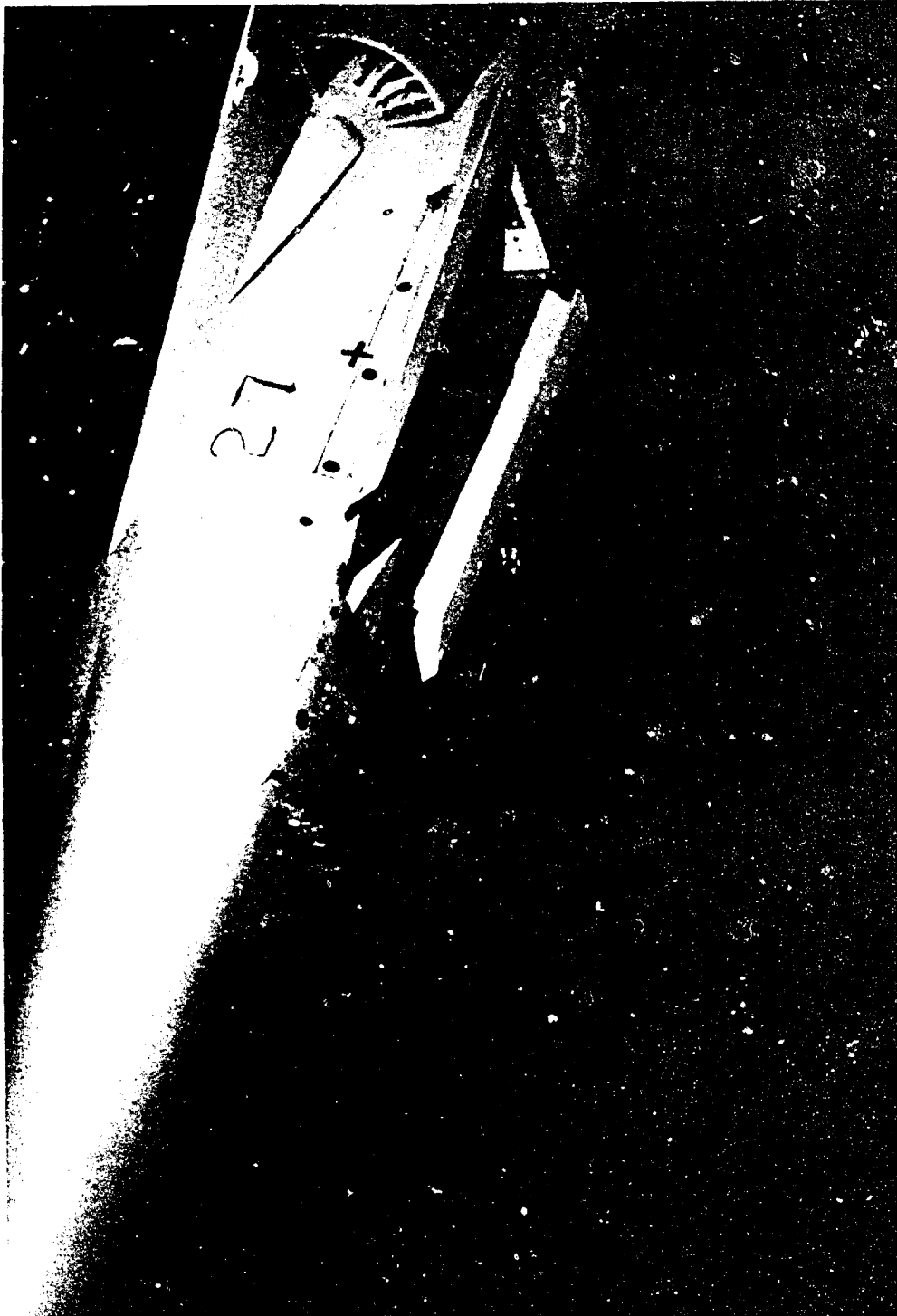


Figure 19. Installation of Suppressor B (Vortex Generators)



Figure 20. Installation of Suppressor C (Rear Facing Step)

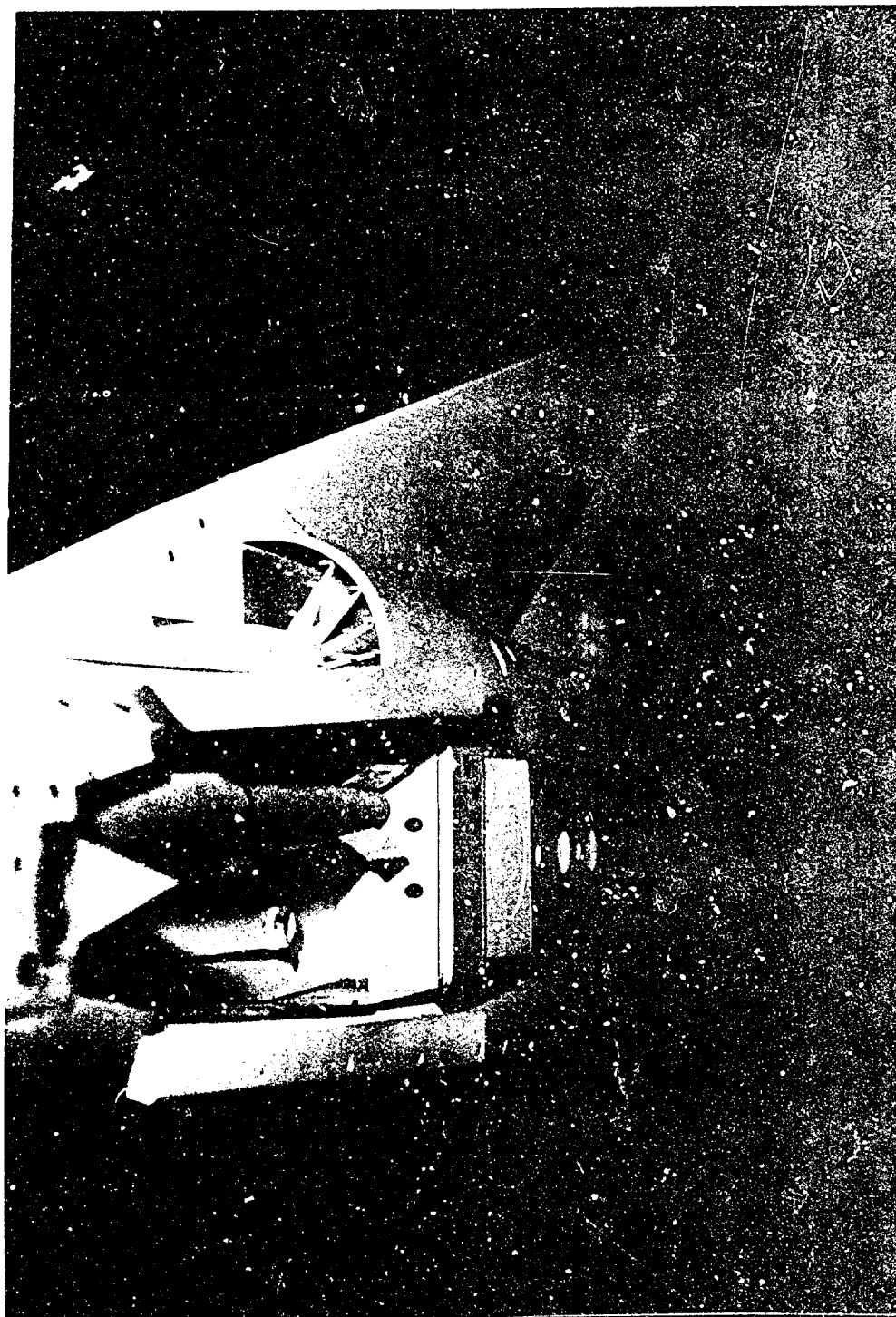


Figure 2L. Installation of Suppressor D (Rear Ramp Deflector)



Figure 22. Combination of Suppressors A and D



### 3.2 Test Conditions

During Phase 1, a Mach range of .7 to 1.5 was investigated; however, the major portion of the test program was limited to Mach 1.3 and below by the tunnel installed equipment required for the drop test phase. Reynolds number ( $R_N$ ) was not a primary variable. Limited data was acquired over a  $R_N$  range of 2.0 to 4.4 million per foot with 2.5 to 3.5 million being the primary test range. Three drop conditions were investigated, and Table 5 lists the associated wind tunnel test conditions. Table 6 lists the ejection parameters applicable to each weapon. The simulated altitude (H) listed in Table 5 is obtained by use of the dynamic pressure ratio where tunnel dynamic pressure is related to the full scale flight dynamic pressure as discussed in Reference 4.

Table 6 lists the ejection parameters applicable to each weapon.

TABLE 5  
DROP TEST CONDITIONS

Mach	Reynolds Number/Ft	Tunnel Dynamic Pressure; Q (psf)	Total Pressure; $P_T$ (psf)	Simulated Altitude; H (ft)
.95	$2.5 \times 10^6$	439	1242	1000
1.20	$3.5 \times 10^6$	700	1683	1000
1.30	$2.8 \times 10^6$	586	1370	10,000

TABLE 6  
WEAPON EJECTION PARAMETERS

WEAPON	Vertical Ejection Velocity			Pitch Rate (deg/sec, nose down)		
	Model (in/sec)/Full Scale (ft/sec)			Model/Full Scale		
B-43	32.53	/	10.5	64.36	/	16.6
B-57	51.43	/	16.6	359.4	/	92.8

Phase 2 testing was conducted over a Mach range of .7 to 1.3 at a constant Reynold's number of 3 million per foot. Model angle of attack ( $\alpha$ ) sweeps were conducted over the range of -1 to +8 degrees. Sideslip ( $\beta$ ) sweeps were conducted from -8 to +8 degrees; however, some of the configurations were only investigated over a beta range of  $\pm 4$  degrees.

## SECTION IV

### DISCUSSION OF RESULTS

#### 4.1 Baseline F-111 Weapon Bay Data

The following presents data in terms of the ratio of  $P_{rms}/Q$  for the basic bay empty and loaded configurations investigated during Phase 1.  $P_{rms}$  is the root mean square of the non-steady dynamic pressure component measured using the Kulite pressure transducers. This data has been normalized by dividing by the tunnel free stream dynamic pressure ( $Q$ ). This provides a non-dimensional ratio easily scaled to other conditions by using appropriate values of dynamic pressure ( $Q$ ). These data represent the acoustic energy or turbulence at each transducer location and the data can be converted to decibels referenced to  $Q$  by using the following equation:

$$dB_{\text{ref to } Q} = 20 \text{ LOG } (P_{rms}/Q)$$

Figure 23 compares the empty bay with data for several weapon loadings at Mach .95. The data is plotted against non-dimensional ( $X/L$ ) location where " $X$ " is measured from the forward bay lip and " $L$ " is the bay length (12.1 inches). Figure 23a presents the centerline bay distribution which is markedly different in character from the left wall distribution presented in Figure 23b. The centerline instrumentation shows the  $P_{RMS}/Q$  levels increasing from front to rear. The centerline data also suggests that the acoustic energy in the bay increases as the volume of the weapons load decreases. No similar trends are observed on the left wall with the single B-43 producing the highest level at the mid-bay position while the empty bay produces next to the lowest overall level.

SYM MACH LEFT BAY RIGHT BAY SUPPR.

NONE  
NONE  
NONE  
NONE

EMPTY  
EMPTY  
B-43  
EMPTY

EMPTY  
B-43  
B-43  
B-57

.95  
.95  
.95  
.95

—  
□  
+  
Y

PRMS / Q

0.2

0.1

0.0

0.0

0.2

0.4

0.6

0.8

1.0

X/L

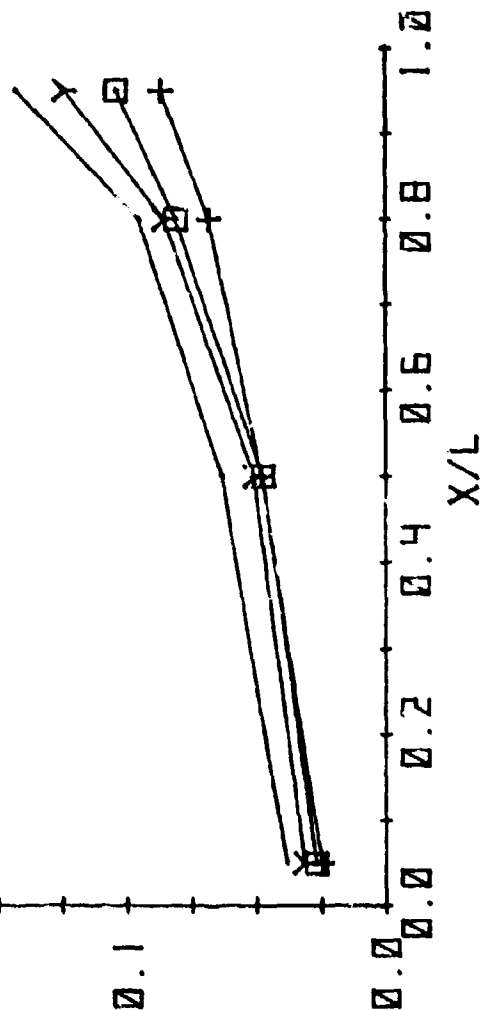


Figure 23a. Comparison of Bay Loadings at Mach .95, Centerline Distribution

SYM	MACH	LEFT BAY	RIGHT BAY	SUPPR.
—	.95	EMPTY	EMPTY	NONE
□	.95	B-43	EMPTY	NONE
+	.95	B-43	B-43	NONE
Y	.95	B-57	EMPTY	NONE

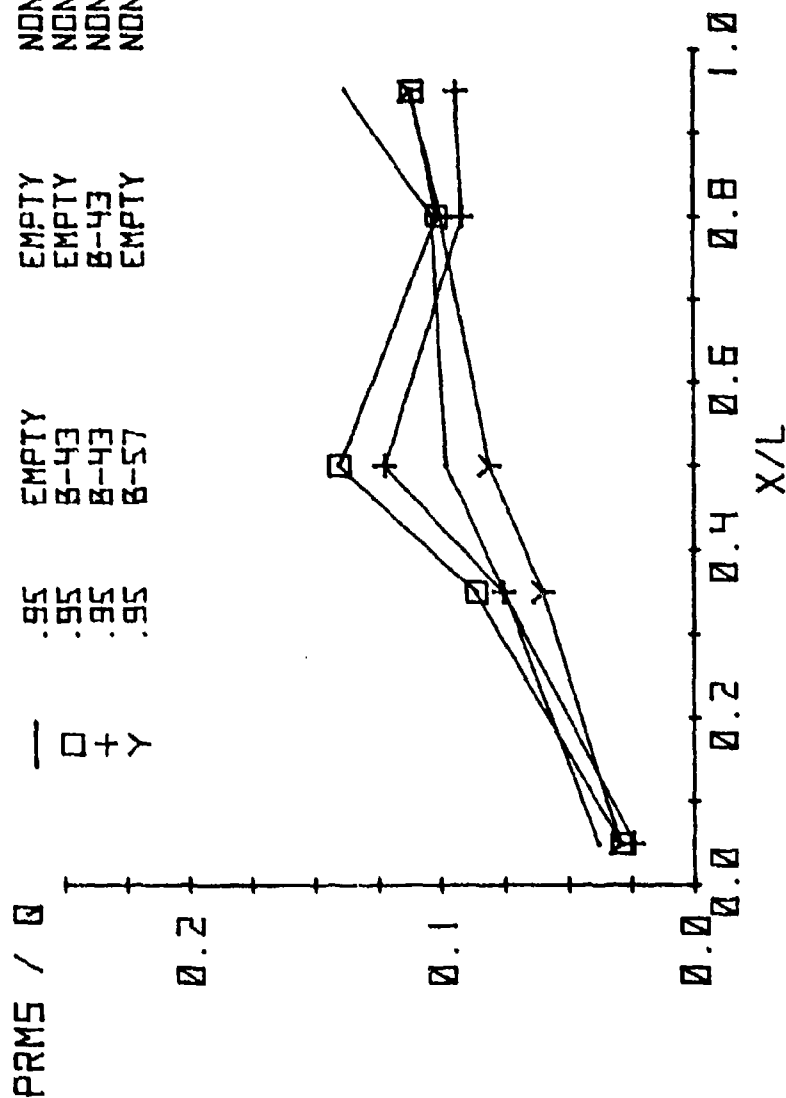


Figure 23b. Comparison of Bay Loadings at Mach .95, Left Wall Distribution

Similar results for Mach 1.3 are presented in Figures 24a. and 24b.

At the X/L .95 station on the left wall, the levels observed for the empty bay and the single B-57 weapon are essentially the same. This location is well aft of the base of the store, which is possibly the reason for this result.

SYM MACH LEFT BAY RIGHT BAY SUPPR.

PRMS / Q	SYM	MACH	LEFT BAY	RIGHT BAY	SUPPR.
0.2	—	1.3	EMPTY	EMPTY	NONE
	□	1.3	B-43	EMPTY	NONE
	+	1.3	B-43	B-43	NONE
	Y	1.3	B-57	EMPTY	NONE

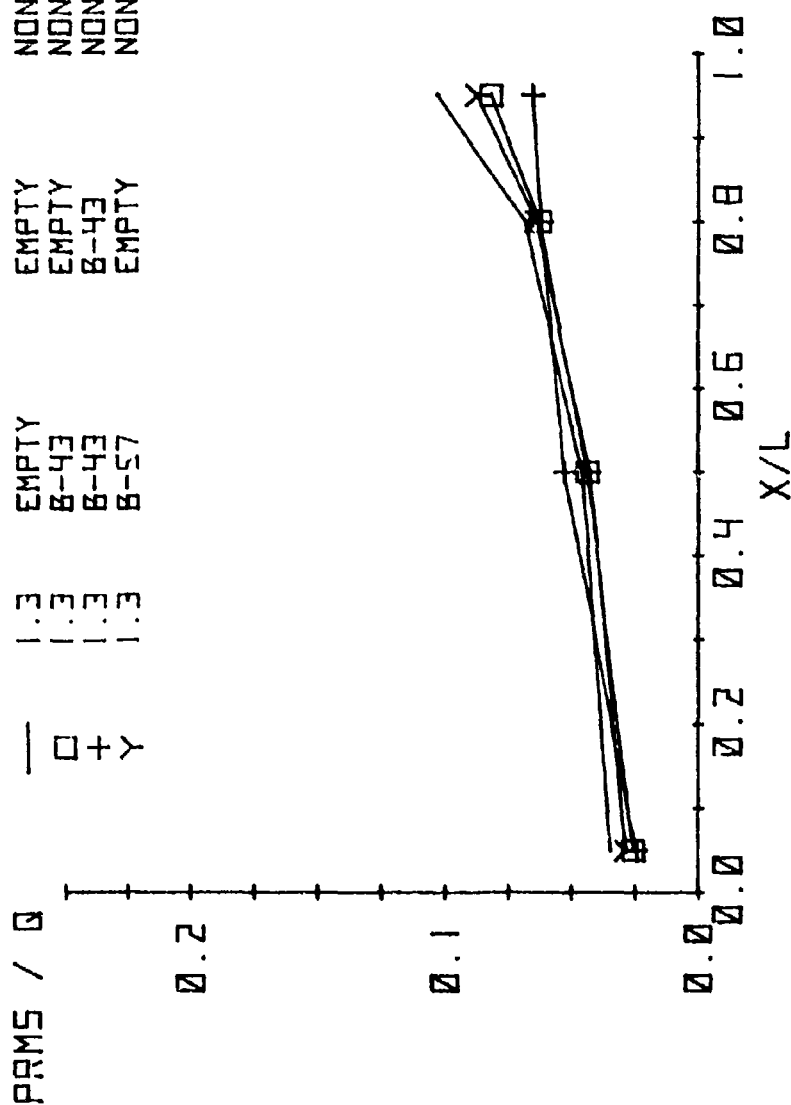


Figure 24a. Comparison of Bay Loadings at Mach 1.3, Centerline Distribution

SYM MACH LEFT BAY RIGHT BAY SUPPR.

NDNE  
NDNE  
NDNE  
NDNE

EMPTY  
EMPTY  
B-43  
EMPTY

EMPTY  
B-43  
B-43  
B-57

1.3  
1.3  
1.3  
1.3

—  
□  
+  
Y

PRMS / 0

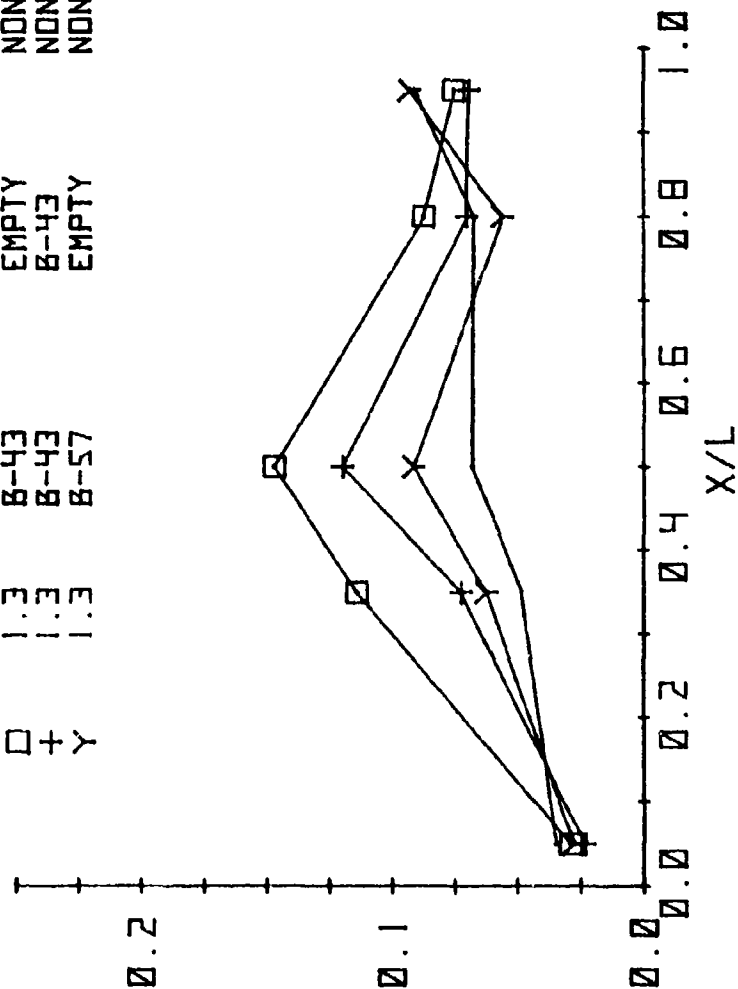


Figure 24b. Comparison of Bay Loadings at Mach 1.3, Left Wall Distribution



#### 4.2 Suppressor Evaluation in PWT-16T

Based upon the above results, the single B-43 left bay installation was determined to be the most severe loading configuration and was used for the following evaluation of candidate suppression devices. The left wall mid-bay position was measured to have the highest levels of acoustic energy for this loading; therefore, this location was selected for presenting a comparison of the various suppression devices.

Figure 25 compares the four suppression devices over the Mach range to the baseline configuration. Suppressor A (saw tooth spoiler) is clearly the most effective device across the complete Mach range investigated. Suppressor D (rear ramp deflector) is the second most effective device; however, this device is more effective at the transonic Mach numbers than at the supersonic conditions. Suppressor C (rear facing step) generally has an adverse effect while Suppressor B (vortex generators) has only a slight beneficial effect transonically and no effect supersonically.

Figure 26 compares each of the three forward mounted suppression devices installed with the rear mounted suppression device. In all instances, the combination is superior to the single device; however, the combination of the saw tooth and the rear ramp deflector is observed to be significantly more effective than the other two combinations. The combination of B and D (vortex generators and rear ramp deflector) is the second most effective combination.

The two most promising suppression configurations, Suppressor A and the combination of A and D, are now compared to the baseline in more detail. Both centerline and left sidewall distributions are compared. Figure 27 compares data at Mach .85 and Figure 28 presents data at Mach 1.3. Except

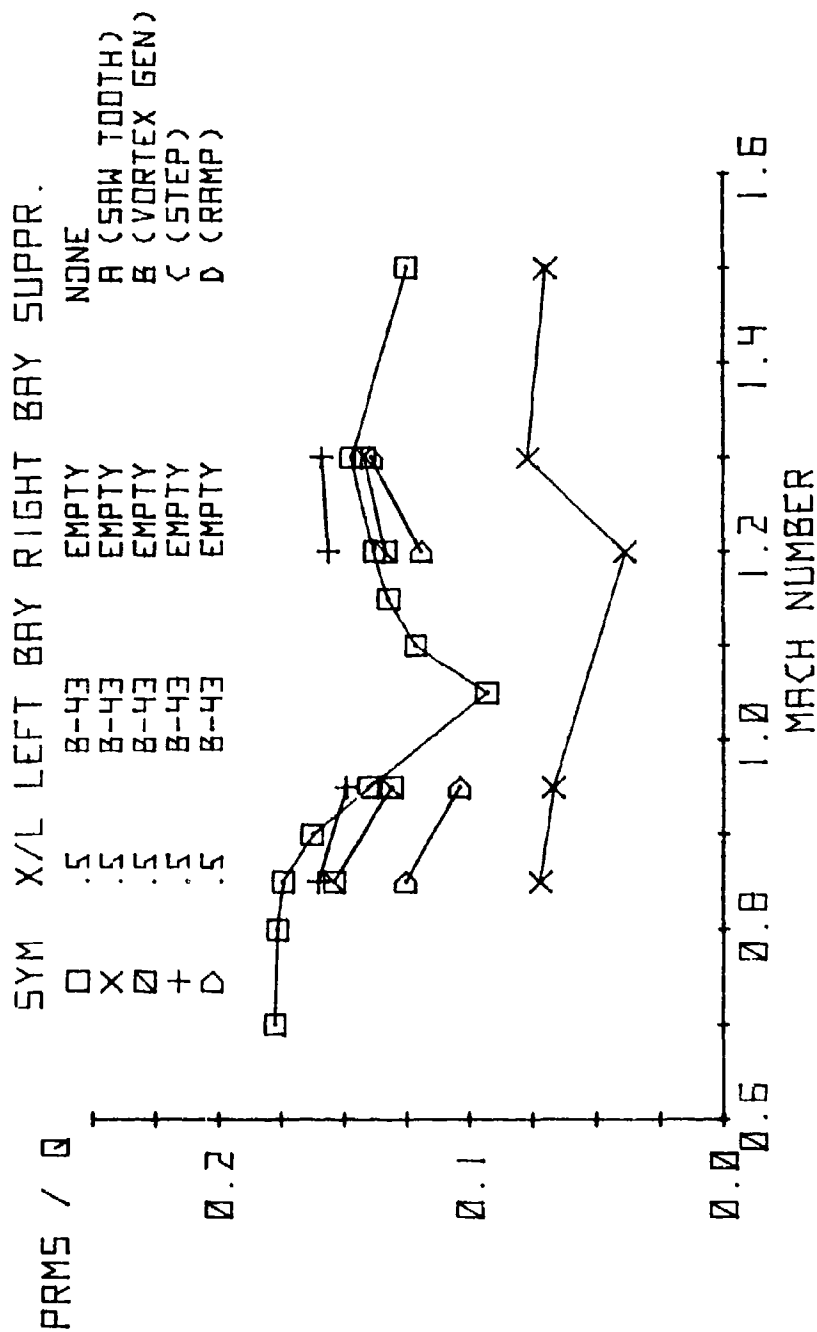


Figure 25. Comparison of Suppressor Effectiveness  
Left Wall Mid-Bay Location

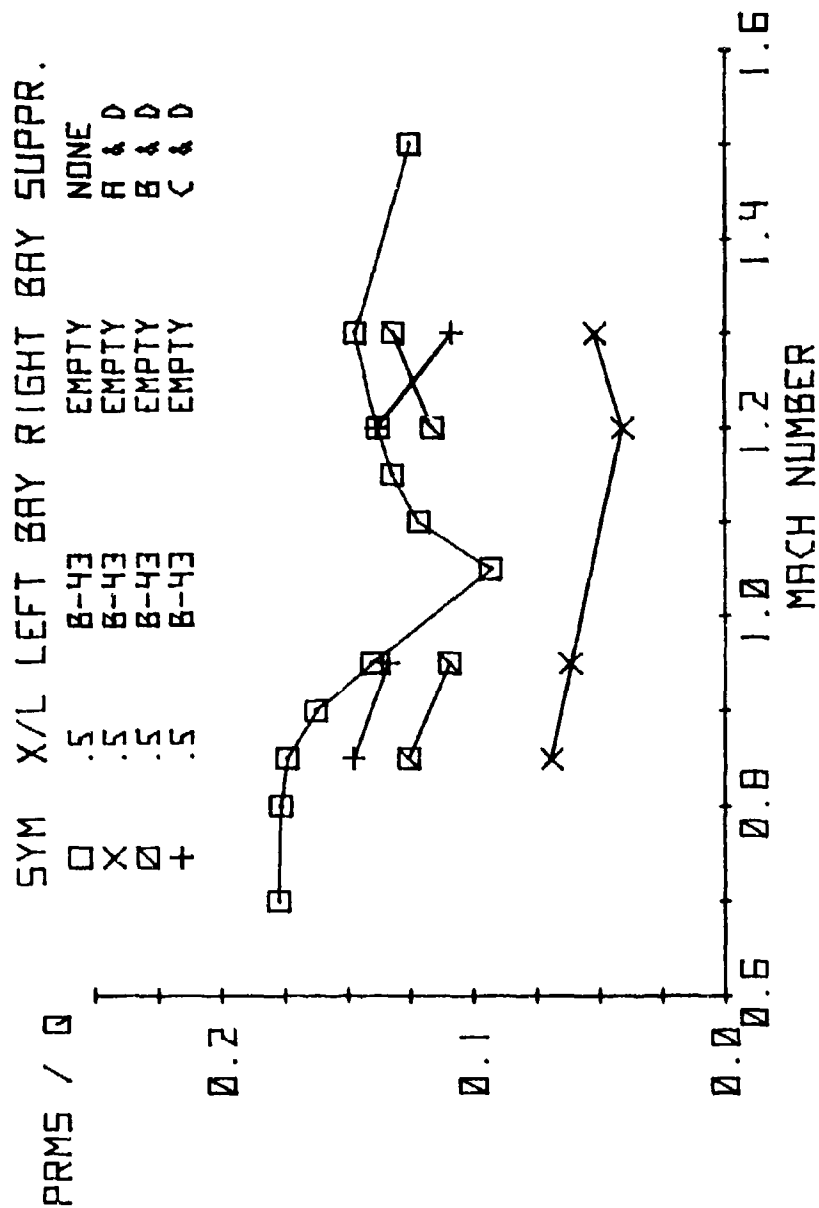


Figure 26. Comparison of Forward Mounted Suppressor  
Devices Combines with Rear Ramp Deflector,  
Left Wall Mid-Bay Location

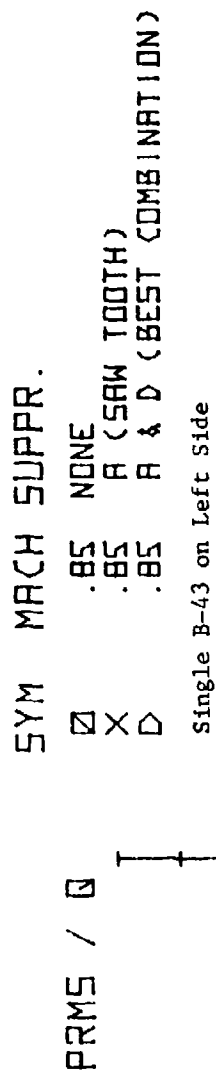


Figure 27a. Detailed Comparison of Suppressor Characteristics of Most Effective Devices at Mach .85, Centerline Distribution

SYM MACH SUPPR.  
 □ .85 NONE  
 X .85 A (SAW TOOTH)  
 ◇ .85 A & D (BEST COMBINATION)

Single B-43 on Left Side

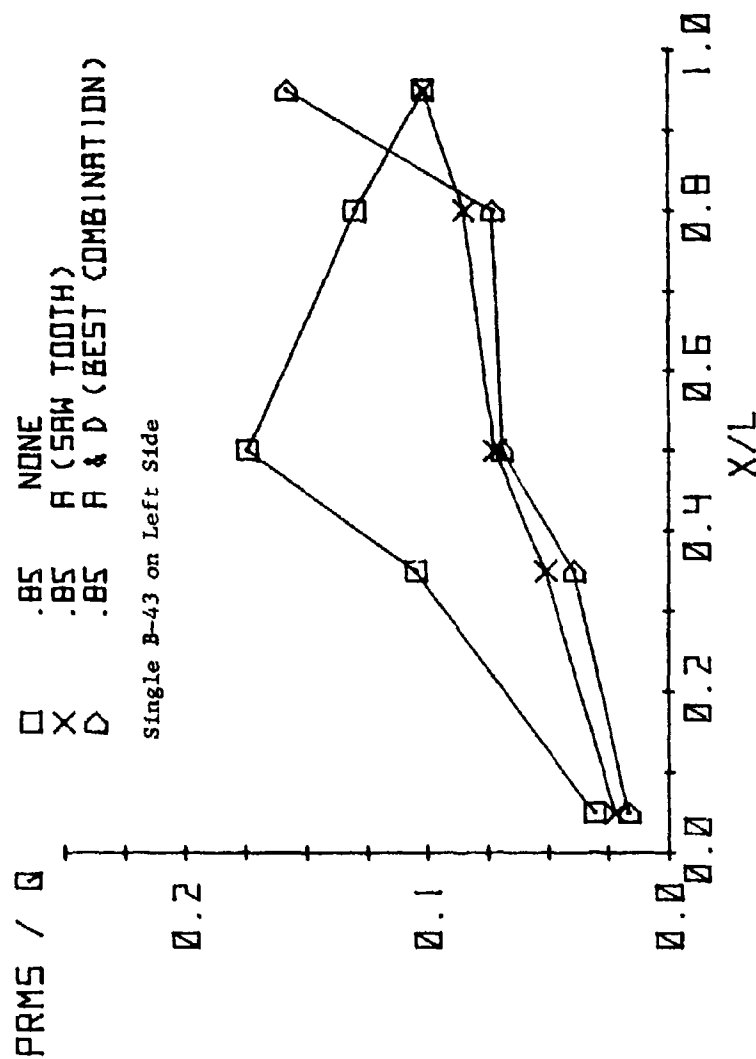


Figure 27b. Left Wall Distribution

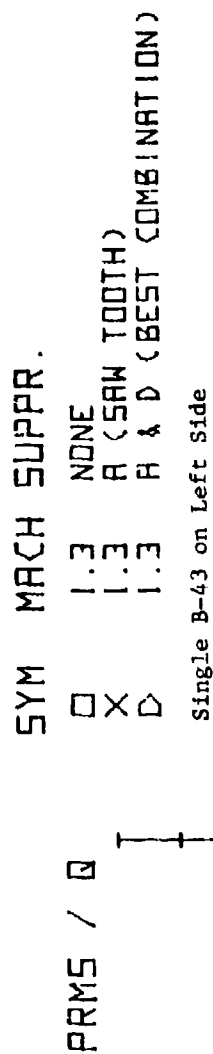


Figure 28a. Detailed Comparison of Suppressor Characteristics of Most Effective Devices at Mach 1.3, Centerline Distribution

SYM    MACH SUPPR.  
 □    1.3    NONE  
 X    1.3    A (SAW TOOTH)  
 ◇    1.3    A & D (BEST COMBINATION)

Single B-43 on Left Side

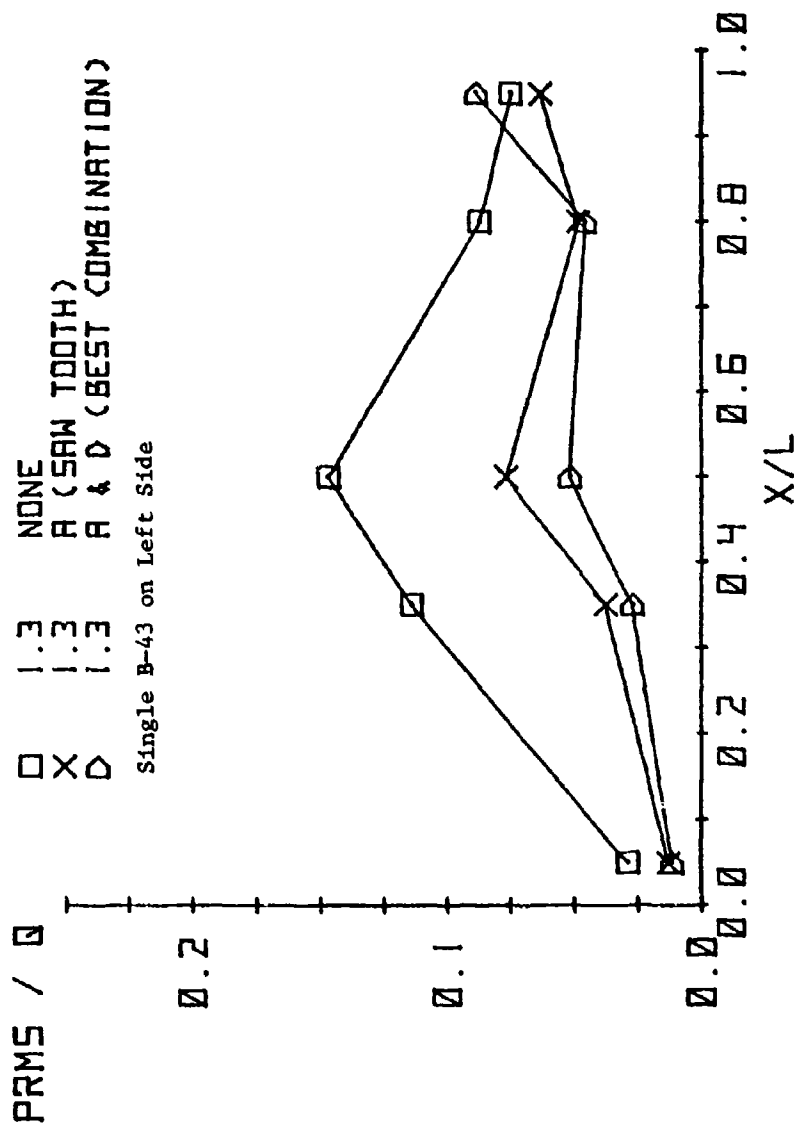


Figure 28b. Left Wall Distribution

for the X/L .95 station on the left side wall, the combination of A and D is superior to Suppressor A alone. The transducer at the X/L .95 location on the left wall is partially covered by the rear ramp, forming a corner. This may be responsible for the increase in Prms/Q at this location; however, this location is sufficiently aft of the store base as to minimize the turbulence effects on the store. Very similar results were observed at each Mach number.

Figure 29 compares the bay environment at Mach .95 with and without Suppressor A and a single B-57 weapon installed on the left side of the bay. Figure 29a presents data along the centerline which shows a small reduction in turbulence level in the aft region of the bay. Figure 29b presents data from the left wall adjacent to the store. Aft of the store at the X/L .95 station, the saw tooth spoiler increases the Prms/Q level. Figure 30 presents directly comparable data from the left wall at Mach 1.3. At this condition, the spoiler clearly improves the bay environment.

Based upon the above results, the saw tooth spoiler was selected as the prime suppression device for testing during the drop test phase. Results of this phase are presented in paragraph 4.3.



PRMS / 0	SYM	MACH	LEFT BAY	RIGHT BAY	SUPPR.
Y	.95	B-57	EMPTY	EMPTY	NONE
X	.95	B-57	EMPTY	EMPTY	A (SAW TOOTH)

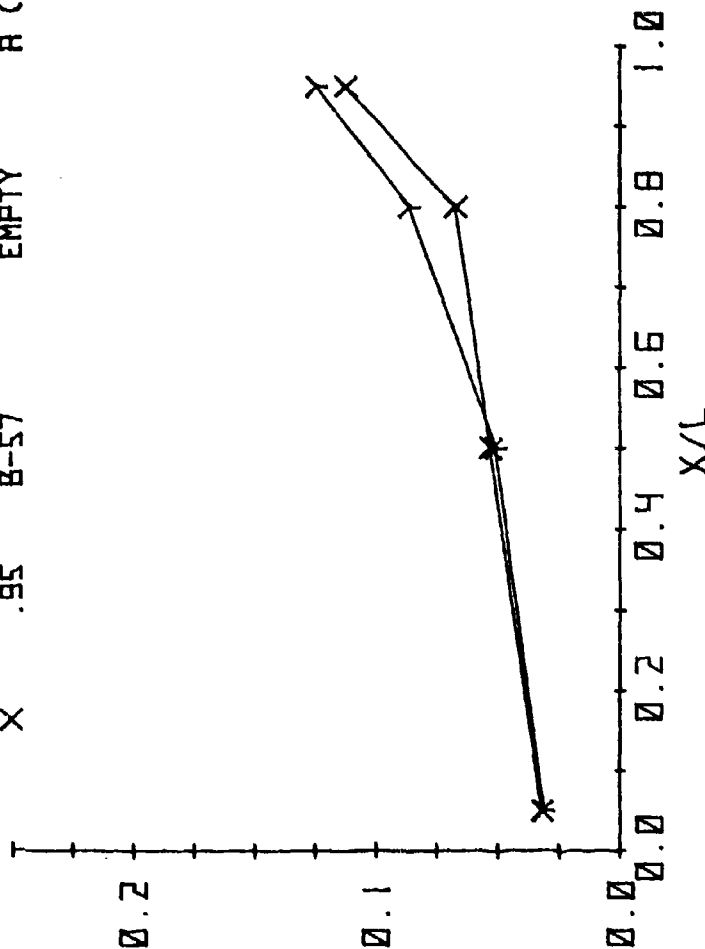


Figure 29a. Bay Environment with and without Suppressor A and a Single B-57 Weapon in the Bay, Centerline Distribution.

SYM		MACH		LEFT BAY		RIGHT BAY		SUPPR.	
Y	X	.95	B-57	EMPTY	EMPTY	NONE	A (SAW TOOTH)		
		.95	B-57						
		.95	B-57						

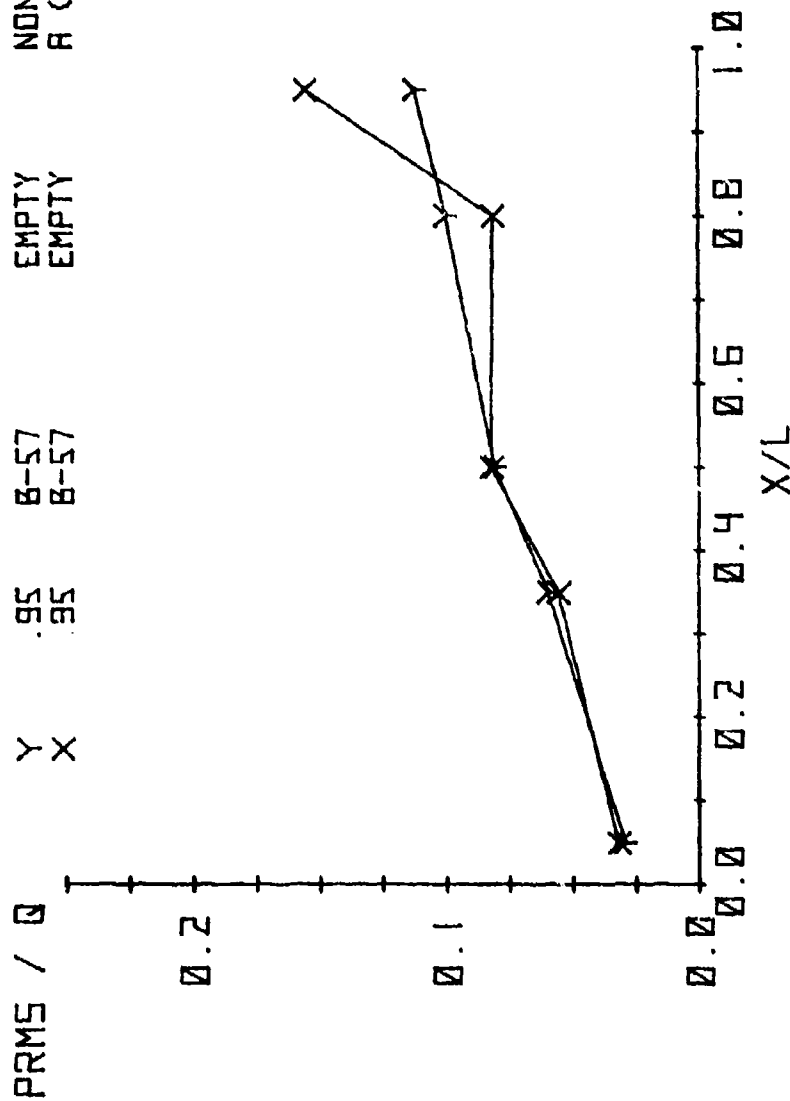


Figure 29b. Left Wall Distribution

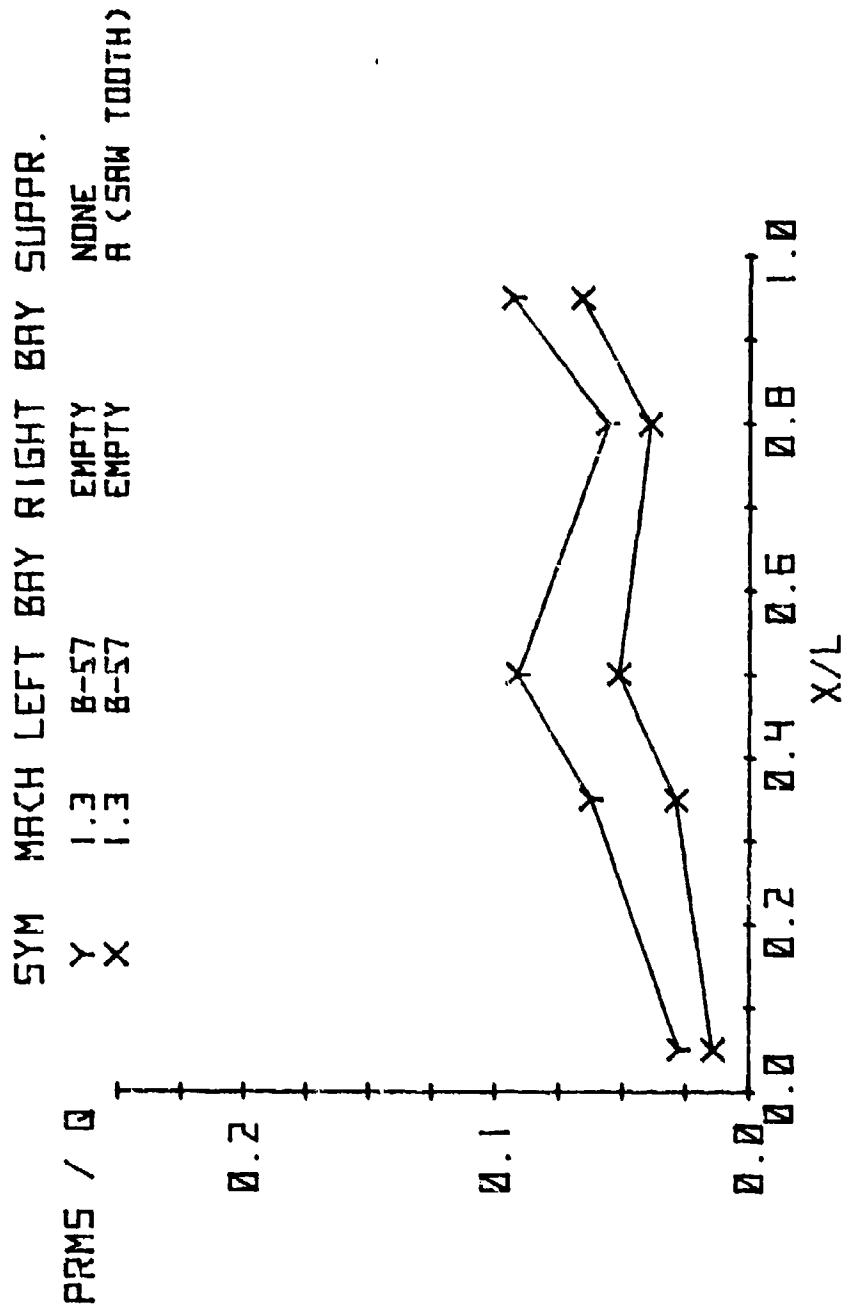


Figure 30. Bay Environment at Mach 1.3 with and without Suppressor A and a Single B-57 Weapon, Left Wall Distribution

#### 4.3 Drop Test Results

Before serious consideration could be given to actual application of a suppression device on an F-111 aircraft, the effect of the device on weapons separation had to be determined. Three drop conditions were selected based upon the presently approved flight limits and the desired expanded envelope. (See paragraphs 3.1.2 and 3.2, and Tables 5 and 6 for the model ejection system description, test conditions, and store ejection parameters.)

Figure 31 compares the critical pitch attitude of the B-43 store with and without the saw tooth spoiler. The maximum nose up pitch attitude is a measure of the risk of the store striking the launch aircraft. Transonically the B-43 generates a lift equal to the store weight at an angle of attack of approximately 15 degrees; therefore, for safe B-43 store separations, the store maximum pitch attitude must remain below this angle. In this figure, for the Mach .95 condition, the spoiler produced a favorable initial pitch down effect and delayed the onset of pitch up, although both trajectories are satisfactory. Figure 32 presents more details of the separation with and without Suppressor A. The store displacements from the carriage position are presented along with the pitch and yaw angles of the store, all as a function of time. All values have been converted to full scale. In Figure 32b, the spoiler suppression device does induce a small yaw oscillation.

SYM MACH LEFT BAY RIGHT BAY SUPPR.  
 □ .95 B-43 EMPTY NONE  
 X .95 B-43 EMPTY A (SAW TOOTH)  
 ALTITUDE - 1000 FT

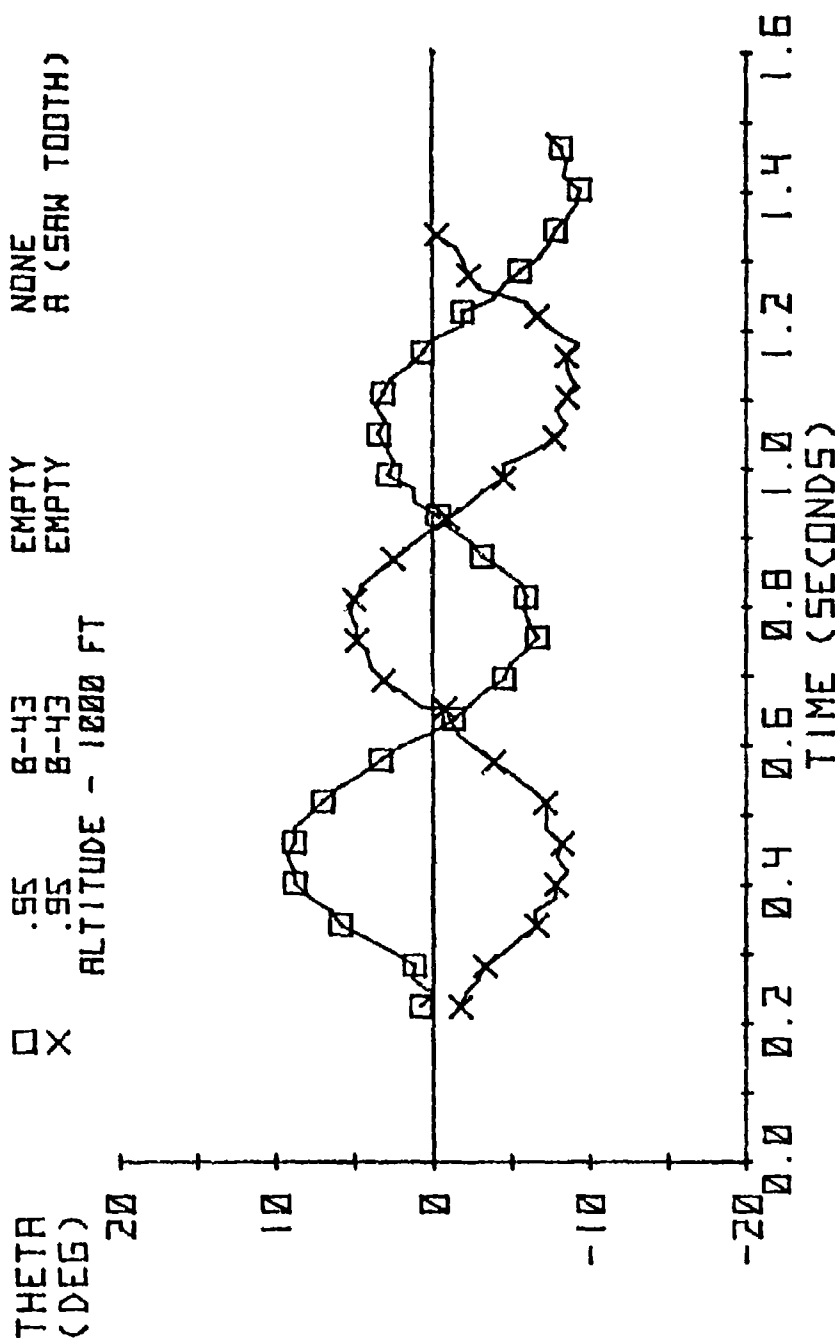


Figure 31. Pitch Attitude of B-43 Store During Separation with  
 and without Suppressor at Mach .95.

SYM	TRAJ	M <sub>0</sub>	CONF	ALFA	H	STORE
O	7	0.95	3	2	1K	B-43

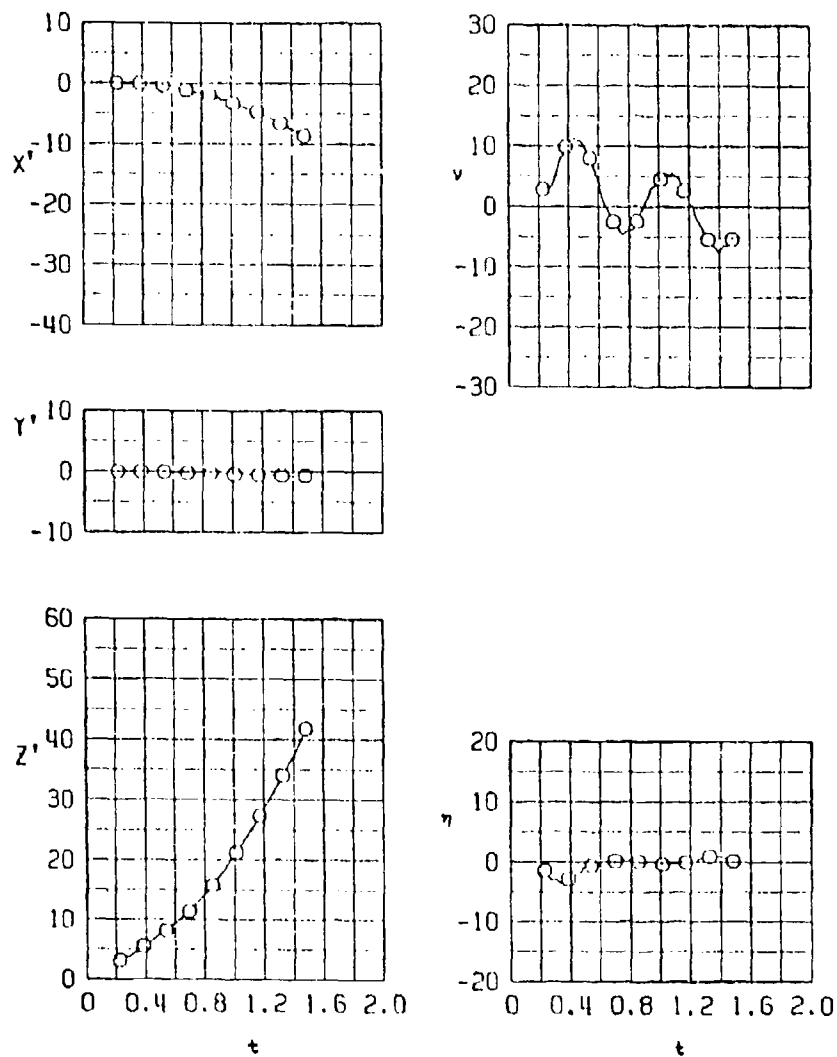


Figure 32a. Baseline F-111/B-43 Weapon Separation Trajectory at Mach .95 and 1000 ft. Altitude

SYM	TRAJ	M <sub>0</sub>	CONF	ALFA	H	STORE
O	12	0.95	20	2	1K	B-43

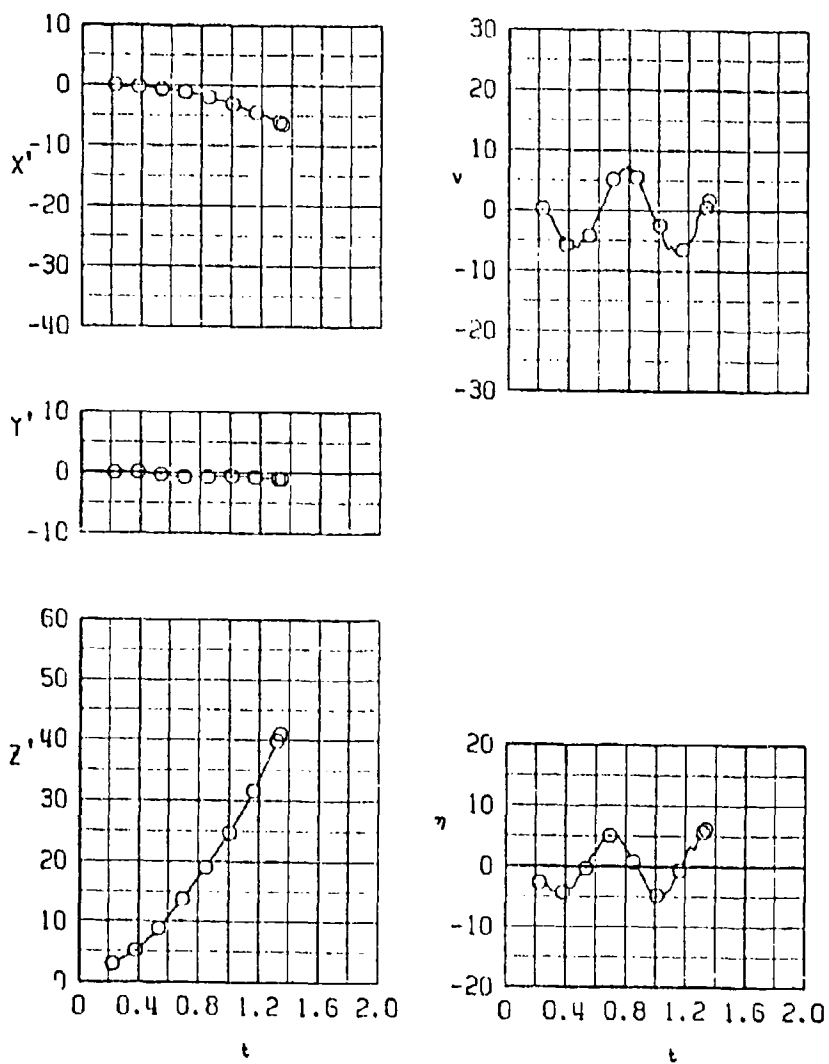


Figure 32b. F-111/B-43 Separation Characteristics with Suppressor A, Mach .95 and 1000 ft Altitude.

Figures 33 and 34 present detailed trajectory data with and without the suppressor at Mach 1.2 and 1.3 conditions. Without a suppression device, the pitch oscillations are significantly greater and exceed the critical 15 degree nose up attitude discussed above. Mach 1.3 is the worst case with a peak pitch angle of approximately 21 degrees. With the saw tooth spoiler installed, these trajectories are significantly improved with the maximum pitch attitude reduced to approximately 12 degrees. In Figure 34a, the store after rotating through the maximum pitch attitude can be seen to float briefly approximately seven feet below the release position at Mach 1.3.

All of the above trajectories were initiated with the model F-111 at a body angle of attack of 2 degrees. Figure 35 presents data with the model at a 5 degree (6 degree wing) angle of attack. No significant changes are noted due to the higher angle of attack.



SYM	TRAJ	M <sub>L</sub>	CONF	ALFA	H	STORE
0	8	1.20	3	2	1K	B-43

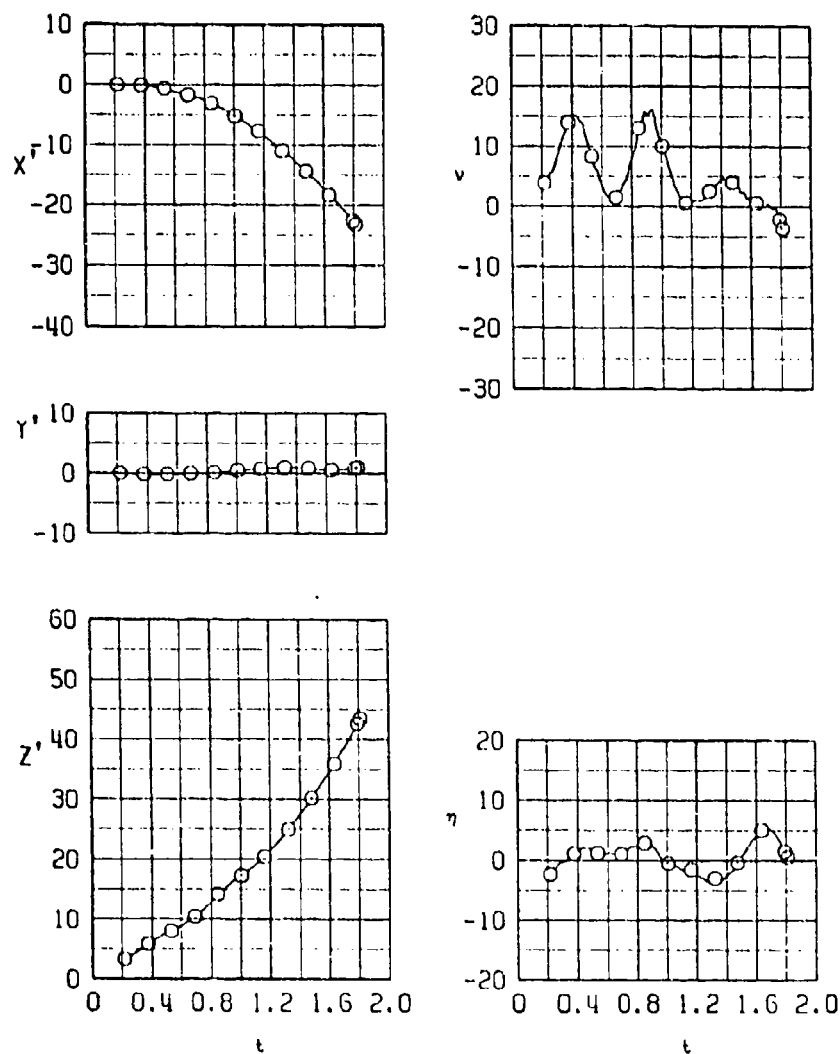


Figure 33a. Baseline B-43 Separation Trajectory at Mach 1.2 and 1000 ft Altitude

SYM	TRAJ	M <sub>0</sub>	CONF	ALFA	H	STORE
O	11	1.20	20	2	1K	B-43

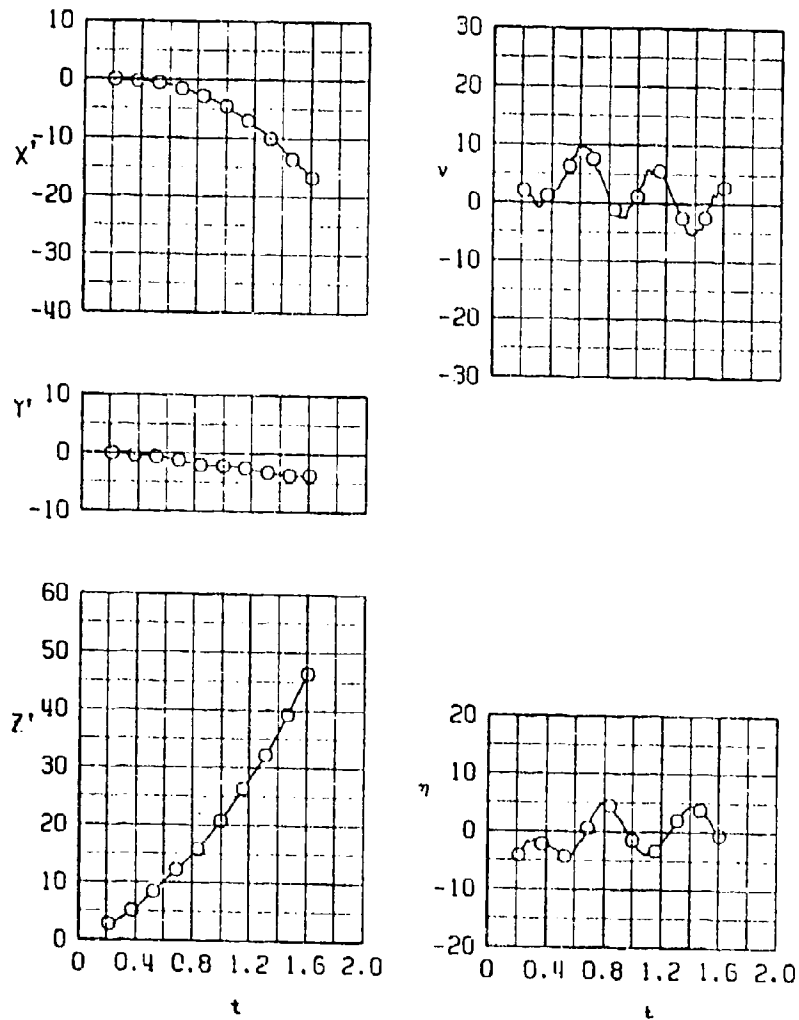


Figure 33b. Trajectory with Suppressor A

SYM	TRAJ	M <sub>0</sub>	CONF	ALFA	H	STORE
○	9	1.30	3	2	10K	B-43

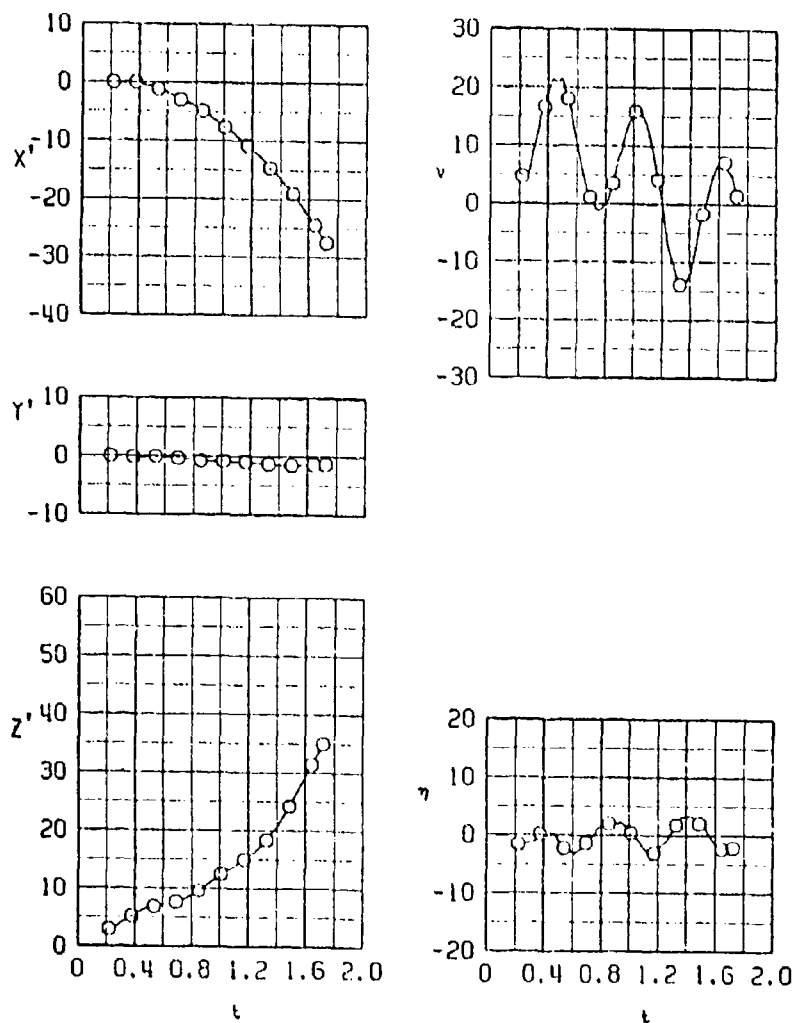


Figure 34a. Baseline B-43 Separation Trajectory at Mach 1.3 and 10,000 ft Altitude

STM	WIND	M <sub>0</sub>	CONF	ALFA	H	STONE
0	10	1.30	20	2	10K	B-43

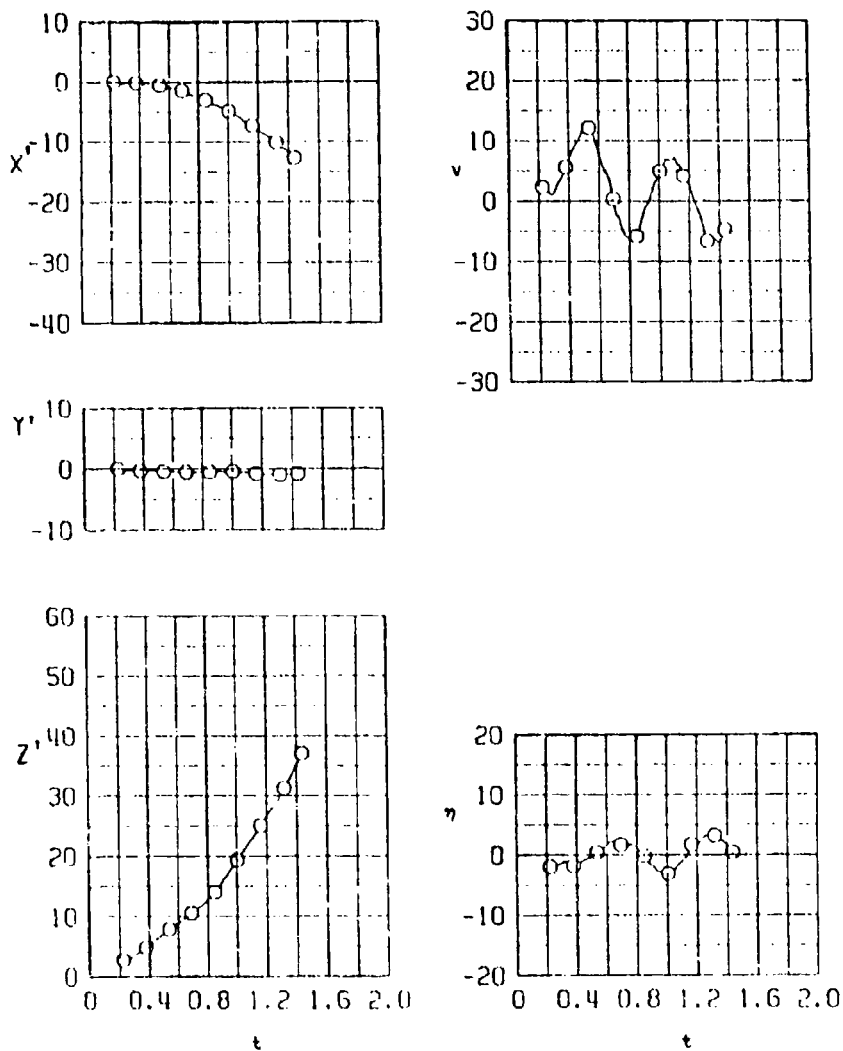


Figure 34b. Trajectory with Suppressor A

SYN	TIME	M <sub>0</sub>	CONF	ALFA	H	STONE
0	15	1.30	20	5	10K	B-43

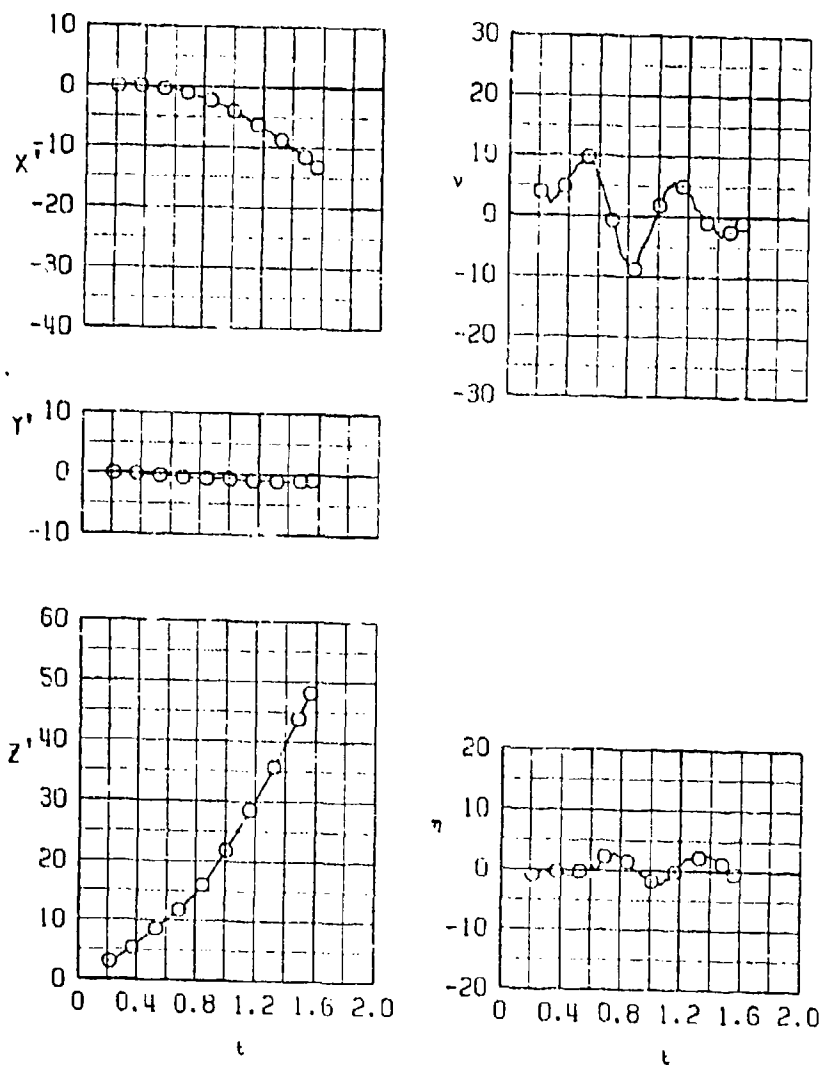


Figure 35a. Baseline B-43 Separation Trajectory with Angle of Attack of 5 Degrees

SYM	TRAJ	M	CONF	ALFA	H	STORE
0	13	1.30	21	2	10K	B-43

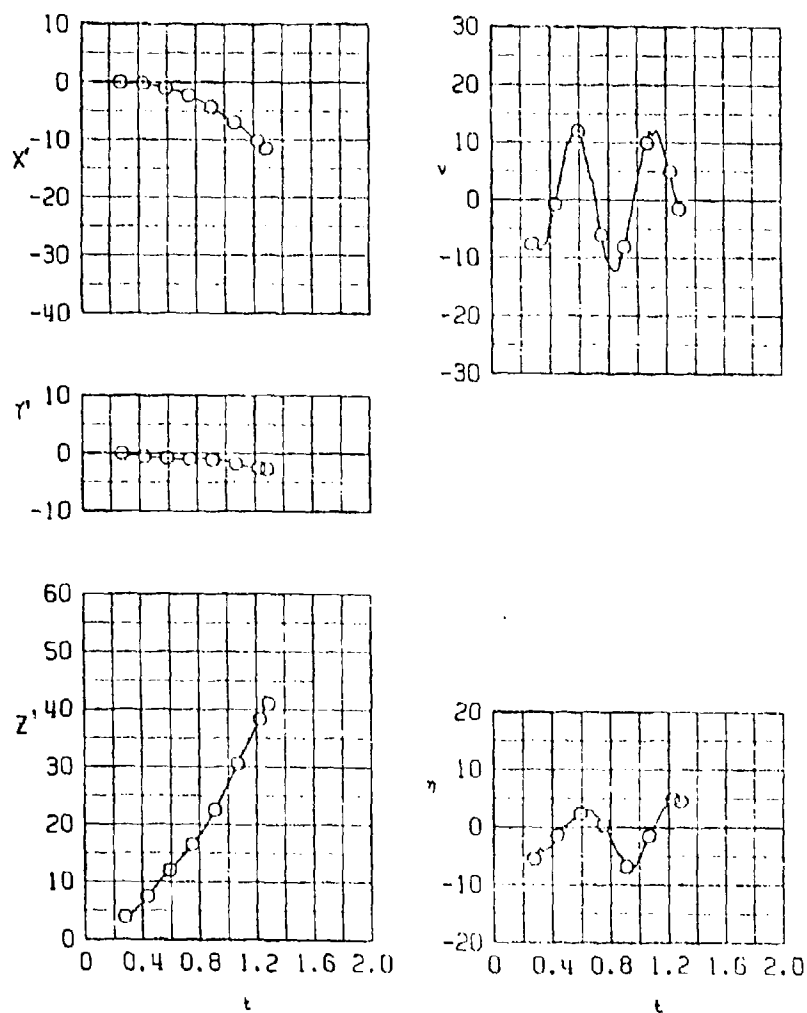


Figure 35b. Trajectory at 5 Degrees Alpha with Suppressor A

Figure 36 presents the trajectory of the B-43 store with both the forward mounted saw tooth and the rear mounted ramp deflector suppressors installed. This figure can be compared to the baseline trajectory at Mach 1.3 (Fig. 34a) and the trajectory with only the saw tooth suppressor (Fig. 34b). These comparisons show a significant improvement over the baseline trajectory in terms of the maximum pitch attitude of the store but no significant improvement over the saw tooth (Suppressor A) alone configuration.

Separation results with two B-43 stores loaded in the bay were very similar to the above single B-43 loadings. The trajectories were slightly improved relative to the comparable single weapon loadings. It should be noted that only the left weapon station was equipped with an ejector system.

Two additional aircraft configurations were investigated with and without a suppression device. Both included installations of a gun on the right hand side of the bay. The second configuration had an ECM pod added to the external surface of the gun pod. Figure 37 shows the installation of the gun, ECM pod, and suppression device along with a B-43 drop store. The saw tooth spoiler was modified as shown to accommodate the gun installation. Figure 38 presents data for the gun pod configuration at Mach 1.3 with and without the spoiler. Figure 39 presents comparable data with the ECM pod added. The ECM pod produces a lateral displacement of the store for both suppressor on or off. The suppressor has a beneficial effect on both configurations by reducing the maximum pitch attitude of the B-43 store to levels below the critical 15 degree range.

SYM	TRAJ	M	CONF	ALFA	H	STORE
O	13	1.30	21	2	10K	B-43

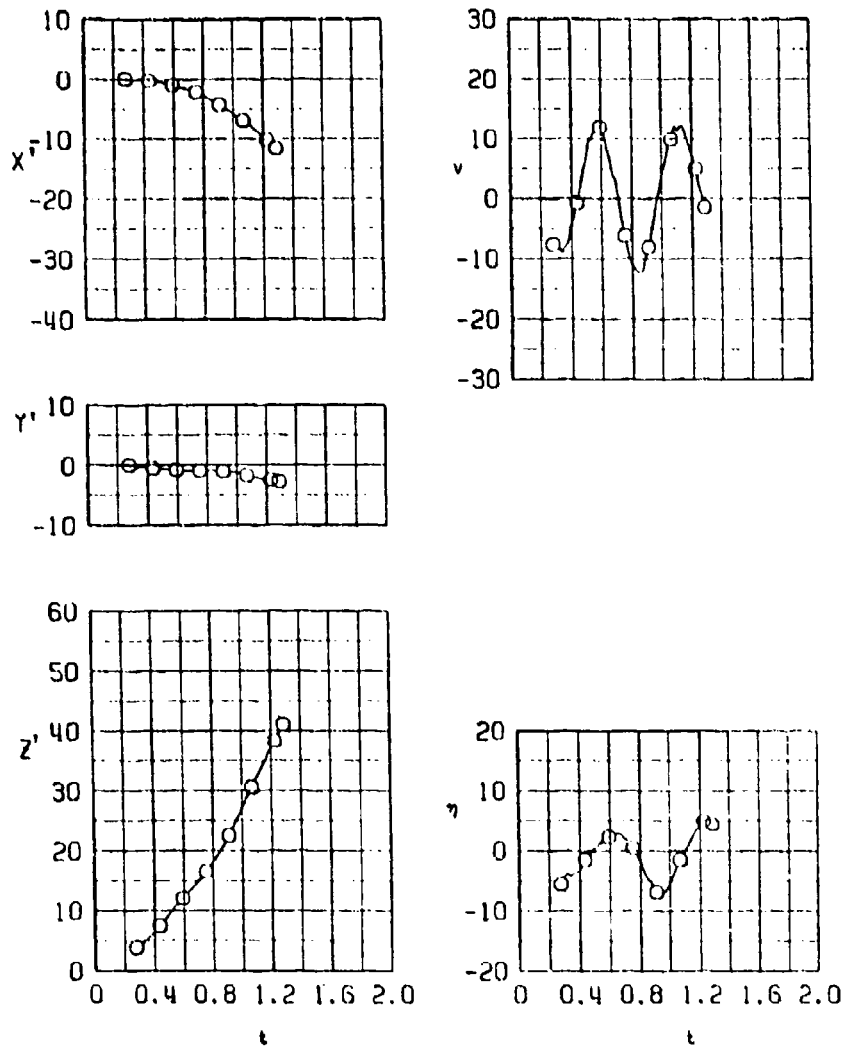


Figure 36. Separation Trajectory with Best Combination of Suppressors, A and D





Figure 37. Model with Internal Bay Mounted Gun, ECM Pod, and Modified Suppressor A

SYM	TRAJ	M <sub>0</sub>	CONF	ALFA	H	STONE
○	22	1.30	16	2	10K	B-43

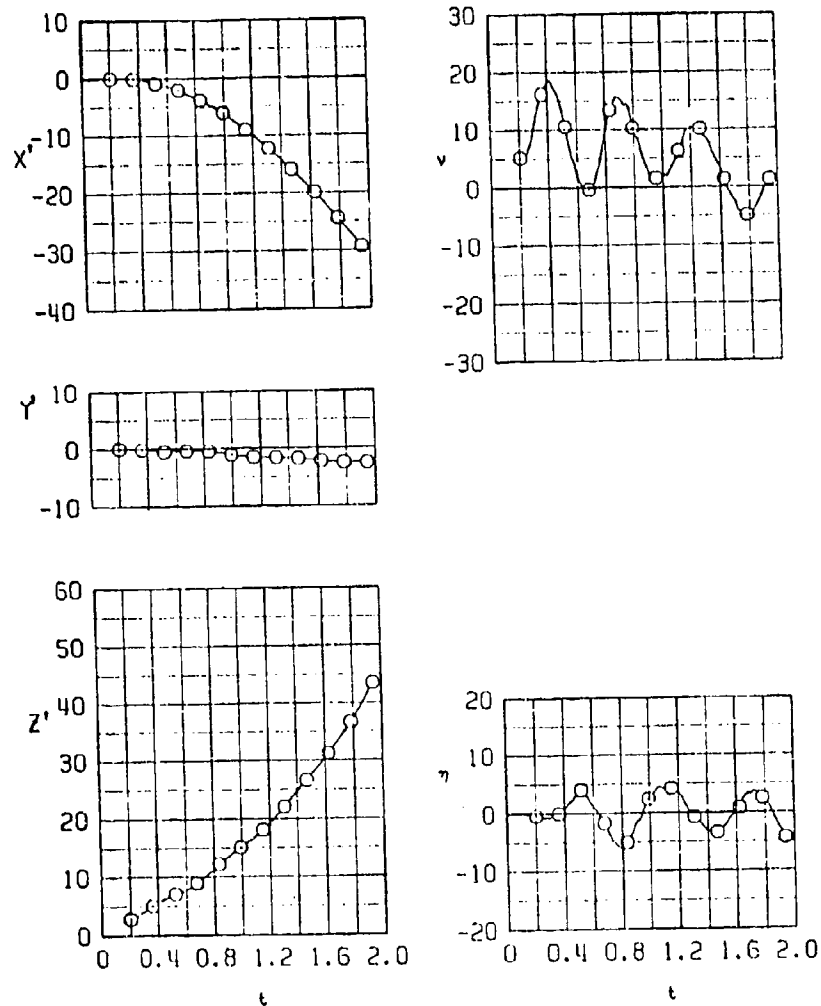


Figure 38a. B-43 Separation Trajectory with Bay Mounted Gun Pod

SYM	TRAJ	M	CONF	ALFA	H	STORE
○	23	1.30	17	2	10K	8-43

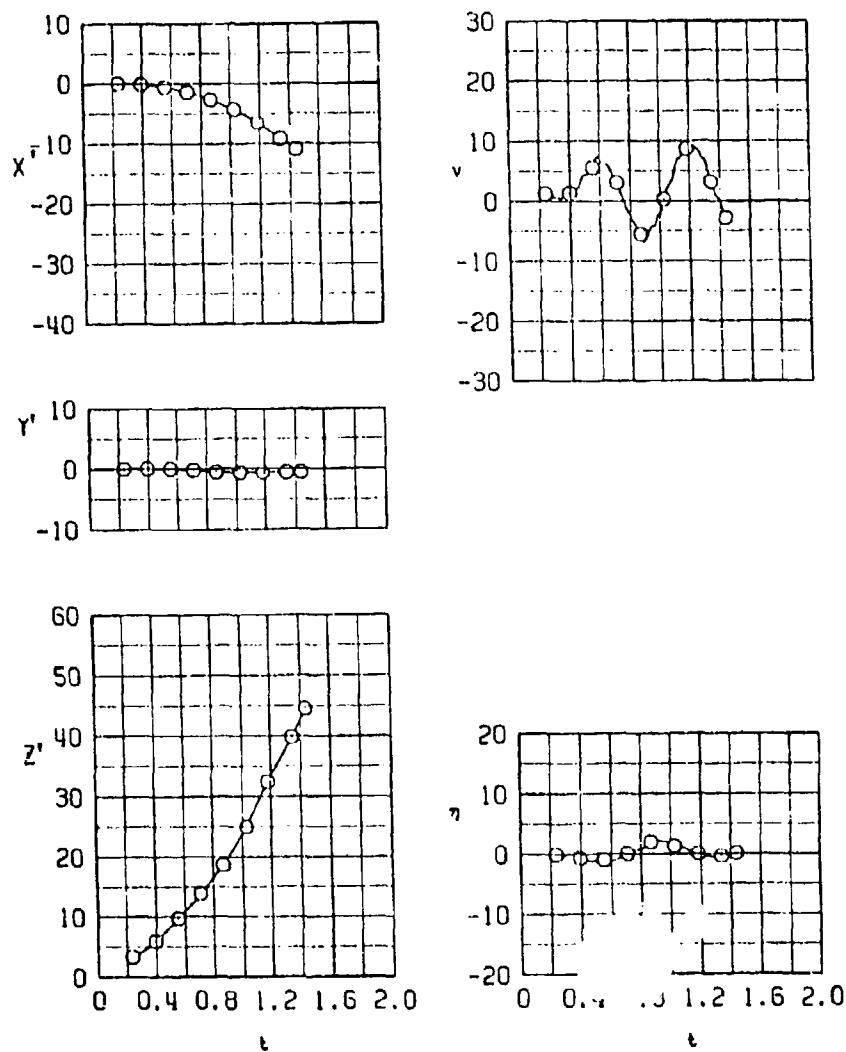


Figure 38b. Trajectory with Gun Pod and Modified Suppressor A

SYM	TRAJ	M <sub>0</sub>	CON	ALT	H	STORE
O	24	1.30	18	2	10K	B-43

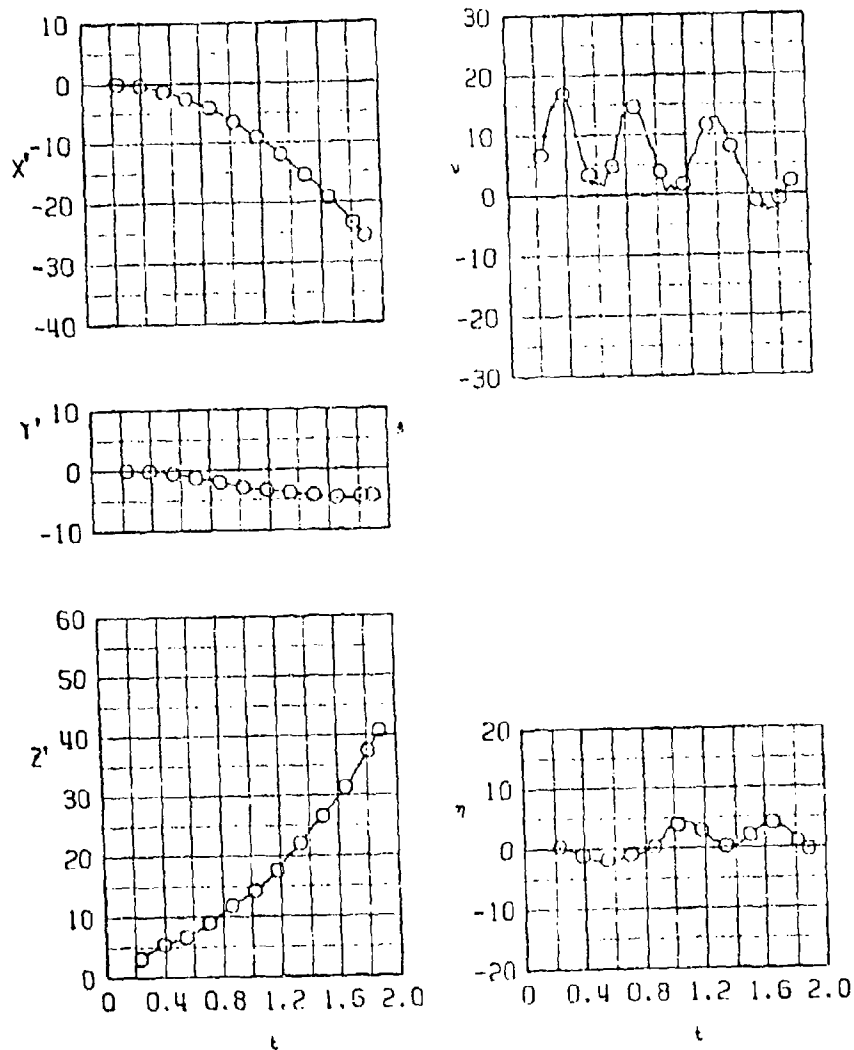


Figure 39a. B-43 Separation Trajectory with Bay Mounted Gun Pod Plus ECM Pod.

SM	TRIJ	M <sub>0</sub>	CONF	ALFA	H	STORE
0	25	1.30	19	2	10K	8-43

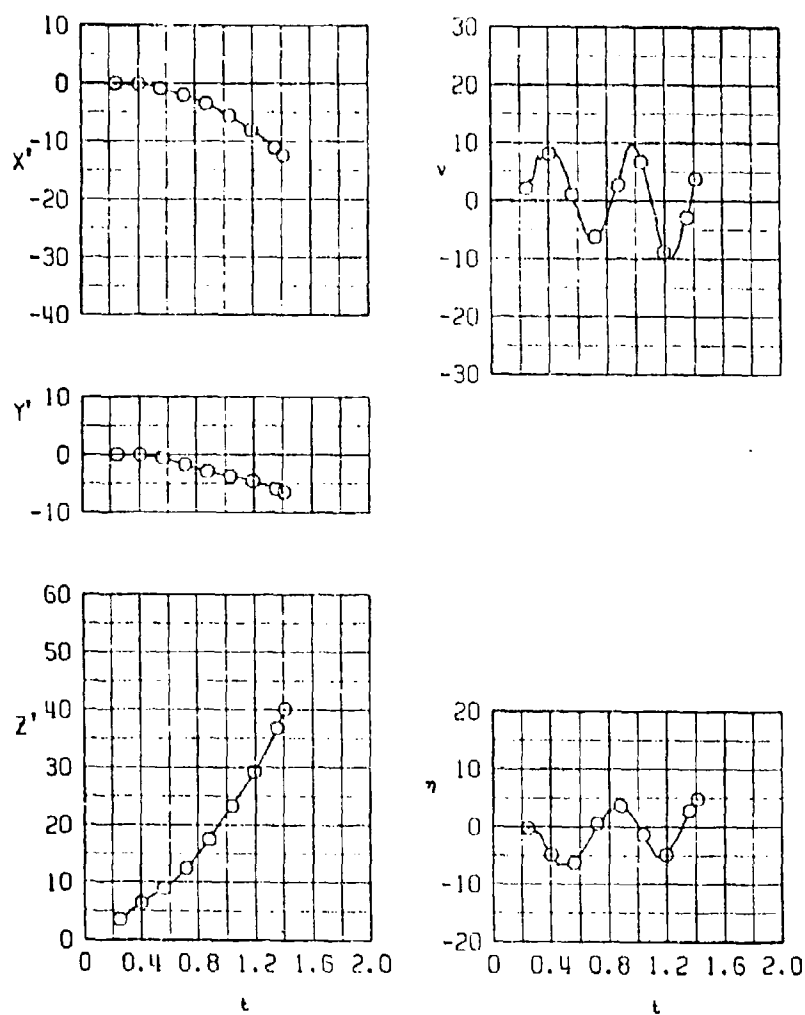


Figure 39b. Trajectory with Gun Plus ECM Pod and Modified Suppressor A

Figures 40 and 41 present separation data for the single B-57 bay loading. Mach .95 and 1.2 data are presented. Addition of the saw tooth suppression device has little or no effect at Mach .95 on the maximum pitch attitude of the store. The vertical separation velocity is increased reducing the risk of striking the launch aircraft. At the higher Mach number, the tendency of the B-57 to float in the region from six to eight feet below the aircraft is completely eliminated by the suppressor.

SYM	TRAJ	M	CONF	ALTA	H	STORE
O	29	0.95	13	2	1K	B-57

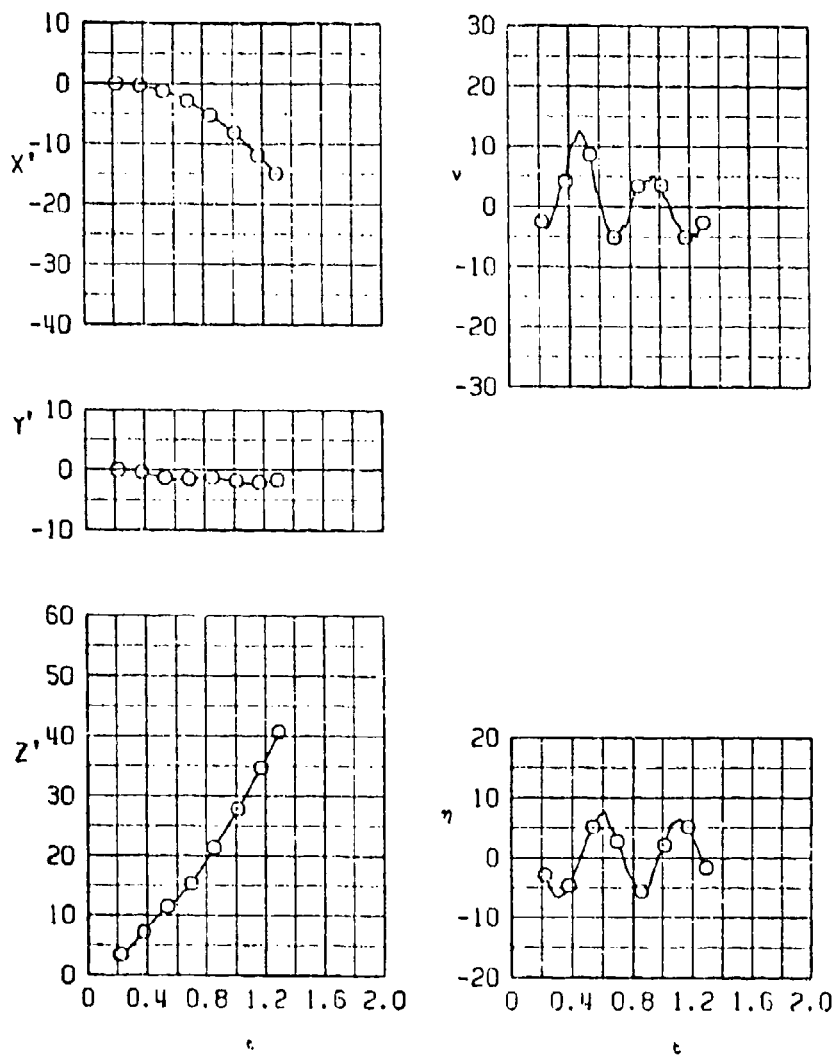


Figure 40a. B-57 Separation Trajectory at Mach .95

SYM	TRAJ	M <sub>0</sub>	CONF	ALFA	H	STORE
0	21	0.95	14	2	1K	B-57

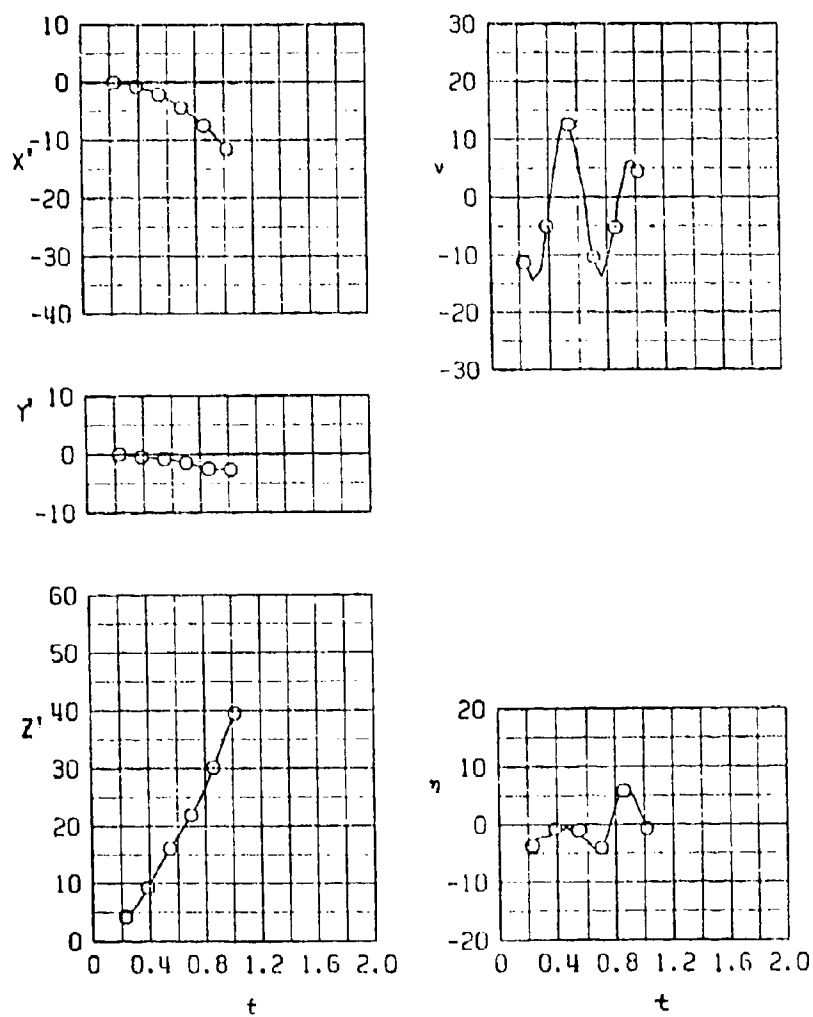


Figure 40b. B-57 Trajectory with Suppressor A at Mach .95



SYM	TRAJ	M	CONF	ALFA	H	STORE
O	19	1.20	13	2	1K	B-57

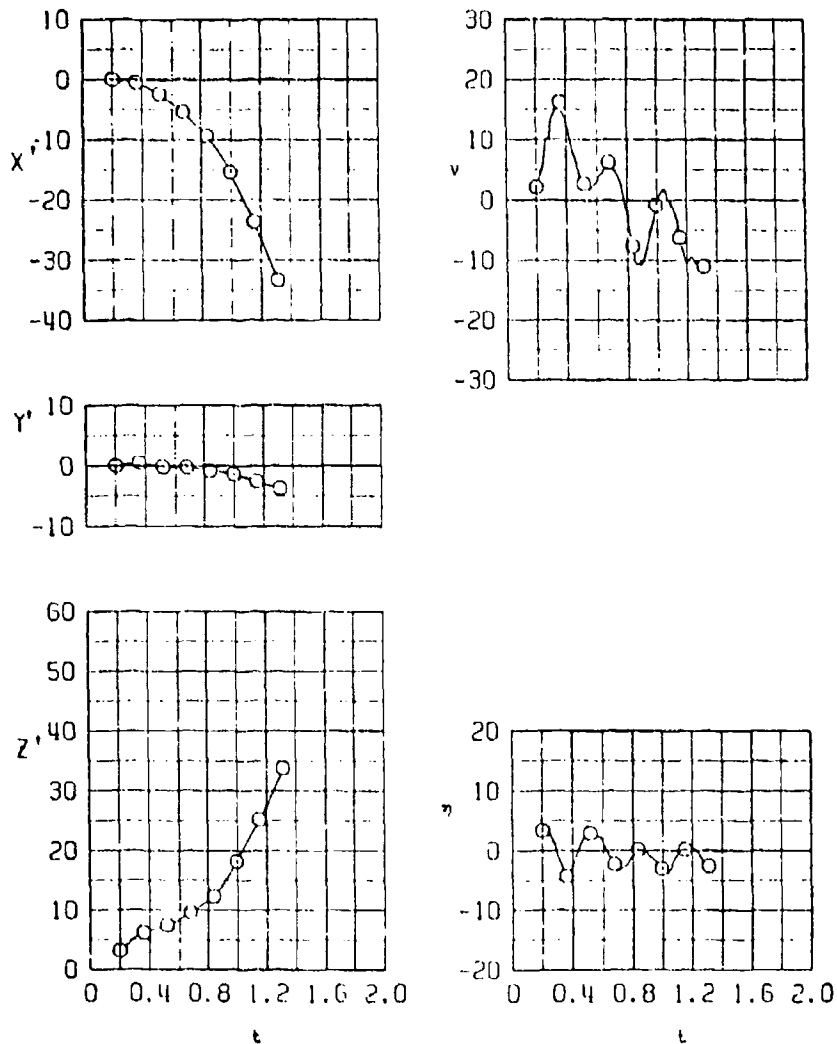


Figure 41a. B-57 Separation Trajectory at Mach 1.2

SYM	TRAJ	M <sub>0</sub>	CONF	ALFA	H	STORE
O	20	1.20	14	2	1K	B-57

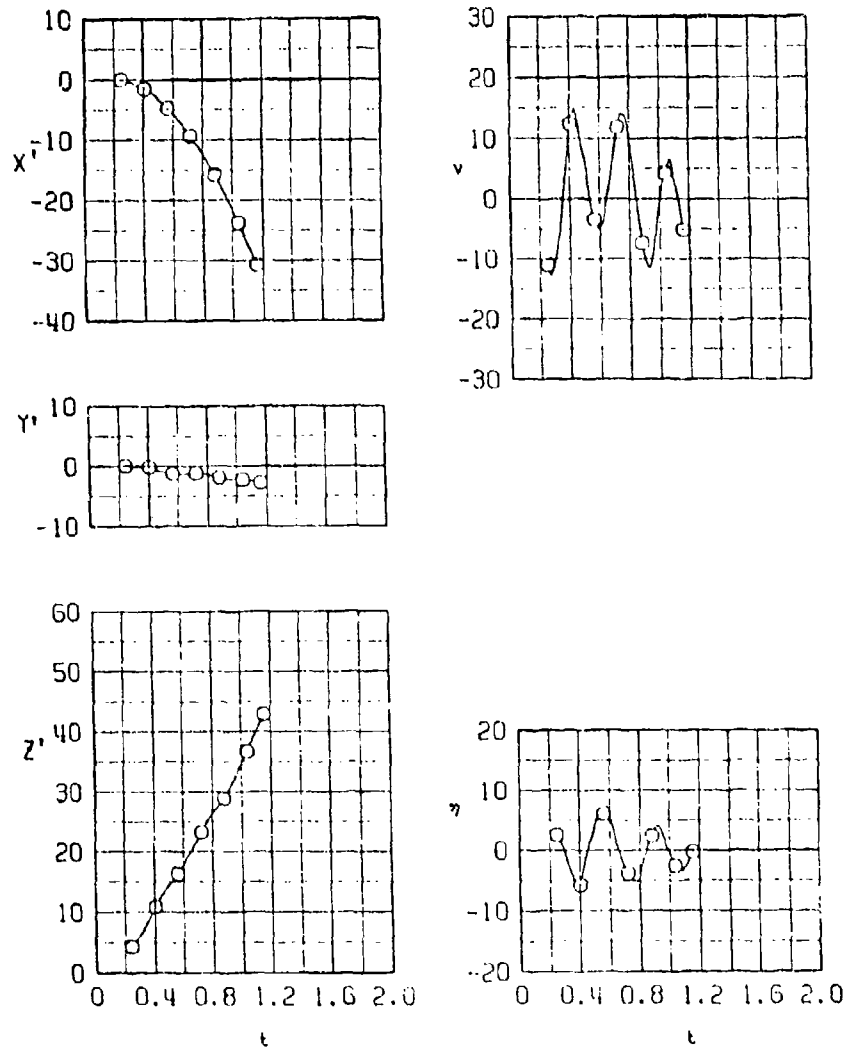


Figure 41b. Trajectory with Suppressor A at Mach 1.2

#### 4.4 Phase 2 Investigation of Saw Tooth Suppression Device in PWT-4T

The saw tooth suppression device (Suppressor A) from the Phase 1 test program was clearly the most promising candidate for further investigation. Therefore, Phase 2 was planned to obtain additional data on the sensitivity of the device to angle of attack ( $\alpha$ ) and sideslip ( $\beta$ ) variations. Also, additional suppressors were fabricated and tested to isolate the effects of height and width.

The first question to be answered during Phase 2 concerned the correlation of data from the two wind tunnels. With a four to one ratio of tunnel size, there was a large change in the tunnel blockage produced by the model. Figures 42 and 43 compare data for the baseline, single B-43 configuration. Data were compared at both Mach .95 and 1.3 conditions and excellent correlation was observed. The  $P_{rms}/Q$  data were generally slightly higher from the larger 16T tunnel. The model instrumentation was unchanged for the two phases; however, the Kulite at the  $X/L$  .5, centerline location was not functioning during Phase 2. Similar results were observed for other bay loadings. Data presented from the left side wall in these and some of the following figures includes data at an  $X/L$  value of 1.0. The data presented is from the Kulite transducer (RMS 13) located on the left side of the rear bulkhead aft of the left store position.

# SYM MACH ALPHA SUPPR TUNNEL

□	.95	2.0	NONE	16T
X	.95	2.0	NONE	4T

BETA = 0

BAY LOADING - SINGLE B-43

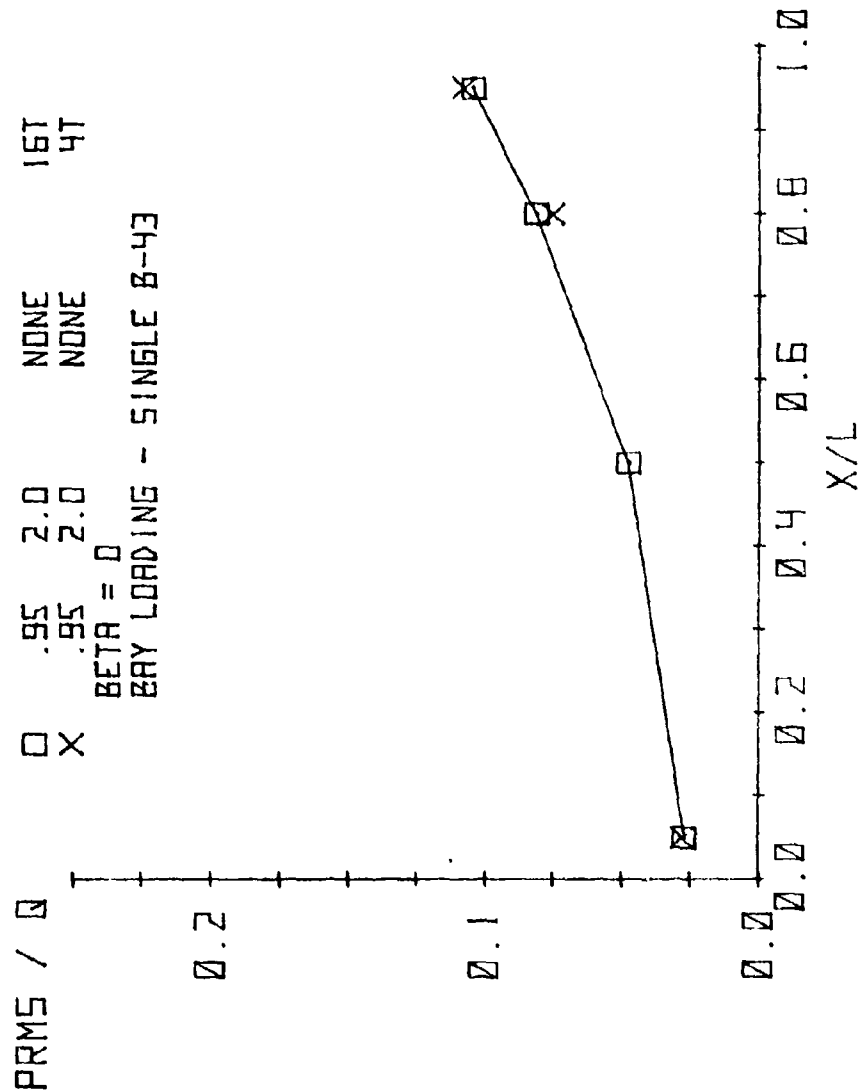


Figure 42a. Comparison of Baseline, Single B-43 Bay Environment as Measured in the 16T and 4T Tunnels, Centerline Distribution

# SYM MACH ALPHA BETA SUPPR LOADING TUNNEL

PRMS / Q	Q	.95	2.0	0.0	NGNE	ONE 8-43	157
X	.95	2.0	0.0	NGNE	ONE 8-43	4T	

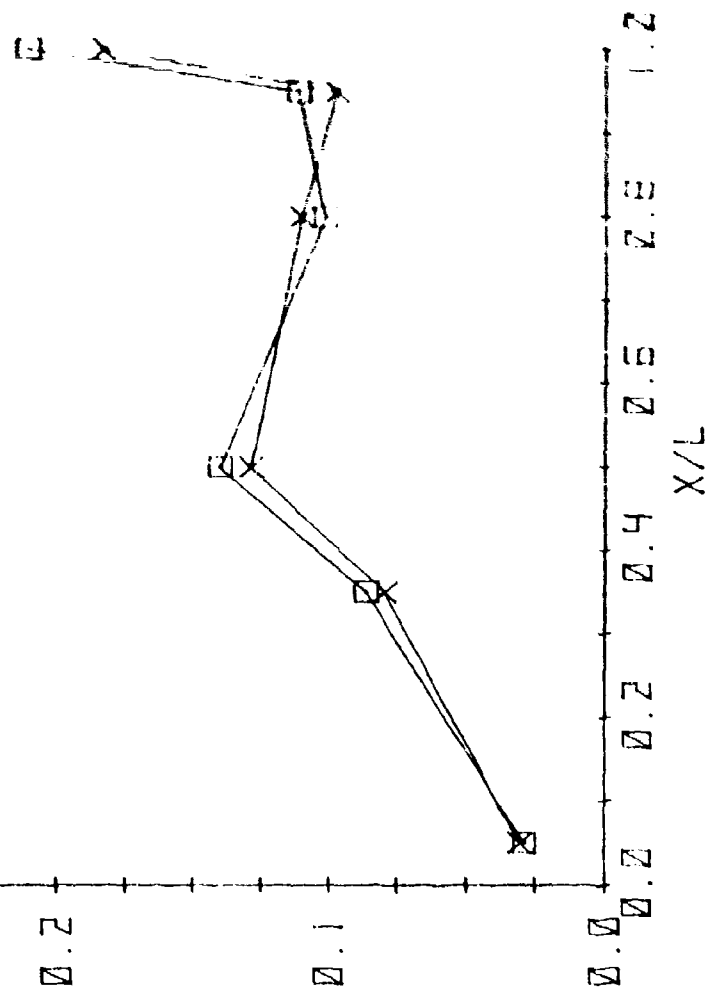


Figure 42b. Left Wall Distribution

SYM MACH ALPHA SUPPR TUNNEL

□ 1.3 2.0 NONE 16T  
 X 1.3 2.0 NONE 4T

BETA = 0

BAY LOADING - SINGLE B-43

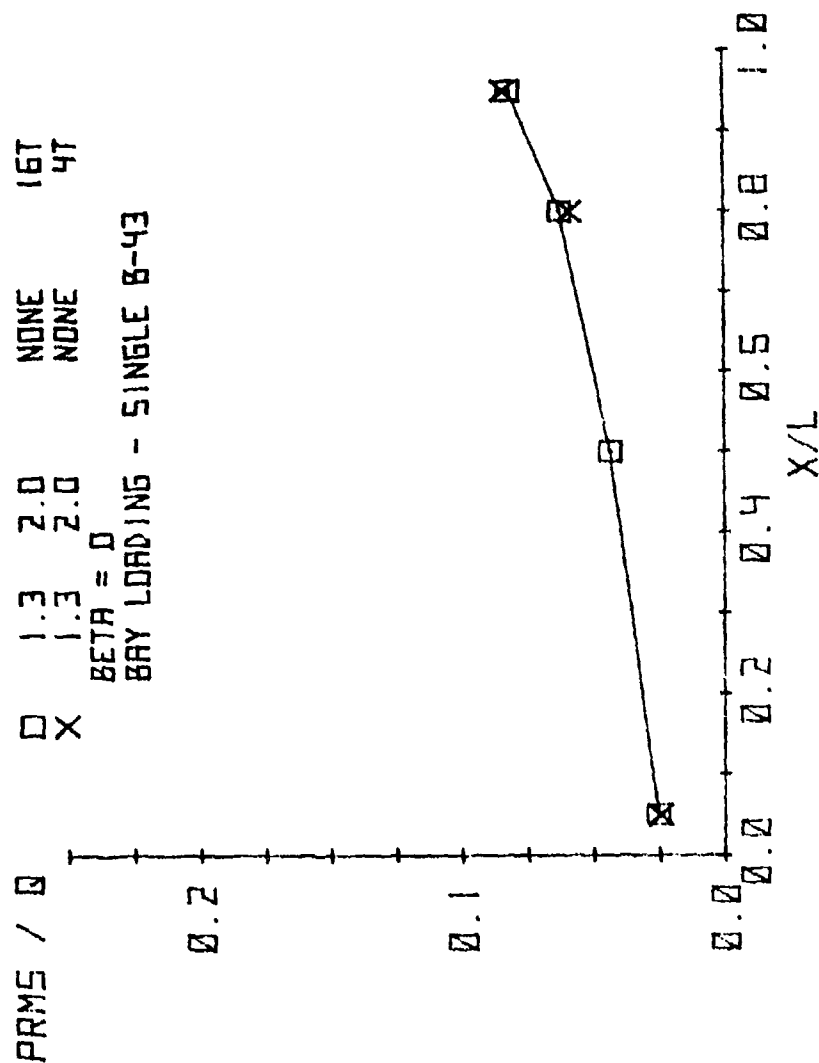


Figure 43a. Comparison of Baseline, Single B-43 Bay Environment at Mach 1.3 as Measured in the 16T and 4T Tunnels, Centerline Distribution

SYM MACH ALPHA SUPPR TUNNEL

SYM	MACH	ALPHA	SUPPR	TUNNEL
□	1.3	2.0	NONE	16T
X	1.3	2.0	NONE	4T

BETA = 0  
BAY LOADING - SINGLE B-43

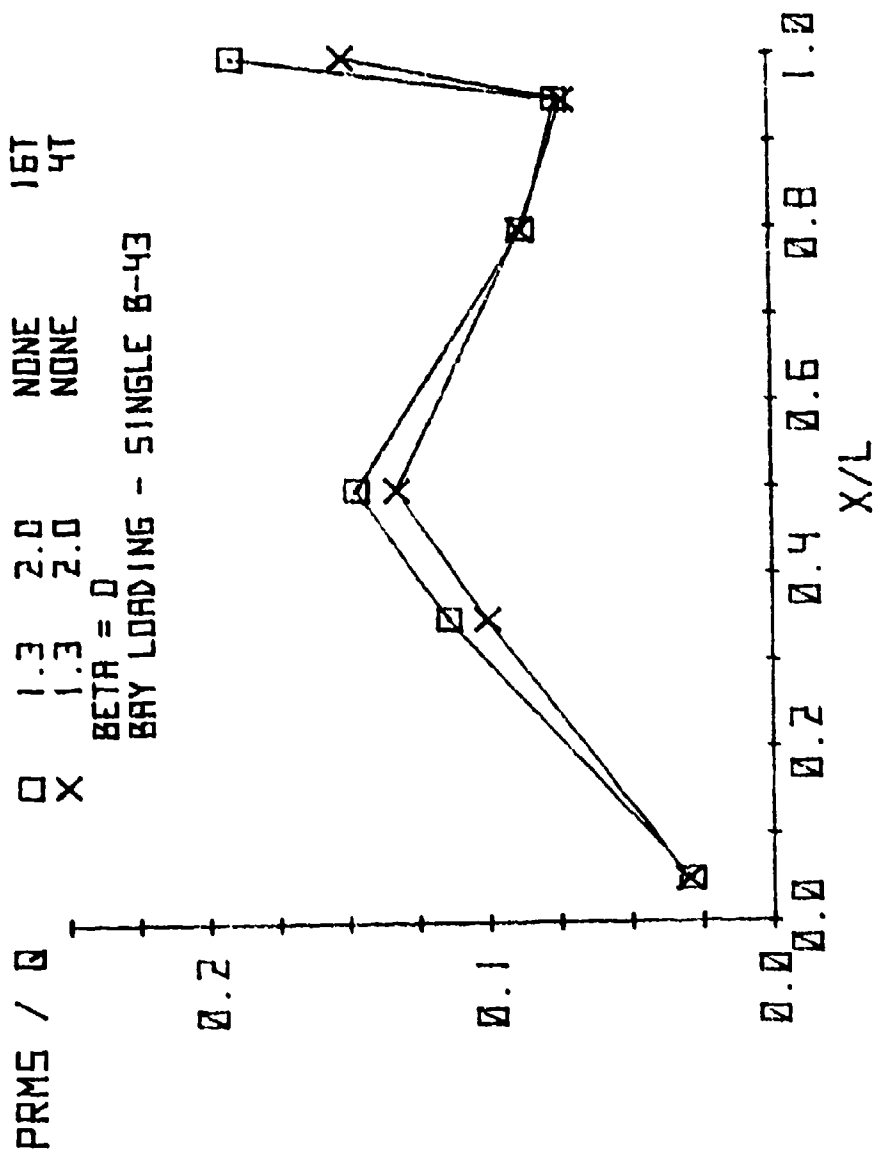


Figure 43b. Left Wall Distribution

#### 4.4.1 Investigation of Suppressor Geometry

Four versions of the saw tooth spoiler were tested and the dimensions of each are included in Figure 44. These can be grouped as follows: Suppressors A and AII were the same height with AII increased in width. AI and AIII were both increased in height to be approximately equal to the model boundary layer height. A and AI are the narrow width suppressors, and AII and AIII were increased in width relative to the A and AI by approximately 17 percent.

Figure 45 compares the four suppressors at Mach .95. Little difference is noted between these devices on the left sidewall. Figure 46 compares the left side wall data at Mach 1.3. Here a significant difference is noted with the taller fences being more effective at most locations. The bay environment achieved with the devices is essentially the same at the  $X/L=.8$  location. This location is adjacent to the store fins and is therefore considered to be the most critical location. The fluctuating pressures or turbulence at this location are assumed to feed loads directly into the region of parachute tail-can to store body attachment that has failed during flight tests.

Based upon the above, the effectiveness of the saw tooth suppression device is more sensitive to height than to width increases. Little difference is noted between the performance of the devices of the same height for the model at zero degrees of sideslip ( $\beta$ ). The data is generally bounded by the A and AIII suppressors which represent the smallest and largest suppressor devices, respectively; therefore, data in the following paragraphs will be presented for these devices only.



SUPPRESSION DEVICE NOMENCLATURE	A	B
A	1.270	0.230
AI	1.270	0.339
AII	1.490	0.230
AIII	1.490	0.339

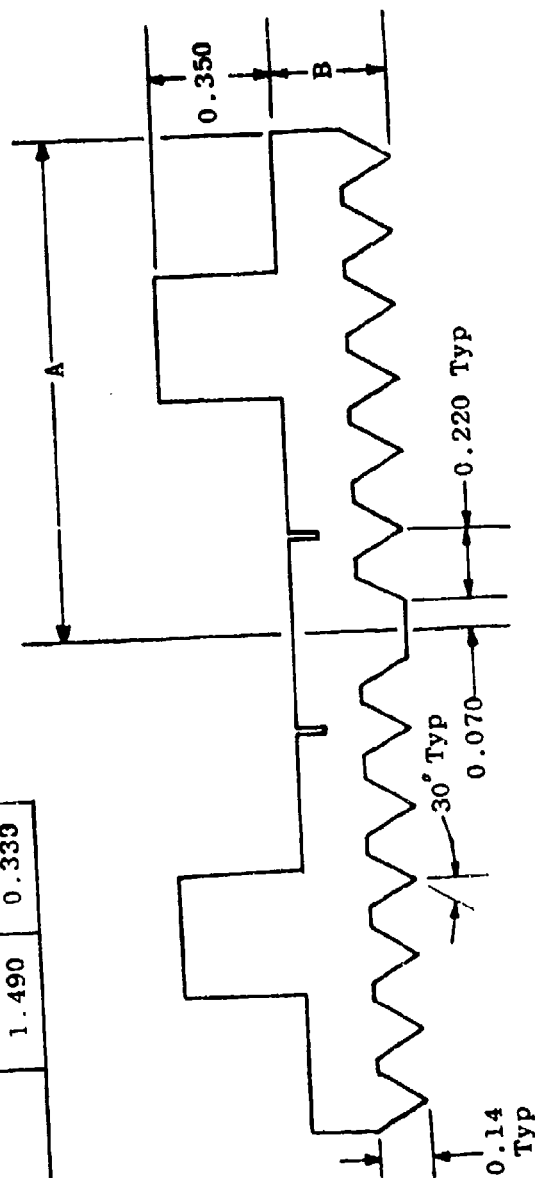


Figure 44. Phase 2 Suppressor Configurations

# SYM MACH ALPHA BETA SUPPR

	X	Y	+	D
.95	2.0	0.0	A	
.95	2.0	0.0	A1	
.95	2.0	0.0	A11	
.95	2.0	0.0	A111	

BAY LOADING - SINGLE B-43

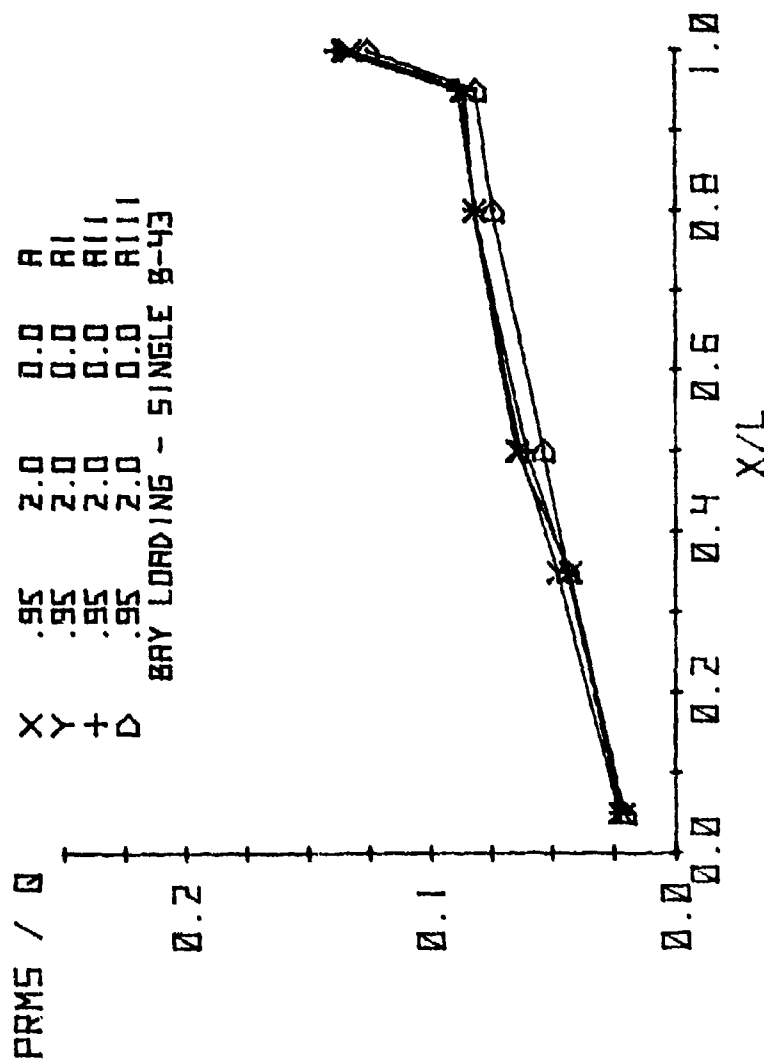


Figure 45. Comparison of Suppressors at Mach .95, Left Wall Distribution

# SYM MACH ALPHA BETA SUPPR

SYM	MACH	ALPHA	BETA	SUPPR
X	1.3	2.0	0.0	A
Y	1.3	2.0	0.0	A1
+	1.3	2.0	0.0	A11
D	1.3	2.0	0.0	A111

BAY LOADING - SINGLE B-43

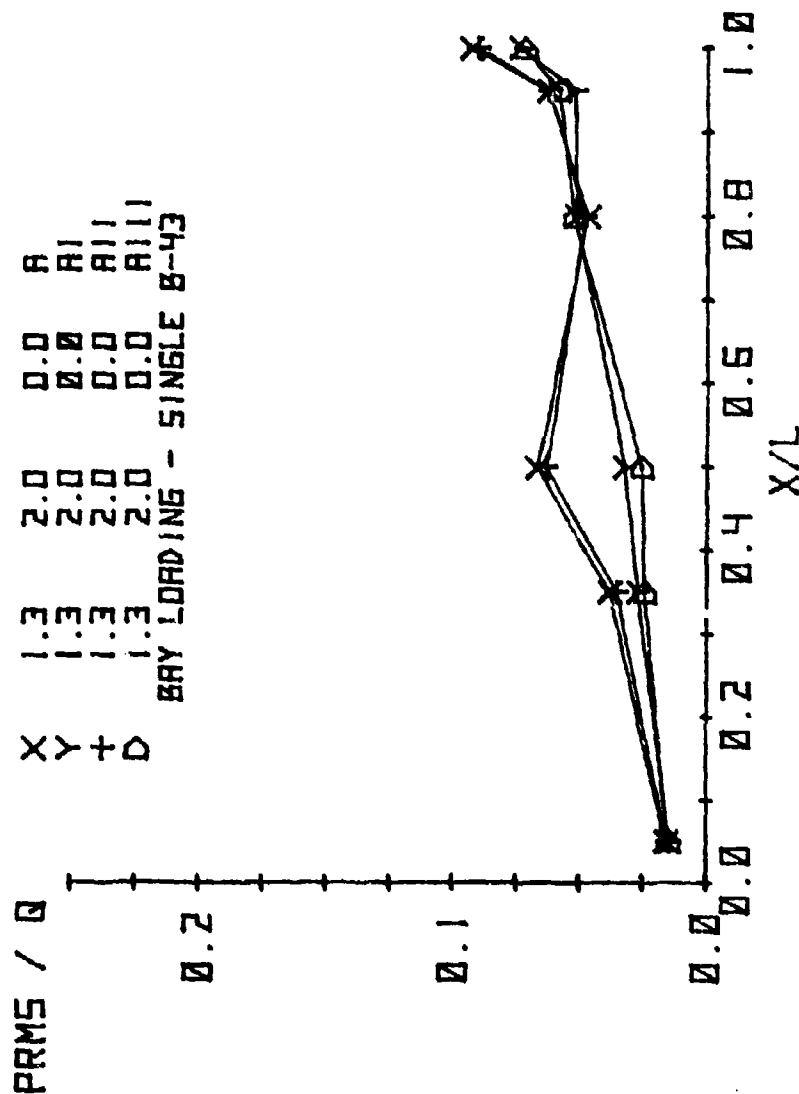


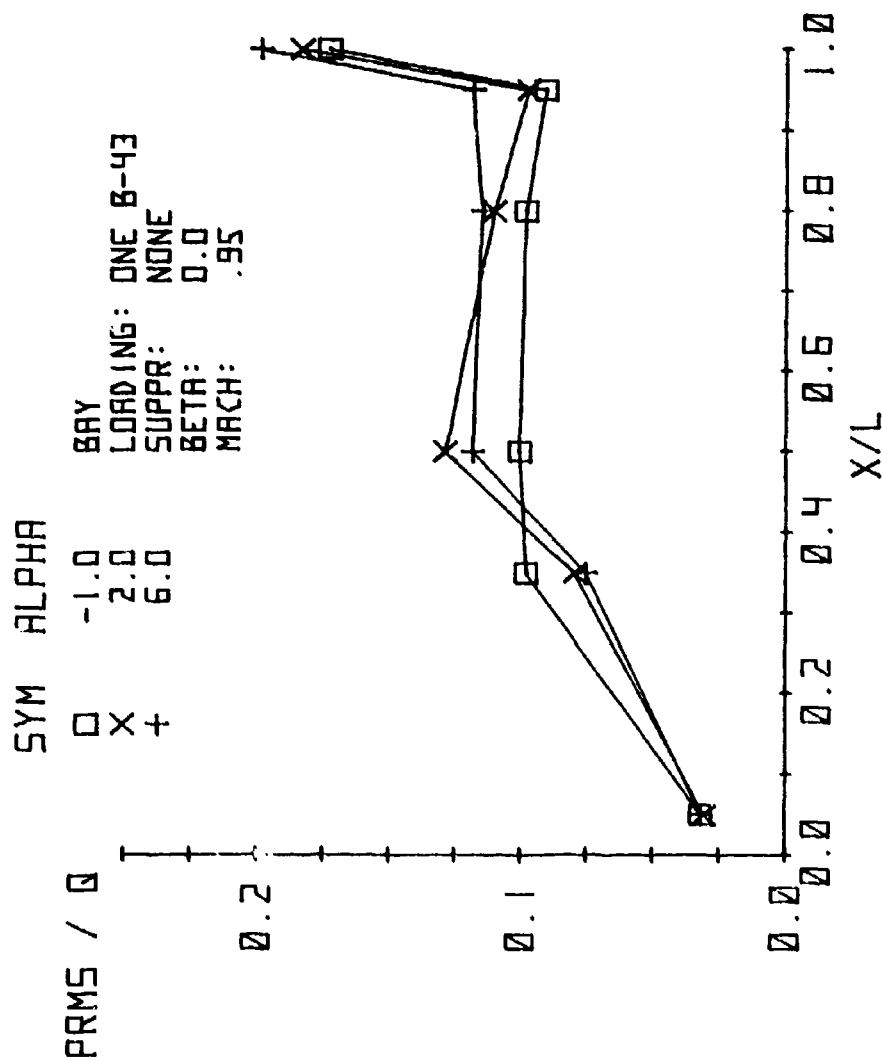
Figure 46. Comparison of Suppressors at Mach 1.3, Left Wall Distribution

#### 4.4.2 Angle of Attack Test Results

Angle of attack effects were investigated and Figures 47 and 48 present baseline data for the suppressor off case at Mach numbers .95 and 1.3. The data at 2 degrees alpha (body angle, 3 degrees wing angle of attack) is representative of the flight angle of attack. The level of turbulence at the mid wall position reaches a maximum at the 2 degree cruise alpha for both Mach numbers.

Angle of attack data at these same Mach numbers are presented in Figures 49 through 52 with Suppressors A and AIII. The bay turbulence levels (Prms/Q) are significantly reduced relative to the suppressor off data. The levels increase slowly as alpha increases up to 6 degrees. At Mach 1.3 with Suppressor A, there is still evidence of peaking of the levels at the X/L .5 location on the left wall. This tendency is not observed with AIII installed.

In general, the bay environment is not strongly affected by angle of attack changes over the range from -1 to +8 degrees, and the suppressor effectiveness is unchanged by alpha variations.



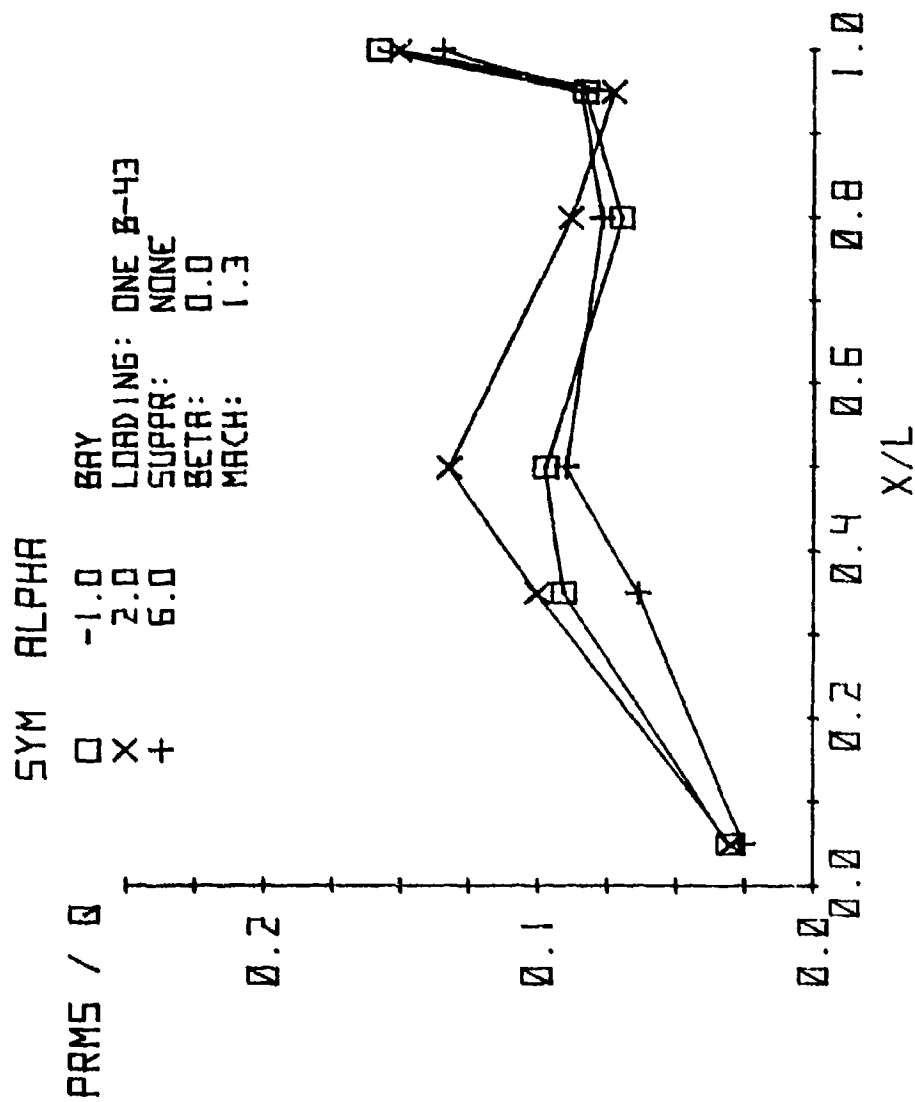


Figure 48. Angle of Attack Effects on Bay Environment at Mach 1.3, Left Wall Distribution

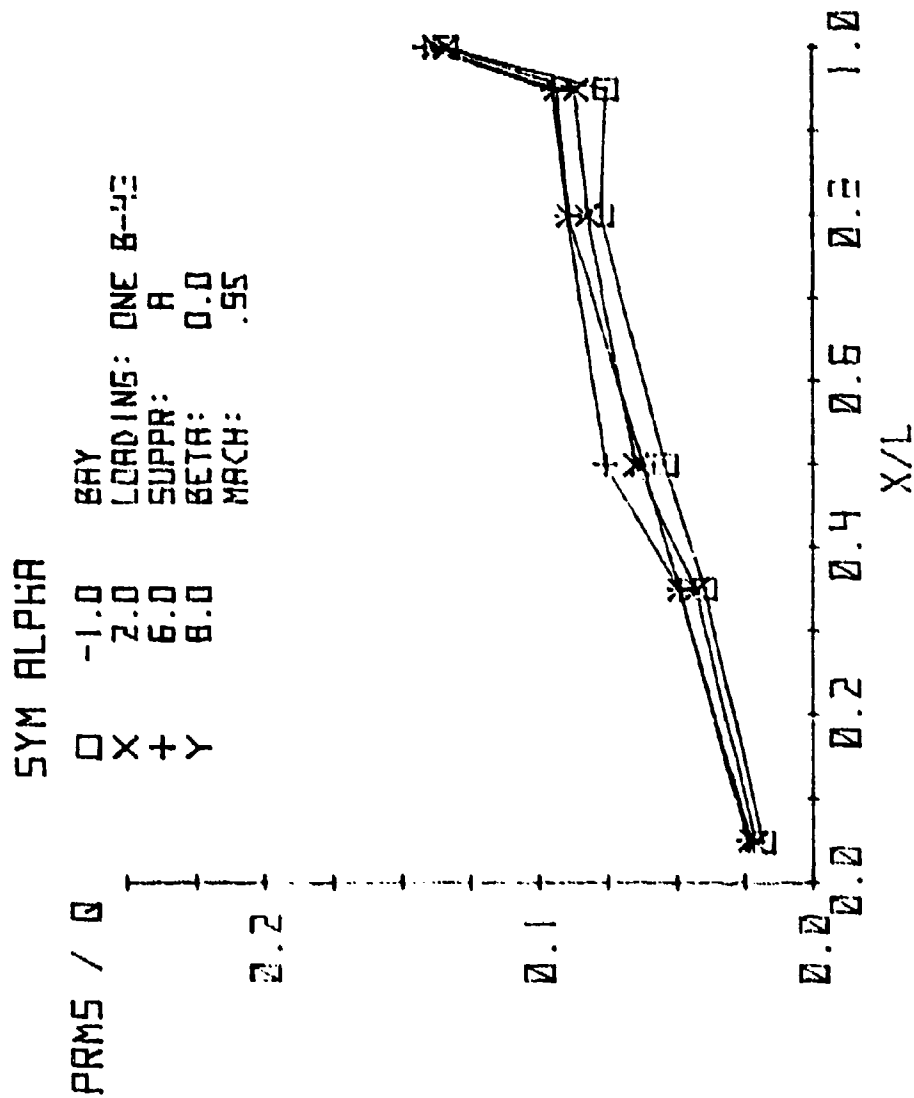


Figure 49. Angle of Attack Effects with Suppressor A  
Installed at Mach .95, Left Wall Distribution

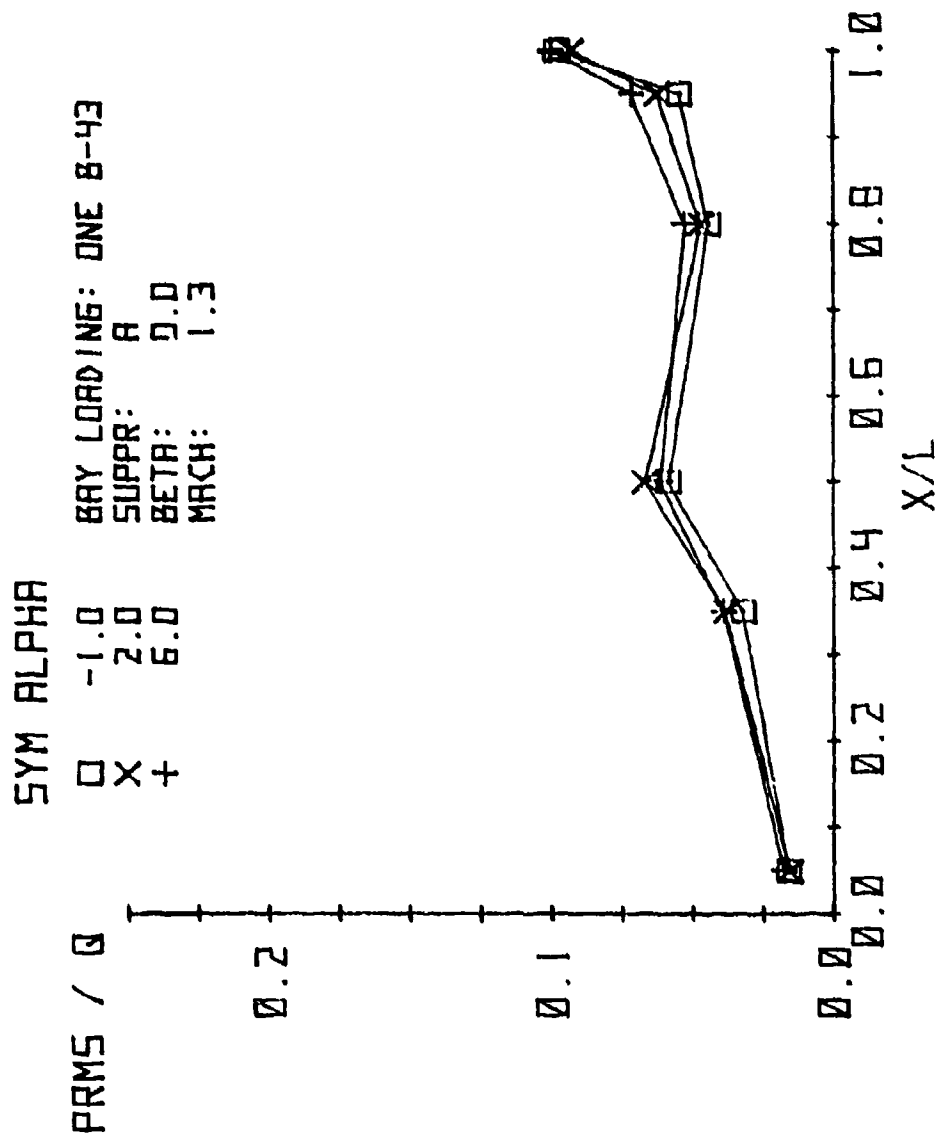


Figure 50. Angle of Attack Effects with Suppressor A  
Installed at Mach 1.3, Left Wall Distribution



SYM ALPHA

□ -1.0  
X 2.0  
+ 6.0

BAY  
LOADING: ONE 8-43  
SUPPR: A111  
BETA: 0.0  
MACH: .95

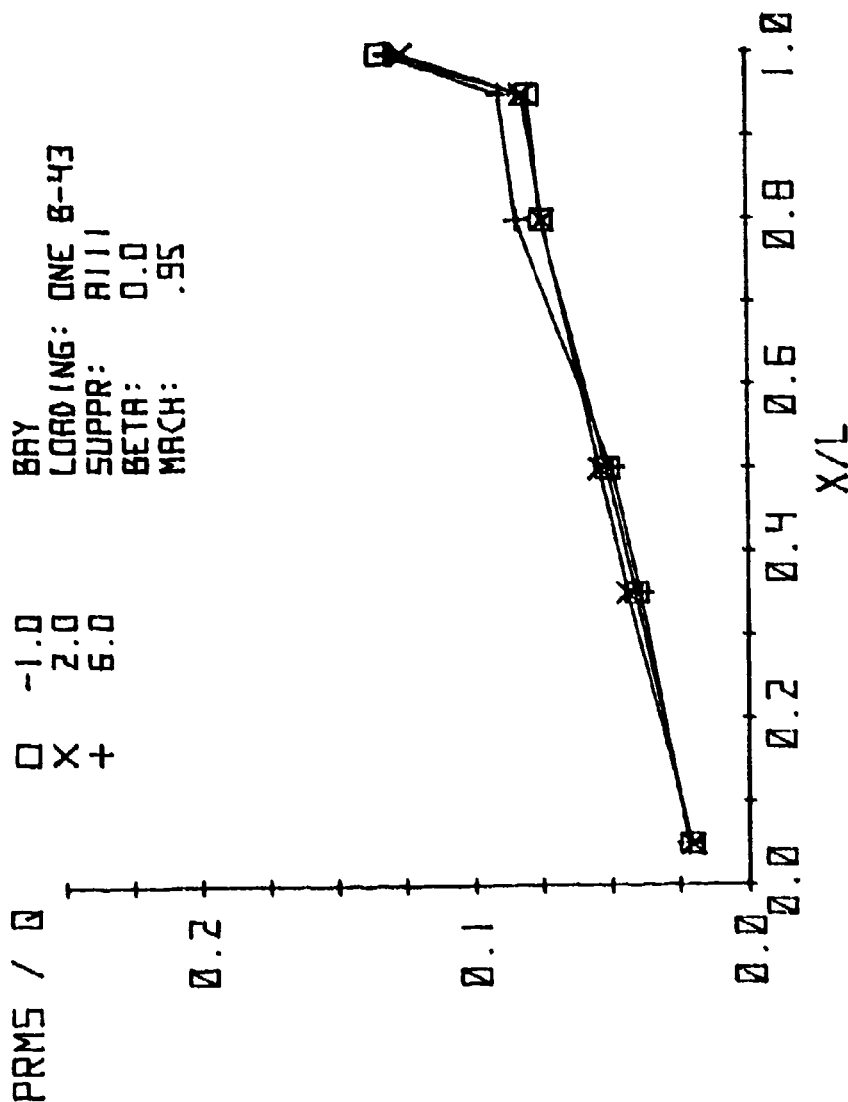


Figure 51. Angle of Attack Effects with Suppressor A111 Installed at Mach .95, Left Wall Distribution

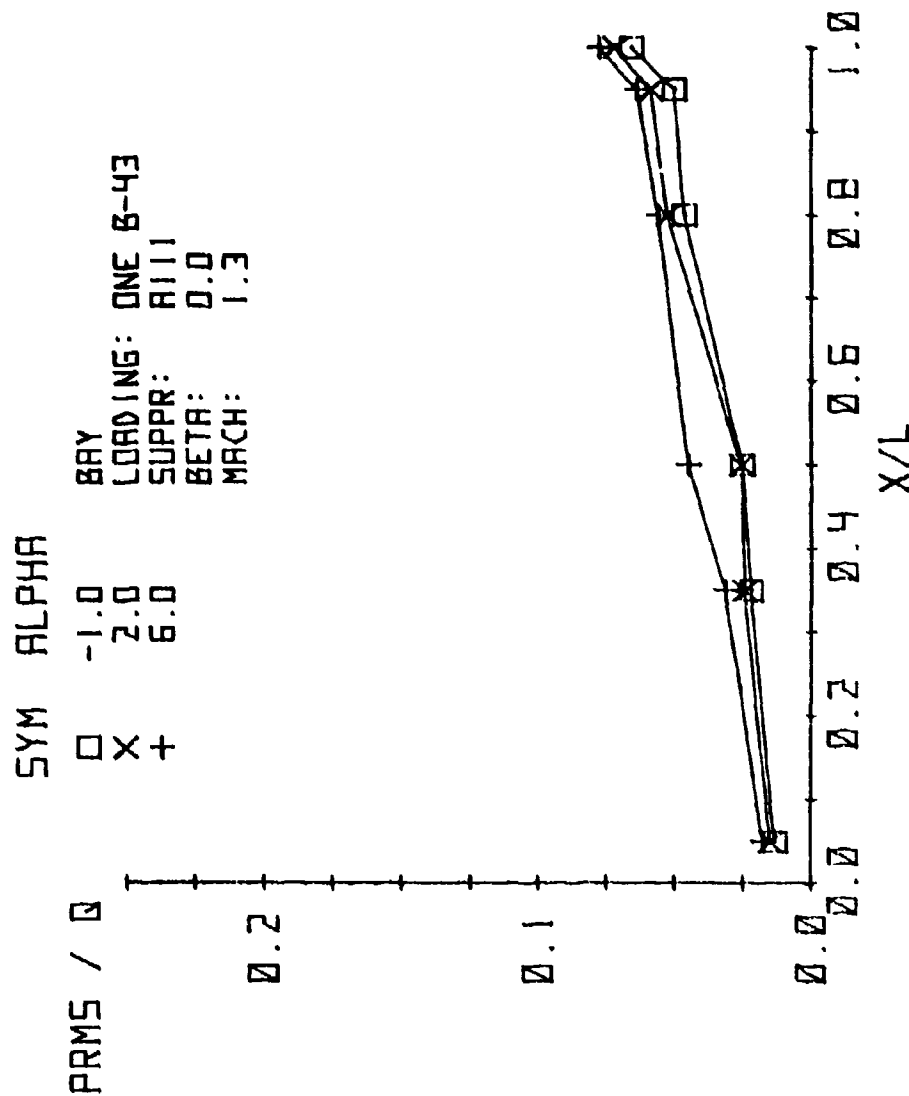


Figure 52. Angle of Attack Effects with Suppressor A111 Installed at Mach 1.3, Left Wall Distribution

#### 4.4.3 Sideslip Test Results

The next variable to be evaluated was sideslip. The data from the inlet rakes installed in the left flow through inlet will be discussed in paragraph 4.4.4, and as expected this data is very sensitive to sideslip (beta) angle variations. Note: Model nose left corresponds to positive beta angles.

Baseline data at Mach .95 and 1.3 are presented in Figures 53 and 54 over a beta range of  $\pm 4$  degrees. Only the data from the left wall and left side of the rear bulkhead are presented because these locations are the most sensitive to sideslip. Referring back to Figure 7b, the taper in bay width should be kept in mind. At two degrees of sideslip, the turbulence level in the bay is increased at all locations relative to the zero beta condition. This may be due to the geometry of the side wall (taper) which aligns the wall more closely with the free stream direction. The data at both Mach numbers is similar; however, the Mach 1.3 data in the aft half of the bay is generally decreased in level relative to the Mach .95 data.

With Suppressor A installed, very little effect of sideslip is observed. Figures 55 through 57 present data at Mach numbers of .8, .95, and 1.3. Only at Mach 1.3 is the tendency to peak at the mid bay side wall location still evident.

Similar data at Mach .95 and 1.3 is presented in Figures 58 and 59 with Suppressor AIII. The bay environment achieved with both suppression devices is essentially the same except at the X/L .5 and 1.0 locations.

Both suppression devices produced dramatic improvements in the bay environment at all sideslip angles, and AIII was only moderately more effective than the substantially smaller device A.

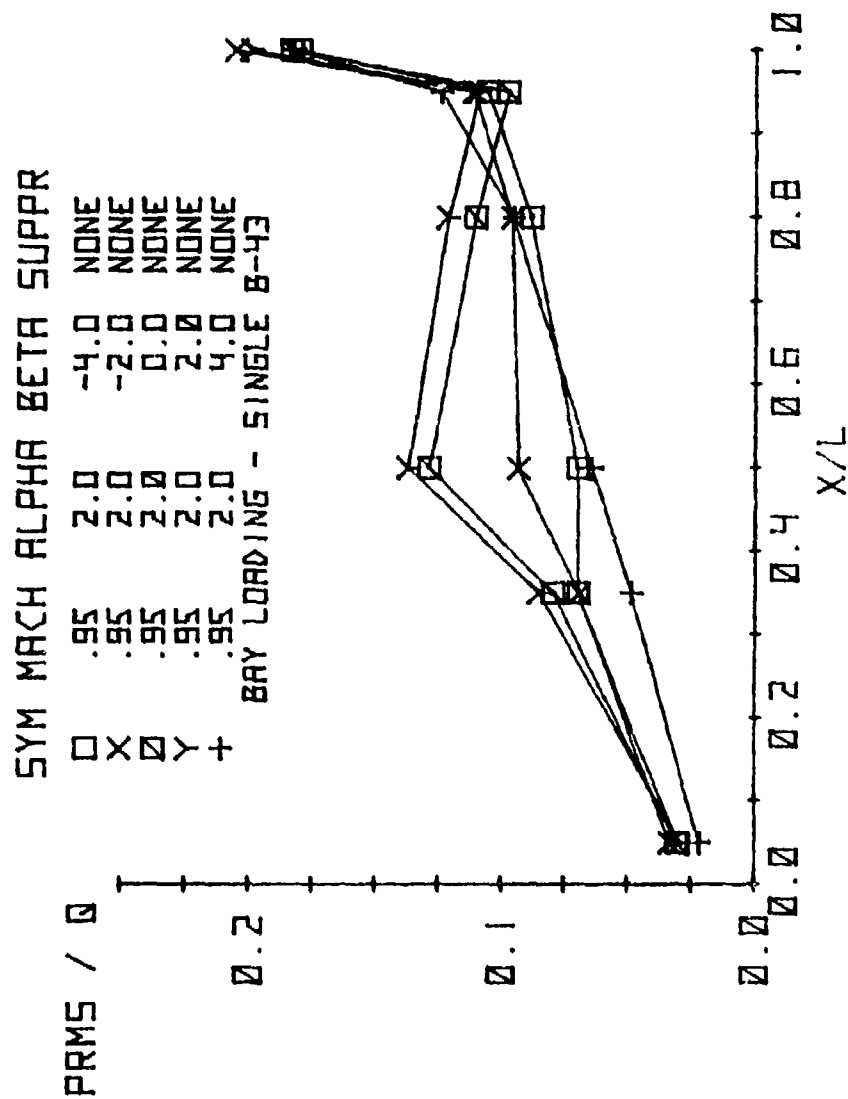


Figure 53. Baseline Sideslip Data at Mach .95,  
Left Wall Distribution

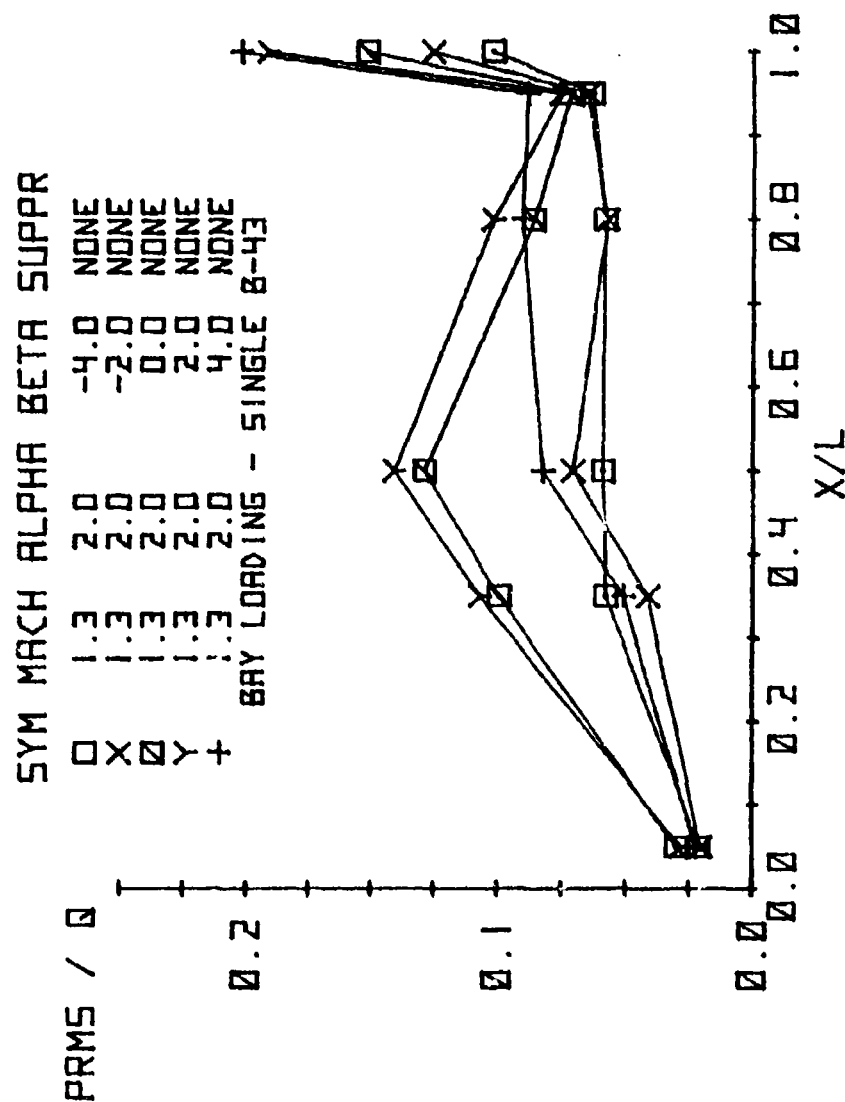
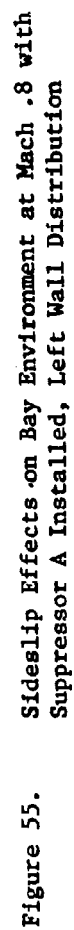


Figure 54. Baseline Sideslip Data at Mach 1.3,  
Left Wall Distribution



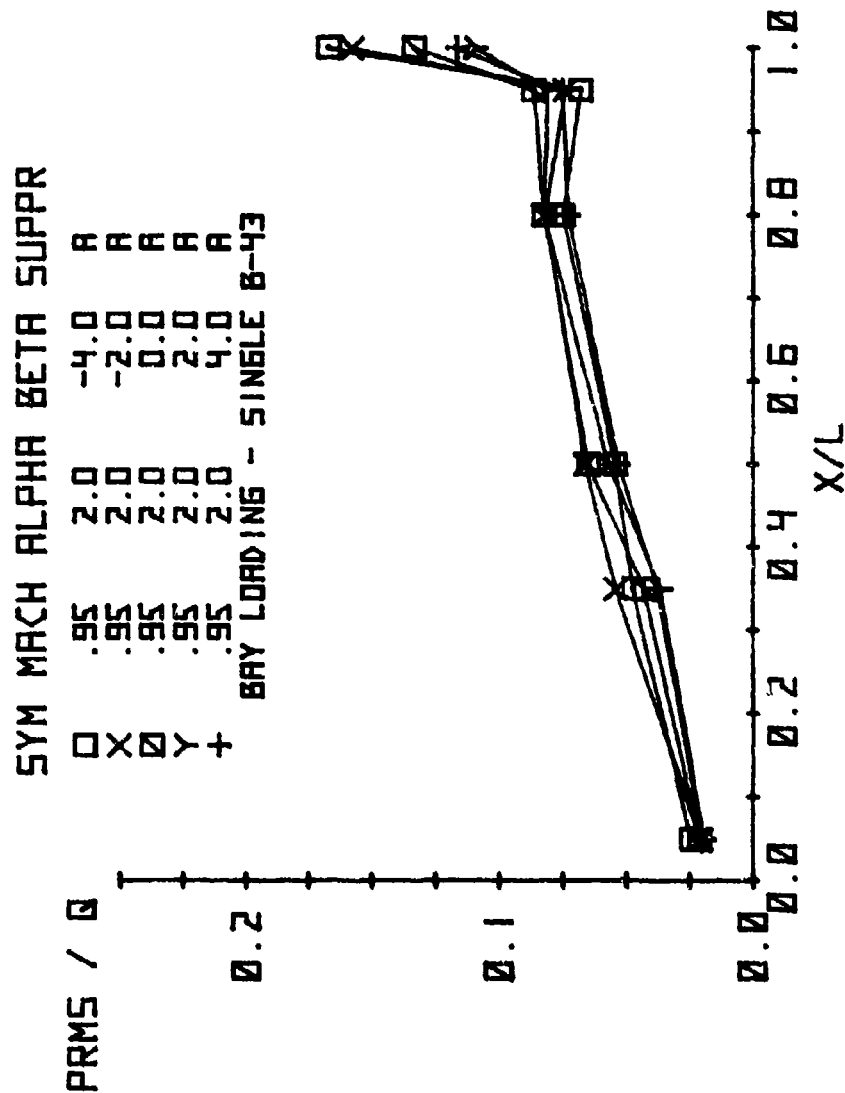


Figure 56. Sideslip Effects on Bay Environment at Mach .95 with Suppressor A Installed, Left Wall Distribution.

# SYM MACH ALPHA BETA SUPPR

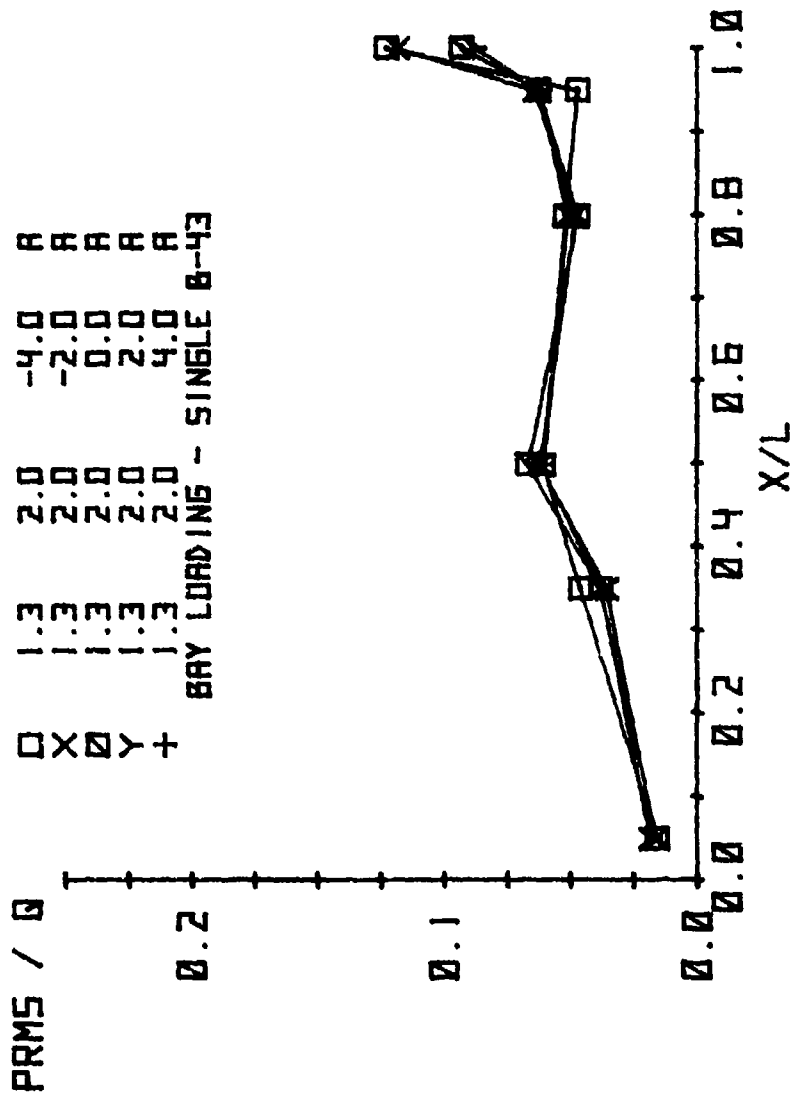


Figure 57. Sideslip Effects on Bay Environment at Mach 1.3 with Suppressor A Installed, Left Wall Distribution



# SYM MACH ALPHA BETA SUPPR LOADING TUNNEL

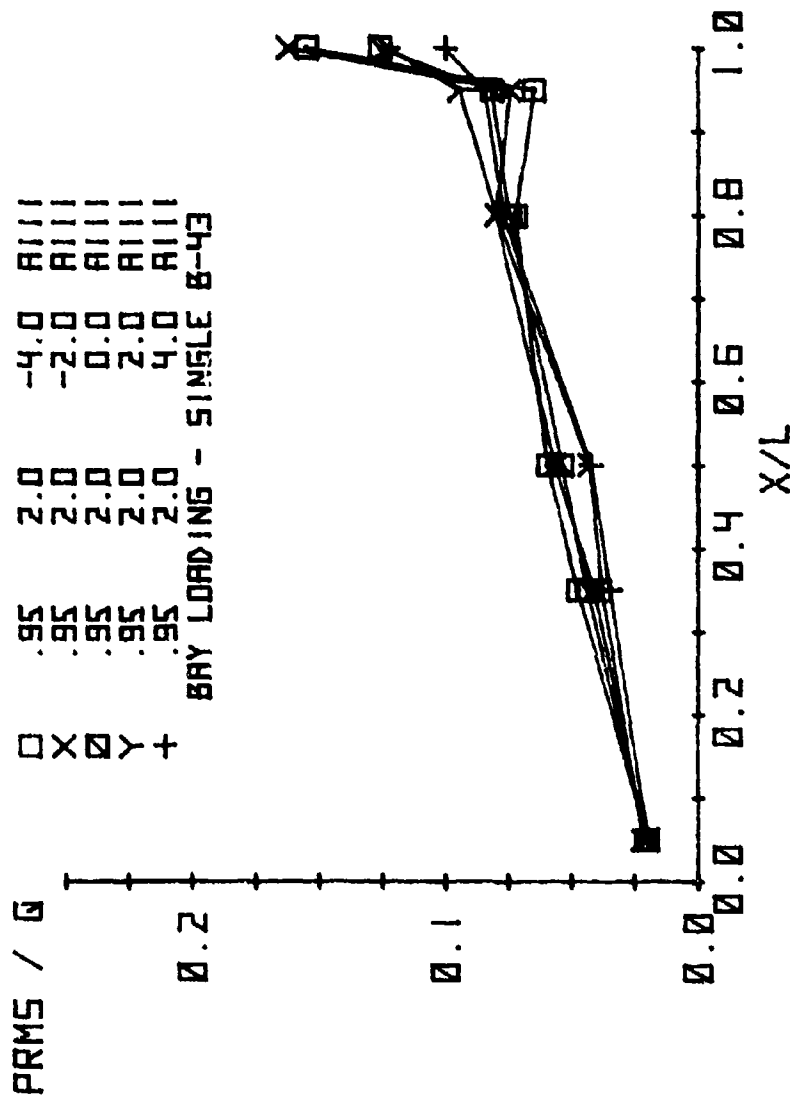


Figure 58. Sideslip Effects on Bay Environment at Mach .95 with Suppressor AIII Installed, Left Wall Distribution

# SYM MACH ALPHA BETA SUPPR

□	1.3	2.0	-4.0	RIII
X	1.3	2.0	-2.0	RIII
□	1.3	2.0	0.0	RIII
Y	1.3	2.0	2.0	RIII
+	1.3	2.0	4.0	RIII

BAY LOADING - B-43

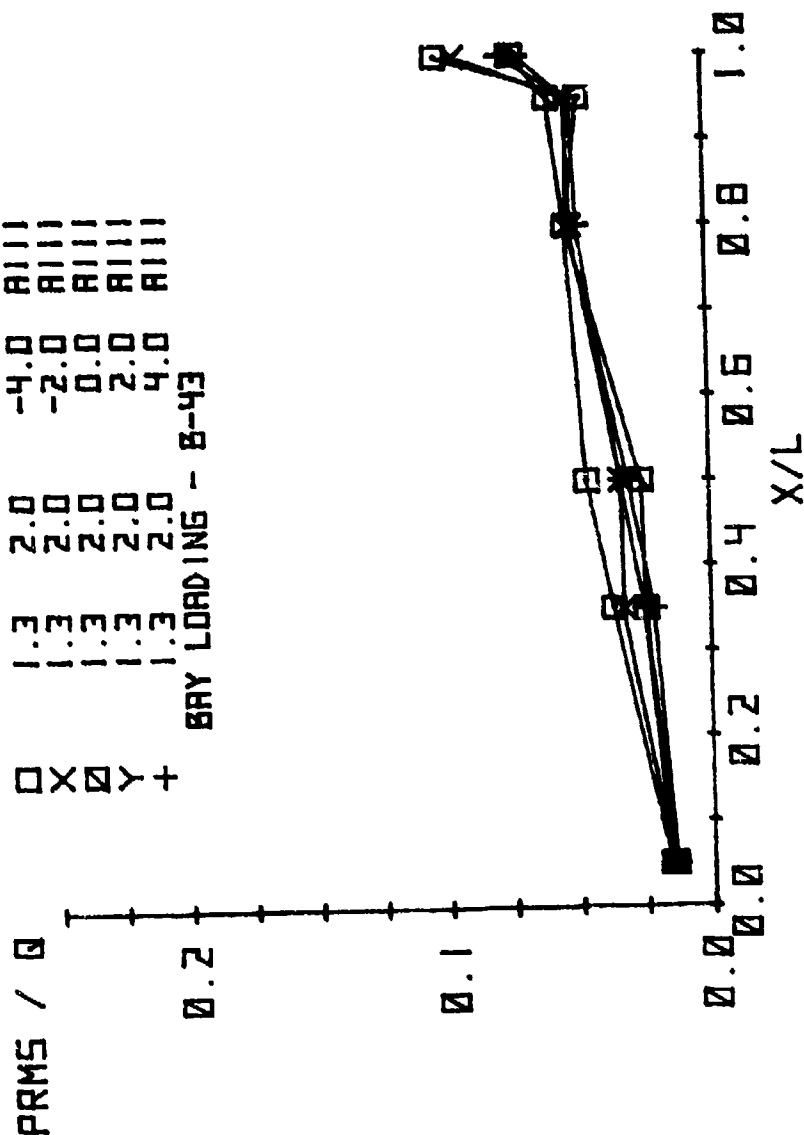


Figure 59. Sideslip Effects on Bay Environment at Mach 1.3 with Suppressor AIII Installed, Left Wall Distribution

#### 4.4.4 Inlet Pressure Recovery Results

One of the primary questions to be answered concerns the effect of the installation of the spoiler type suppressor on the engine inlet flow. With the spoiler raised into position while the bay doors are open, airflow may be diverted around to the sides of the aircraft where the inlets are located. Sideslip will increase the effect of the spoiler on the lee inlet. Figures 60 and 61 show the physical relationships of the bay, spoiler, and inlets. The inlet geometry is representative of the Triple Flow II Configuration; however, no attempt was made to match the correct mass flow.

Inlet total pressure data was acquired for all configurations tested. The data are reduced to a ratio of total pressure at the rake tap location to the freestream total pressure. Interpolated constant pressure recovery contours are then plotted as shown in the series of figures starting with Figure 62. The contours are plotted at increments of .01 between .90 and 1.0. Values of pressure recovery less than .9 are not plotted. The locations of the twelve pressure tapes are indicated by the small circle symbols shown in these plots.

The inlet pressure recovery contours for the basic configuration are contained in Figure 62. The bay doors are open and one B-42 is loaded in the bay. Mach 1.3 data is shown for sideslip angles of zero (Figure 62a) and two degrees (figure 62b). This Mach number produces the greatest loss and the small positive sideslip has an additional effect on the lee inlet. A significant area in the lower inboard portion of the inlet has a pressure recovery of less than 90%. Figures 63 through 66 present the inlet data at the same conditions for each of the saw tooth suppression devices.

A more detailed comparison of the data from the rake located in this corner of the inlet are presented in Figure 67. The rake taps are numbered from the inlet center body down with Tap #3 located closest to the lower inboard corner. At zero beta, Suppressor A produces approximately 2% reduction in pressure recovery relative to the basic configuration across the Mach range. With only two degrees of sideslip, this reduction increases to 4 to 5 percent except at Mach 1.1 for Tap #3 where a reduction of 8 percent is noted relative to the suppressor off configuration. All of the other devices produced larger increments with AIII producing the lowest pressure recovery at all Mach numbers. Larger positive sideslip angles produced even larger areas of low pressure recovery at the inlet plane.

The height of the saw tooth suppression device again is the most significant geometry variable with respect to the effect on the inlet at all Mach numbers. It is apparent that the smallest device (A) produces the least installation problem from the inlet standpoint and that the two tall fences (AI and AIII) produced the greatest inlet losses.



Figure 60. Model Frontal View in I6T Showing Inlet and Inlet Rake Details

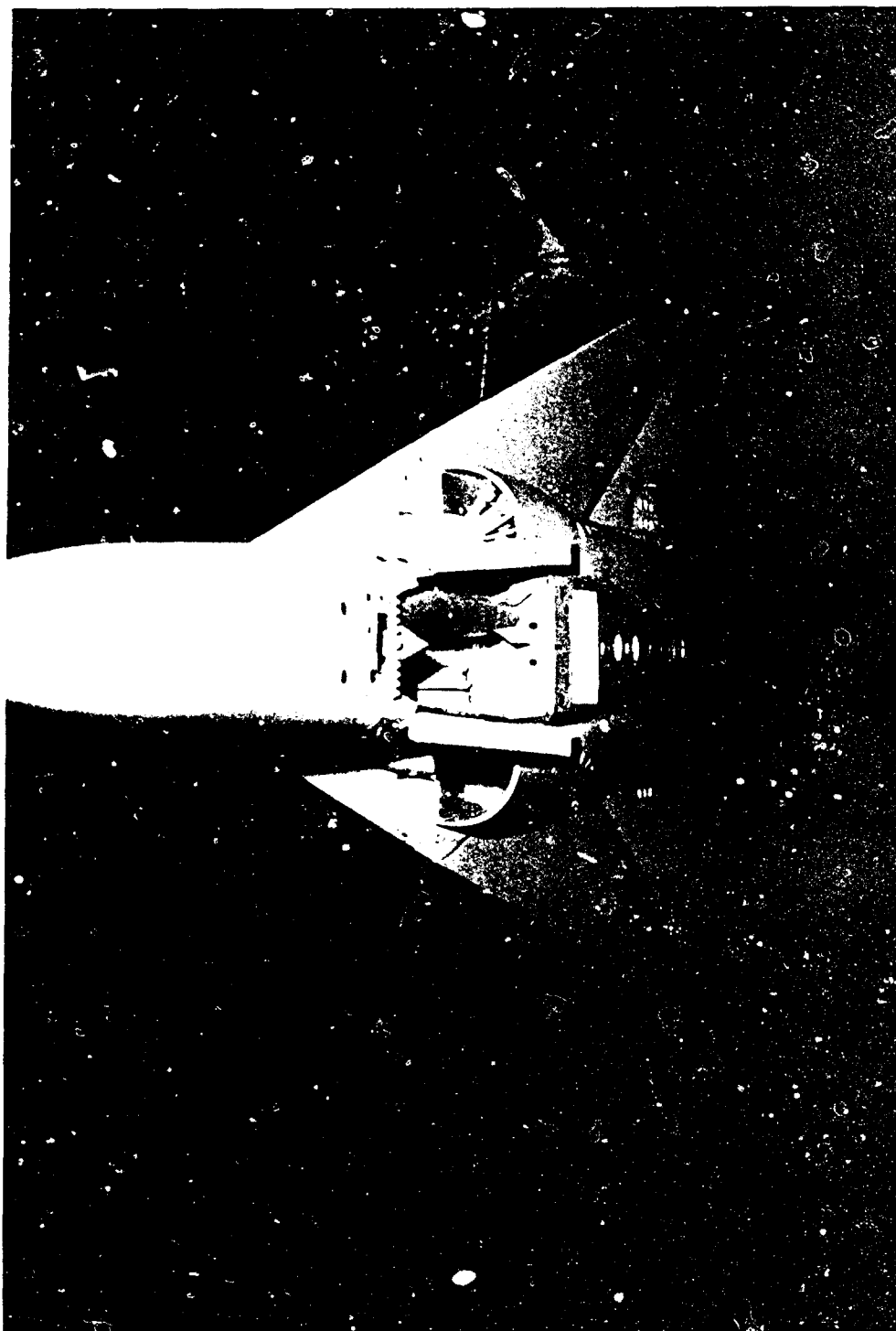


Figure 61. Model Viewed from Below Showing Physical Relationship of Suppression Device A to Inlets and Bay Doors

R/F-H  
 2.00  
 REI  
 3.00  
 MOD 10  
 1.30  
 6  
 618.52

Suppressor  
 None  
 Beta  
 0°

PRT 1000  
 15.000

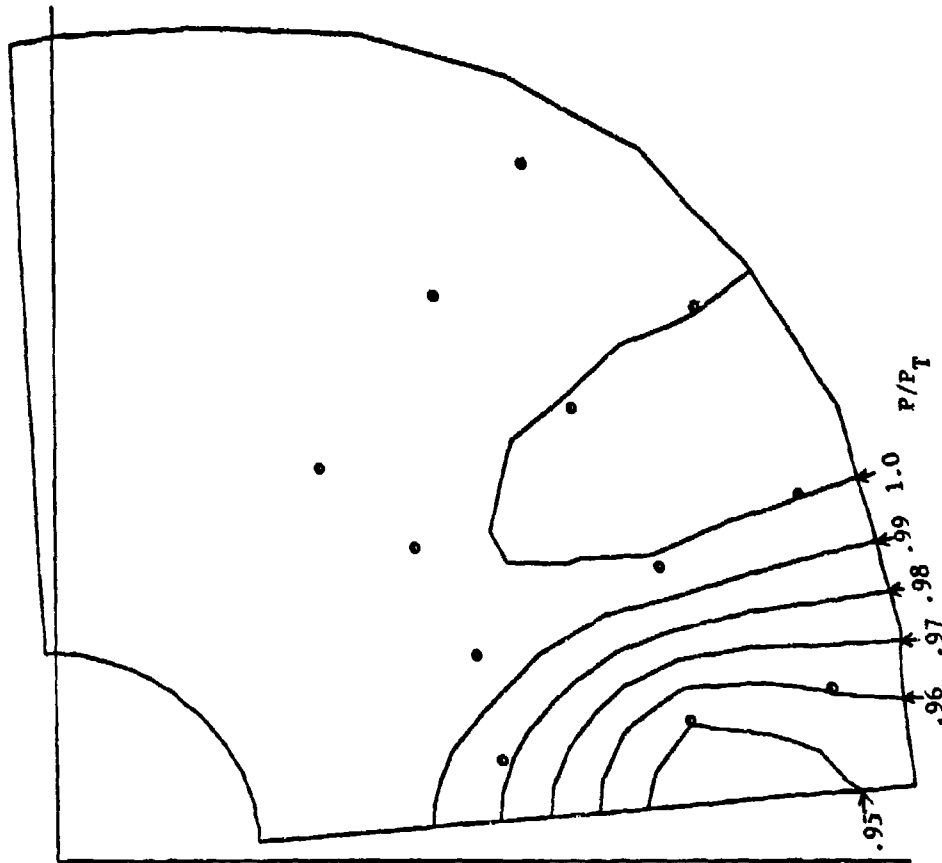


Figure 62a. Inlet Pressure Recovery Contours for Baseline Configuration, Beta = 0 degrees

RF-4  
1.50

RF-4  
3.00

RF-4  
1.30

RF-4  
619.43

Suppressor  
None  
Beta  
20

RF-4  
3.00

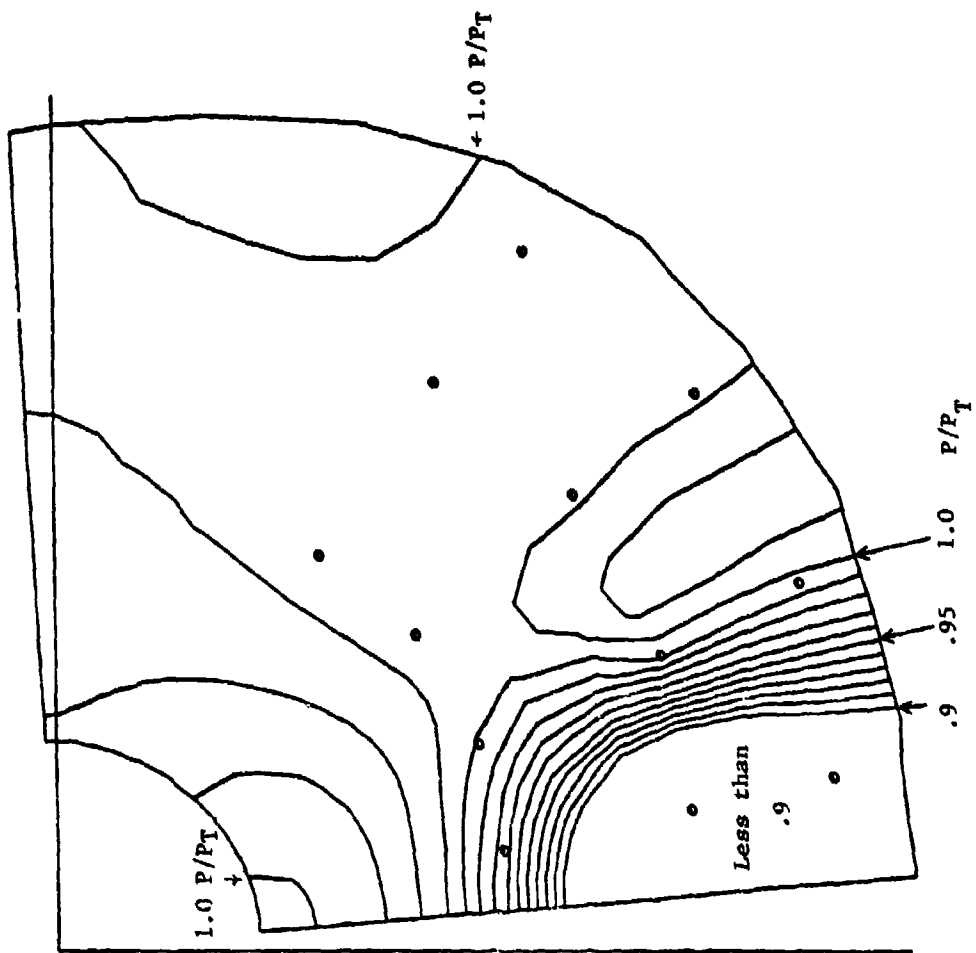


Figure 62b. Inlet Pressure Recovery Contours for Baseline Configuration, Beta = 2 degrees



2.00  
 3.00  
 1.30  
 6  
 620-15

Suppressor  
 A  
 Beta  
 2

PART NUMBER  
 620-15

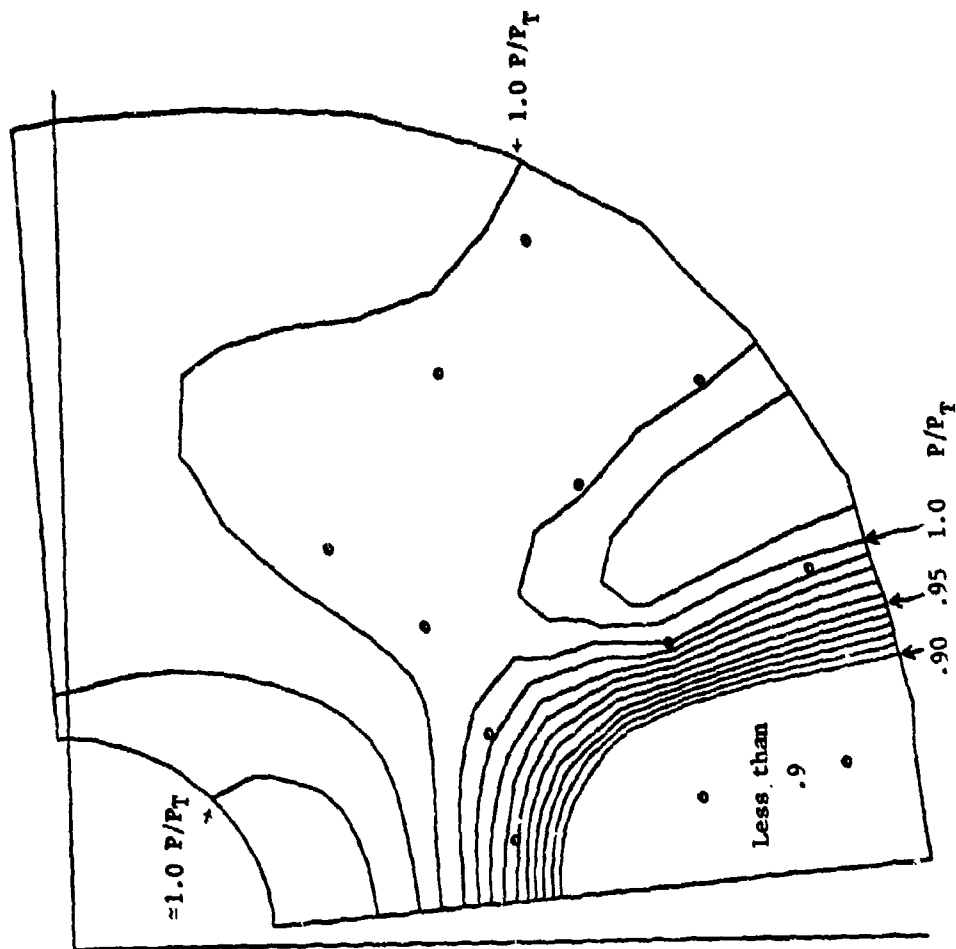


Figure 63. Inlet Pressure Recovery Contours with Suppressors A Installed

ALJ-M  
 1.00  
 REX  
 3.00  
 PACH NO  
 1.30  
 0  
 618.85

Suppressor  
 AI  
 Beta  
 20

PART NUMBER  
 99.005

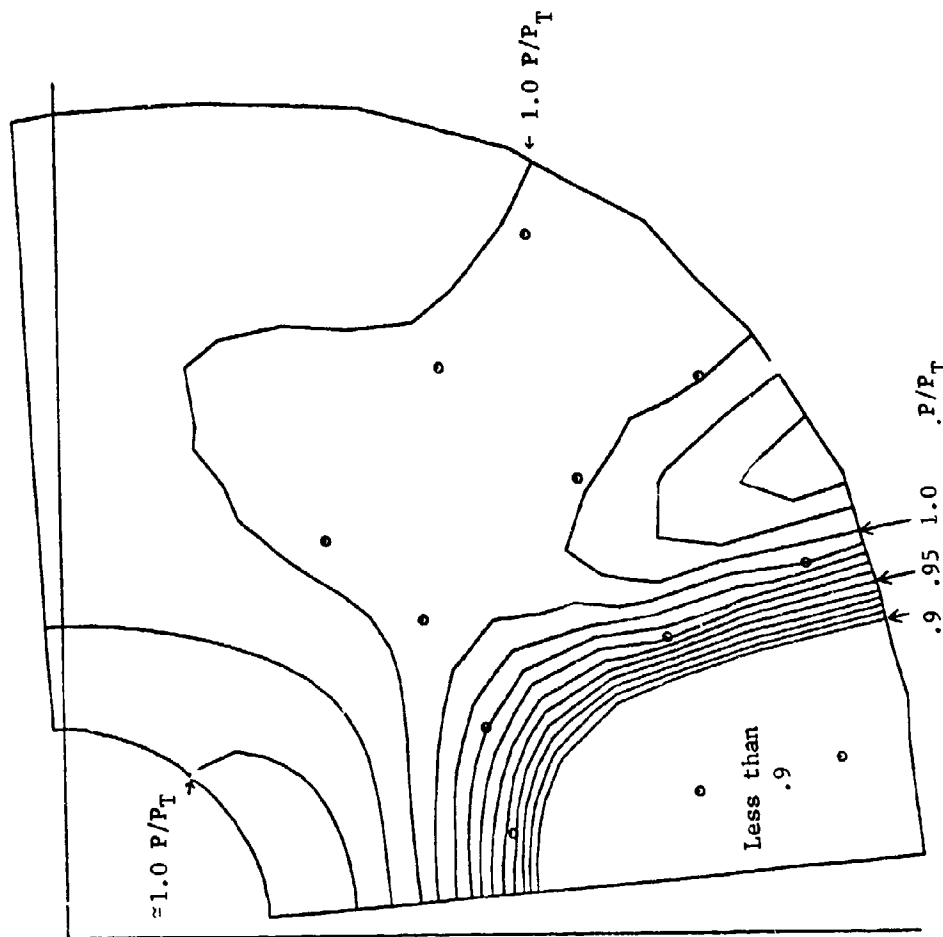


Figure 64. Inlet Pressure Recovery Contours with  
 Suppressor AI Installed

ALF-H  
 2.00  
 REY  
 3.00  
 MCH M0  
 1.30  
 0  
 619.49

Suppressor  
 All  
 Beta  
 20

PART NUMBER  
 S3.005

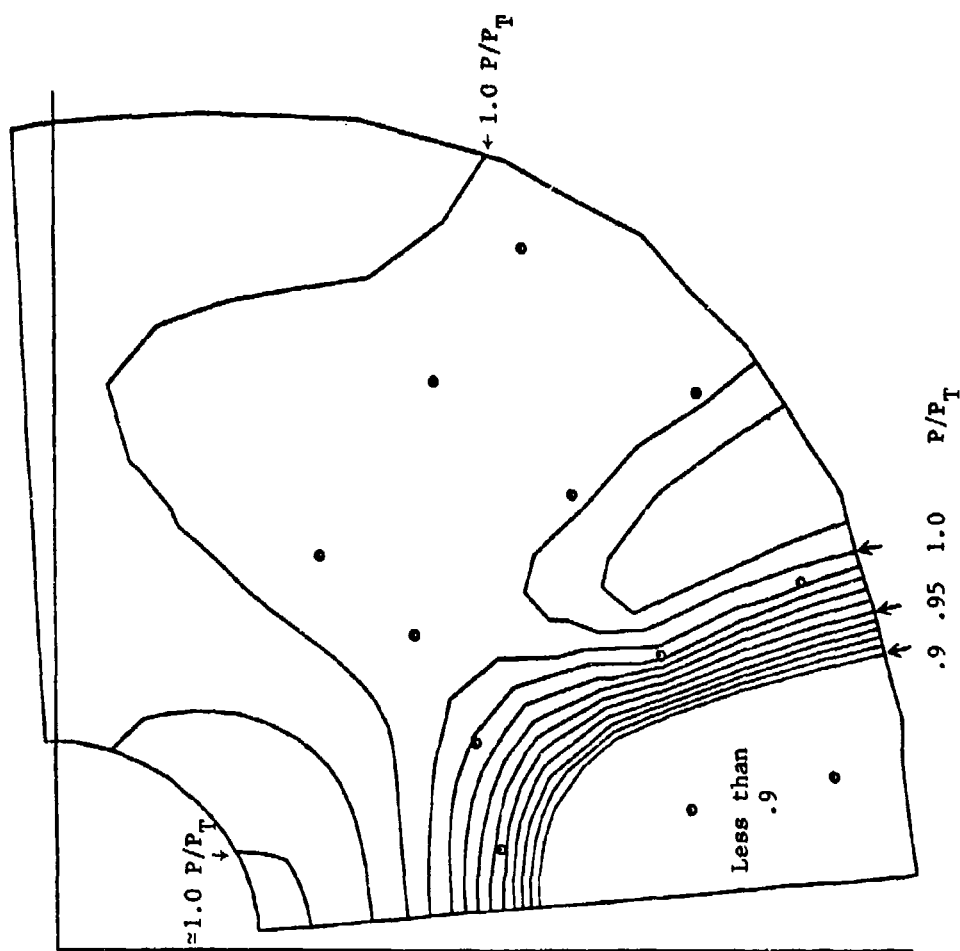


Figure 65. Inlet Pressure Recovery Contours with Suppressor All Installed

RLF-41  
 1.82  
 REX  
 3.00  
 WCH MD  
 1.30  
 0  
 621.92

Suppressor  
 AIII  
 Beta  
 20

PART NUMBER  
 304.008



Figure 66. Inlet Pressure Recovery Contours with Suppressor AIII Installed

#### 4.5 Static Pressure Data

The following figures summarize the static pressure data acquired with a single B-43 store installed on the left side of the bay. These data may be useful in estimating the airload changes resulting from installation of a suppression device. The data are presented in terms of the static pressure coefficient,  $C_p$ . Figure 68 compares the static pressure data at Mach .95 acquired with the baseline configuration from the AEDC 16T and 4T wind tunnels. The centerline distributions show excellent agreement; however, the left wall distribution (Figure 68b) can be seen to differ significantly in the aft region near the rear bulkhead. With Suppressor A installed (Figure 69), the data agreement between the tunnels is excellent for both the centerline and left wall distributions.

The effects of sideslip on the basic configuration are presented in Figure 70 at Mach .95. The centerline distributions, presented in Figure 70a, show that the 2 and 4 degree sideslip angles produce a relatively linear increase in  $C_p$  from front to rear. For the other sideslip conditions, the levels initially decrease then rise aft of the mid-bay tap. The pressure distribution along the left wall adjacent to the store reveals a much greater sensitivity to sideslip (Figure 70b).

The addition of Suppressor A (Figure 71) reduces the  $C_p$  levels along both the centerline and the left wall. The left wall distribution (Figure 71b) shows a dramatically reduced sensitivity to sideslip.

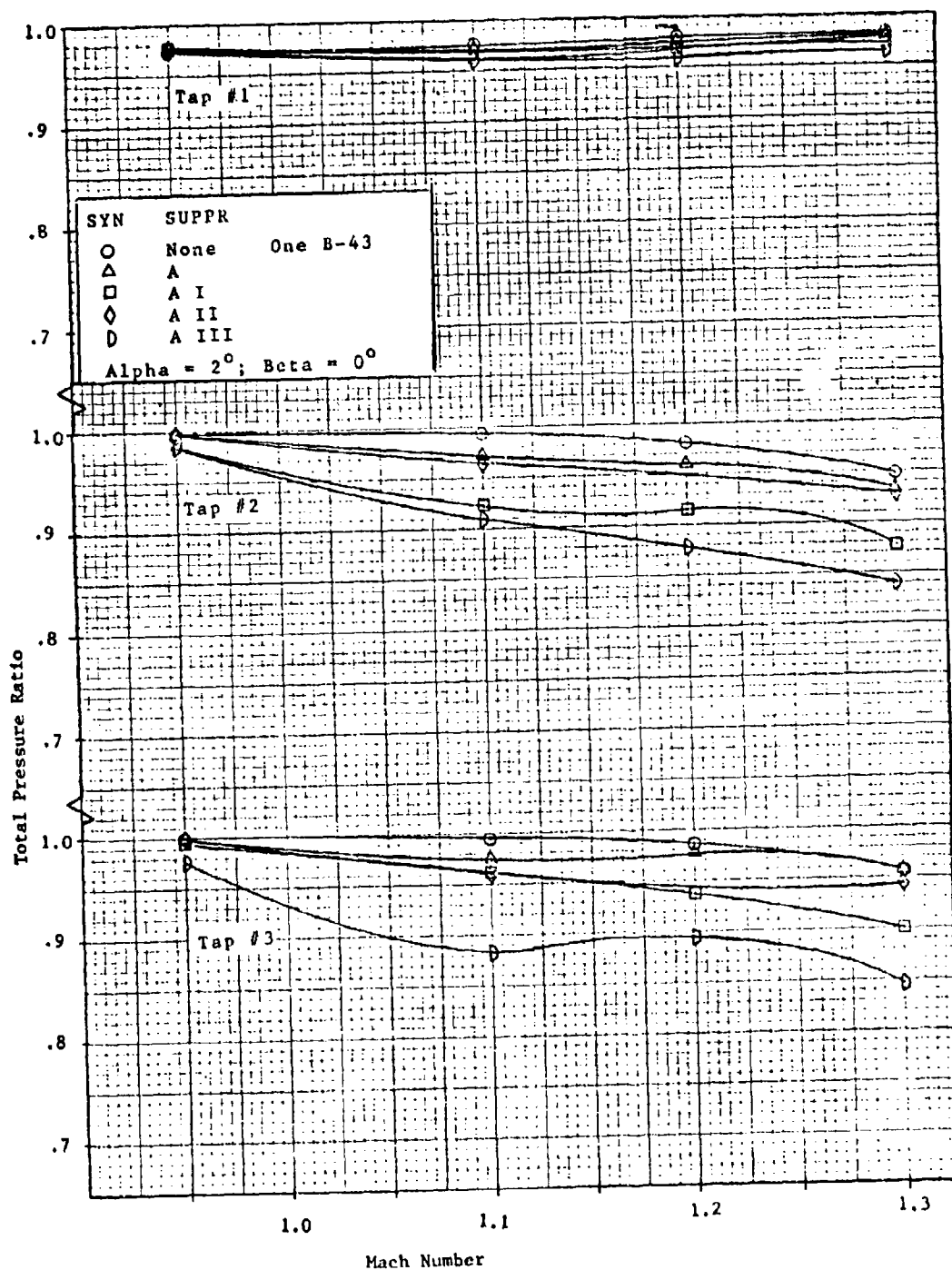


Figure 67a. Inlet Pressure Recovery Measured with Rake Located in Lower Corner of Left Inlet, Beta = 0 degrees

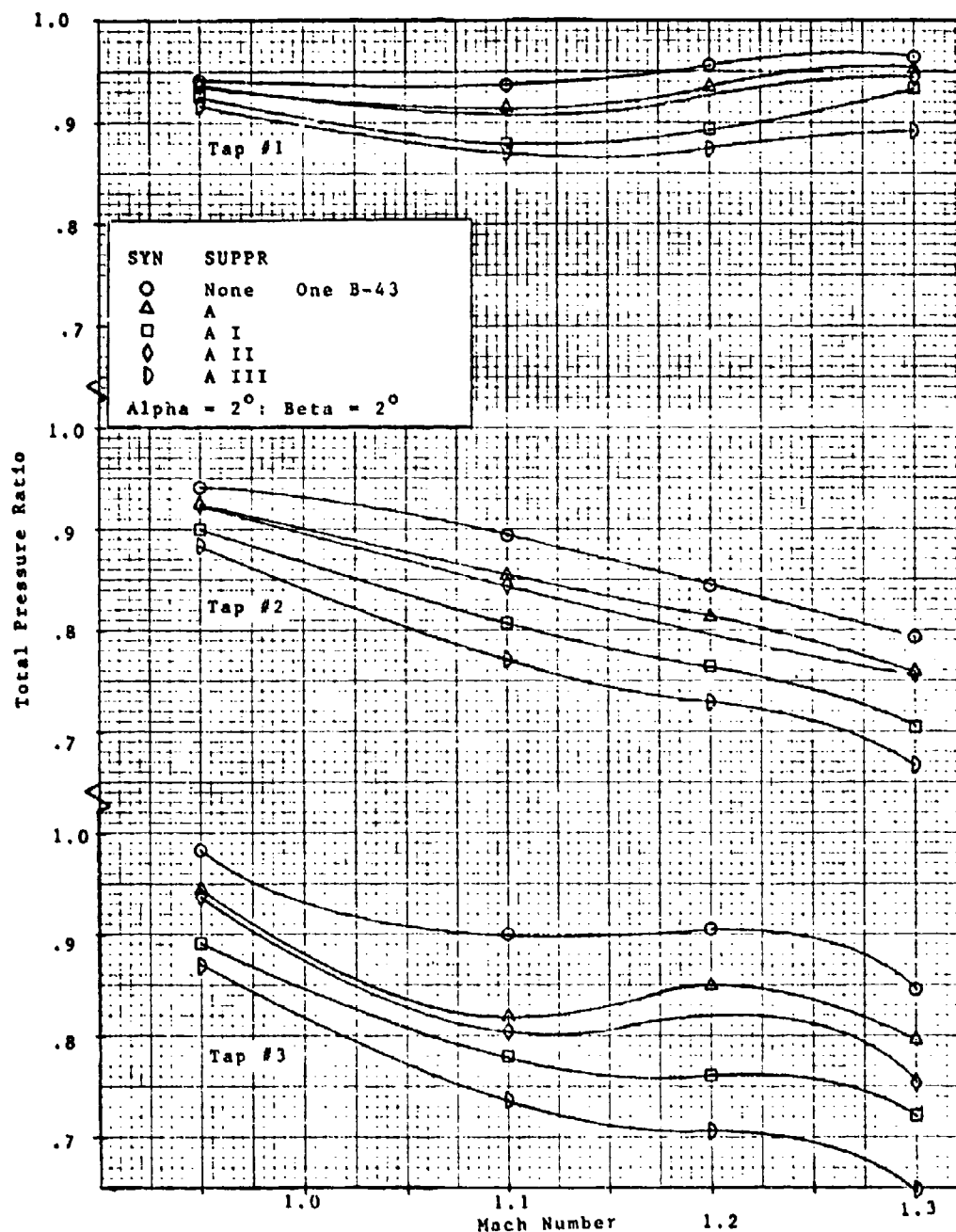


Figure 67b. Inlet Pressure Recovery in Lower Corner of Inlet, Beta = 2 degrees

# SYM MACH ALPHA BETA SUPPR TUNNEL

□ .95 2.0 0.0 NONE 4T  
 X .95 2.0 0.0 NONE 16T

BAY LOADING - SINGLE 8-43

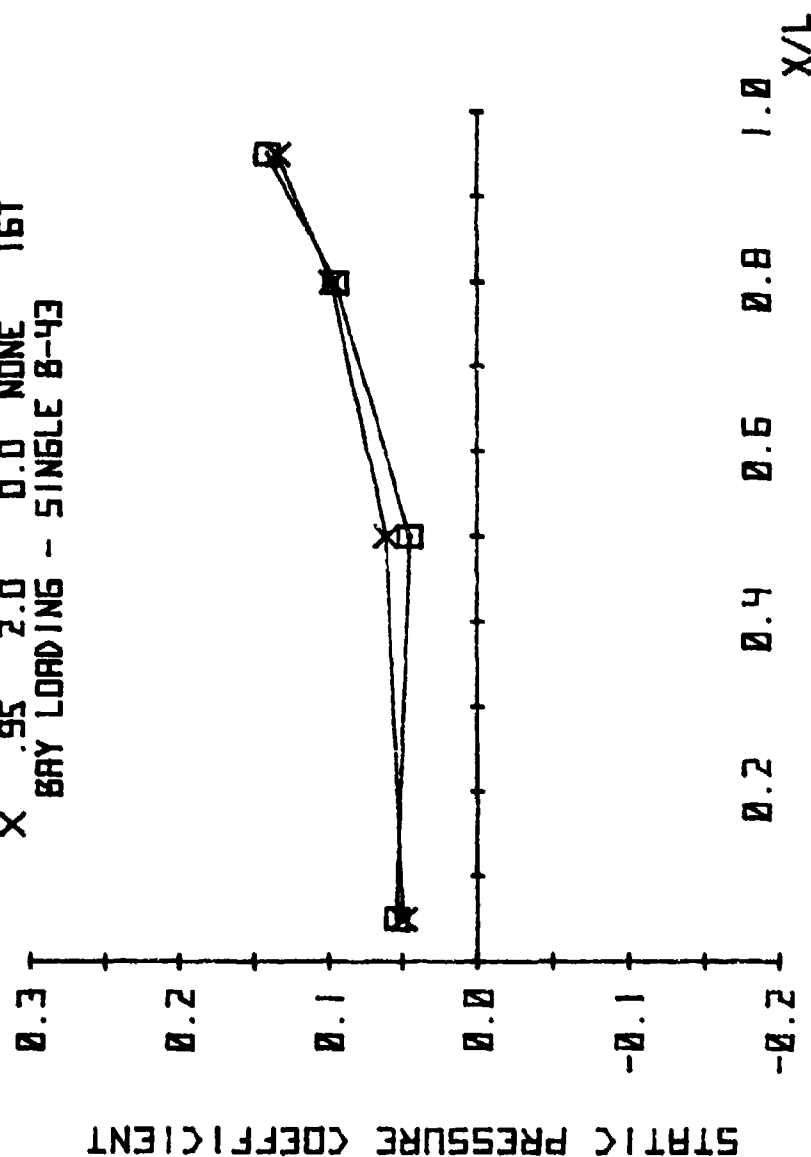


Figure 68a. Static Pressure Distributions Along Centerline of Baseline Configuration at Mach .95 Obtained in AEDC PWT 4T and 16T Wind Tunnels.



# SYM MACH ALPHA BETA SUPPR TUNNEL

□ .95 2.0 0.0 NONE 4T  
 X .95 2.0 0.0 NONE 16T  
 BAY LOADING - SINGLE B-43

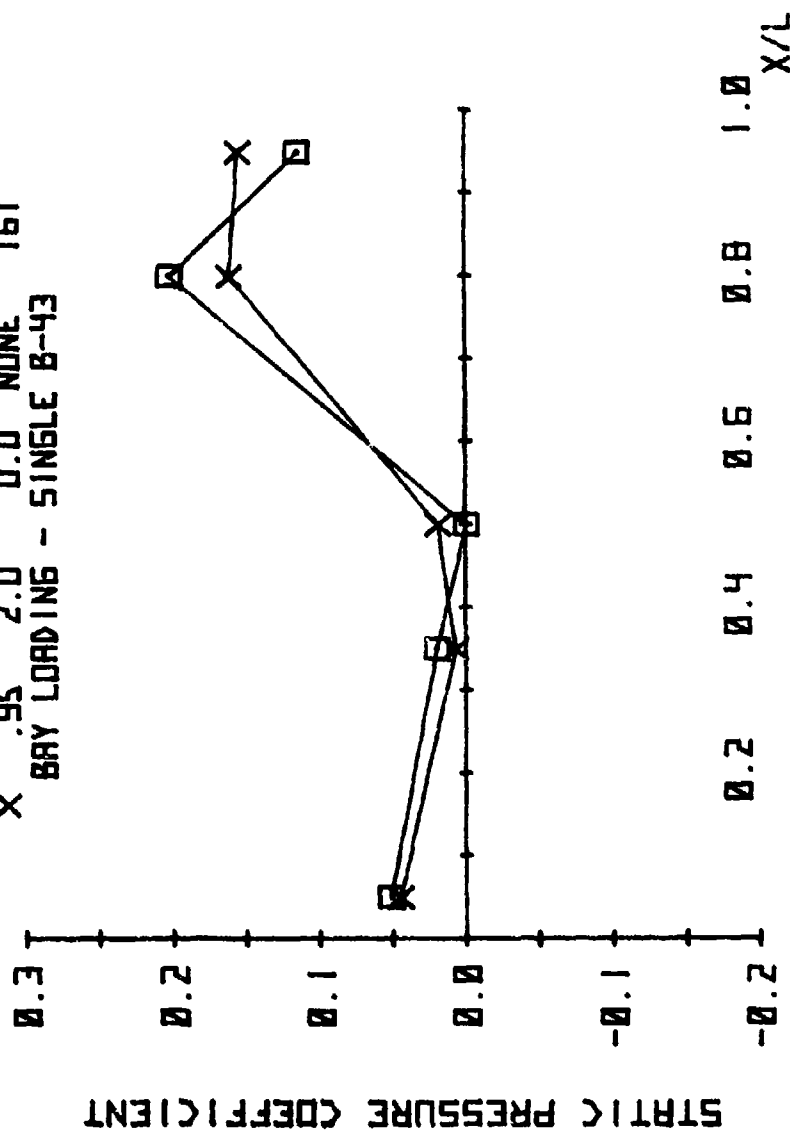


Figure 68b. Comparison of Static Pressure Distributions on Left Wall, Mach .95

# SYM MACH ALPHA BETA SUPPR TUNNEL

□ .95 2.0 0.0 A 4T  
 X .95 2.0 0.0 A 16T

BAY LOADING - SINGLE B-43

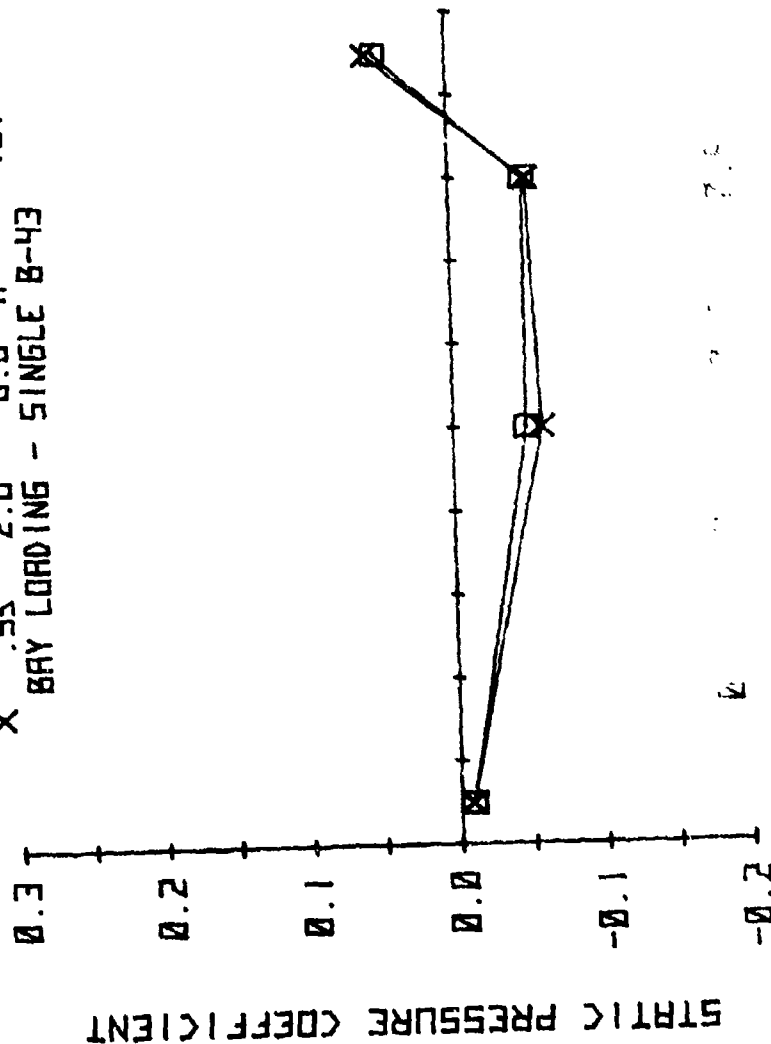


Figure 69a. Comparison of Static Pressure Distributions Along Centerline with Suppressor A Installed, Mach .95

# SYM MACH ALPHA BETA SUPPR TUNNEL

$\square$  .95 2.0 0.0 A 4T  
 $\times$  .95 2.0 0.0 A 16T

BAY LOADINGS - SINGLE B-43

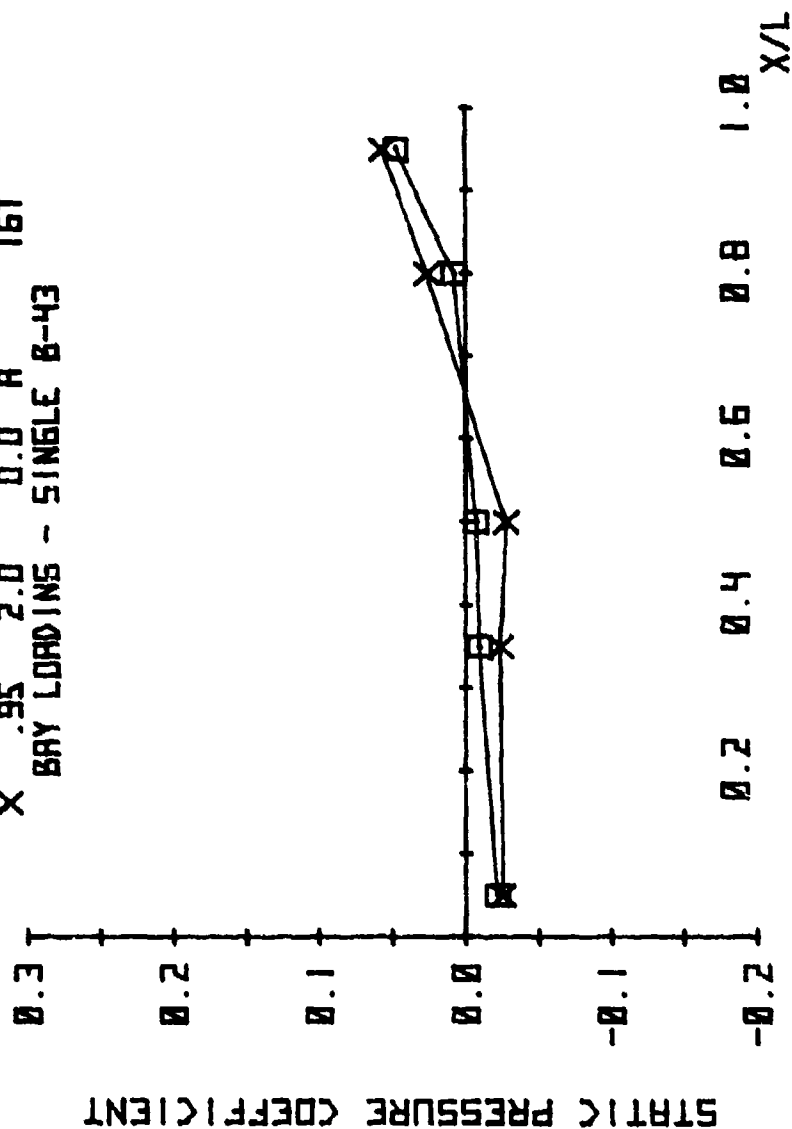


Figure 69b. Comparison of Static Pressure Distributions on Left Wall with Suppressor A Installed, Mach .95

# SYM MACH ALPHA BETA SUPPR

□	.95	2.0	-4.0	NONE
X	.95	2.0	-2.0	NONE
□	.95	2.0	0.0	NONE
Y	.95	2.0	2.0	NONE
+	.95	2.0	4.0	NONE

BAY LOADING - SINGLE B-47

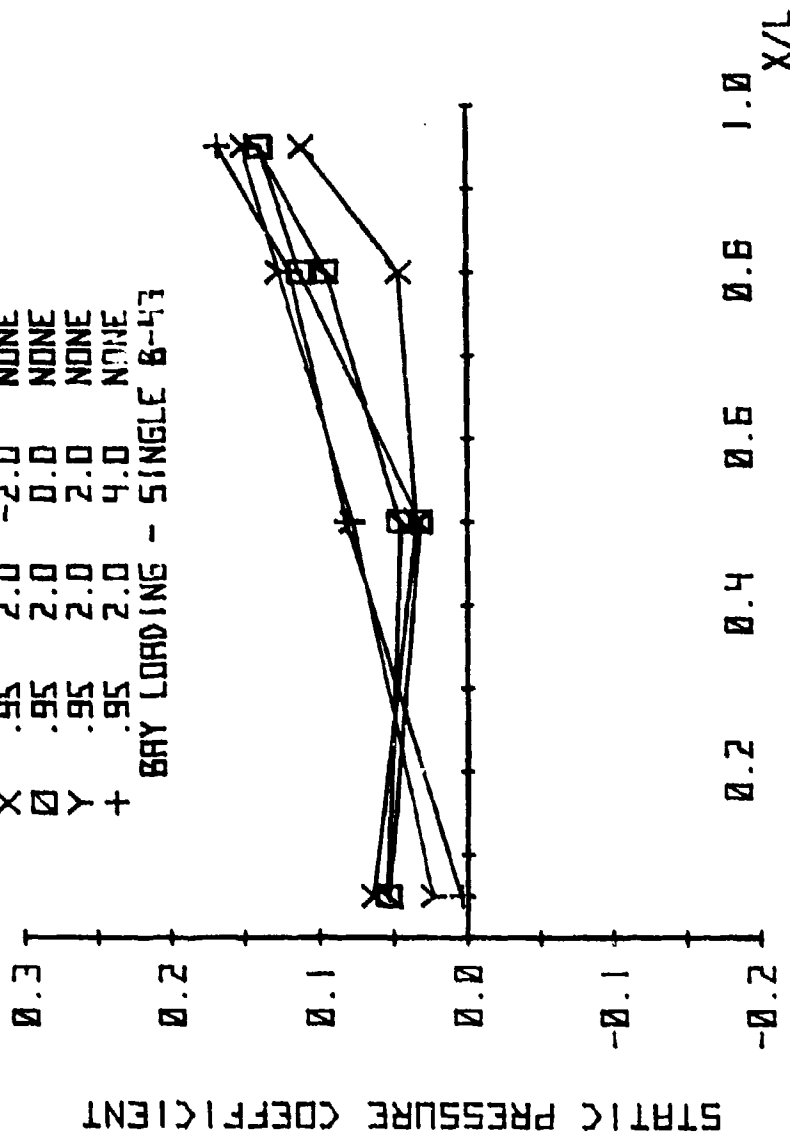


Figure 70a. Effect of Sideslip on Basic Configuration Static Pressure Distribution at Mach .95, Centerline.

# SYM MACH ALPHA BETA SUPPR

□	.95	2.0	-4.0	NONE
X	.95	2.0	-2.0	NONE
□	.95	2.0	0.0	NONE
Y	.95	2.0	2.0	NONE
+	.95	2.0	4.0	NONE

BAY LOADING - SINGLE B-43

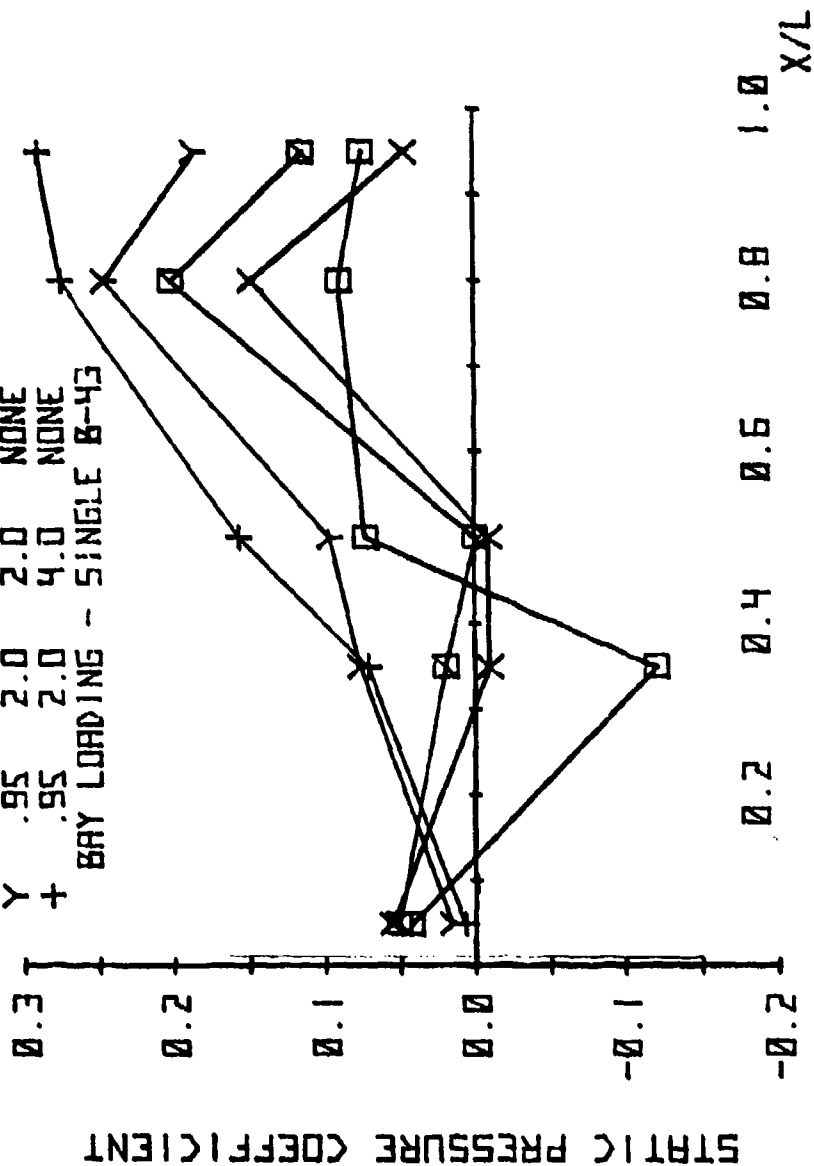


Figure 70b. Effect of Sideslip on Left Wall Static Pressure Distributions at Mach .95.

# SYM MACH ALPHA BETA SUPPR

□	.95	2.0	-4.0	A
X	.95	2.0	-2.0	A
◇	.95	2.0	0.0	A
Y	.95	2.0	2.0	A
+	.95	2.0	4.0	A

BAY LOADING - SINGLE B-43

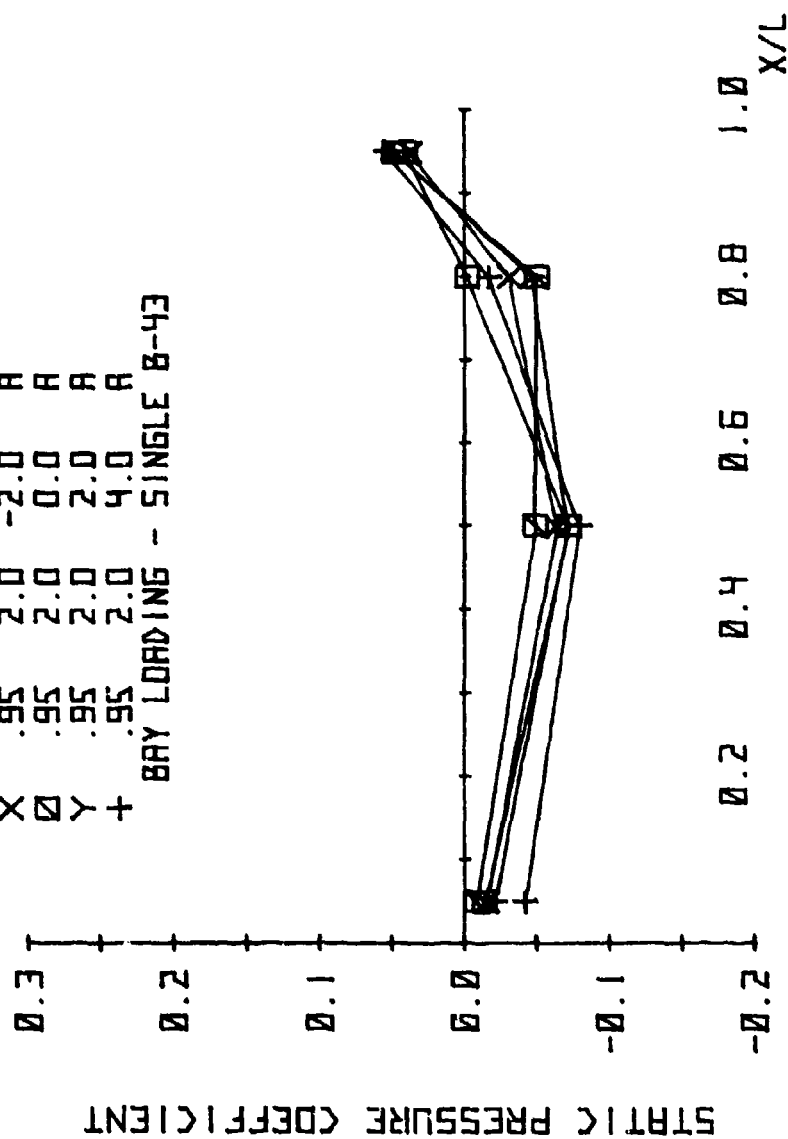


Figure 71a. Effect of Sideslip on Static Pressure Distribution with Suppressor A Installed at Mach .95, Centerline

# SYM MACH ALPHA BETA SUPPR

□	.95	2.0	-4.0	A
X	.95	2.0	-2.0	A
□	.95	2.0	0.0	A
Y	.95	2.0	2.0	A
+	.95	2.0	4.0	A

BAY LOADING - SINGLE B-43

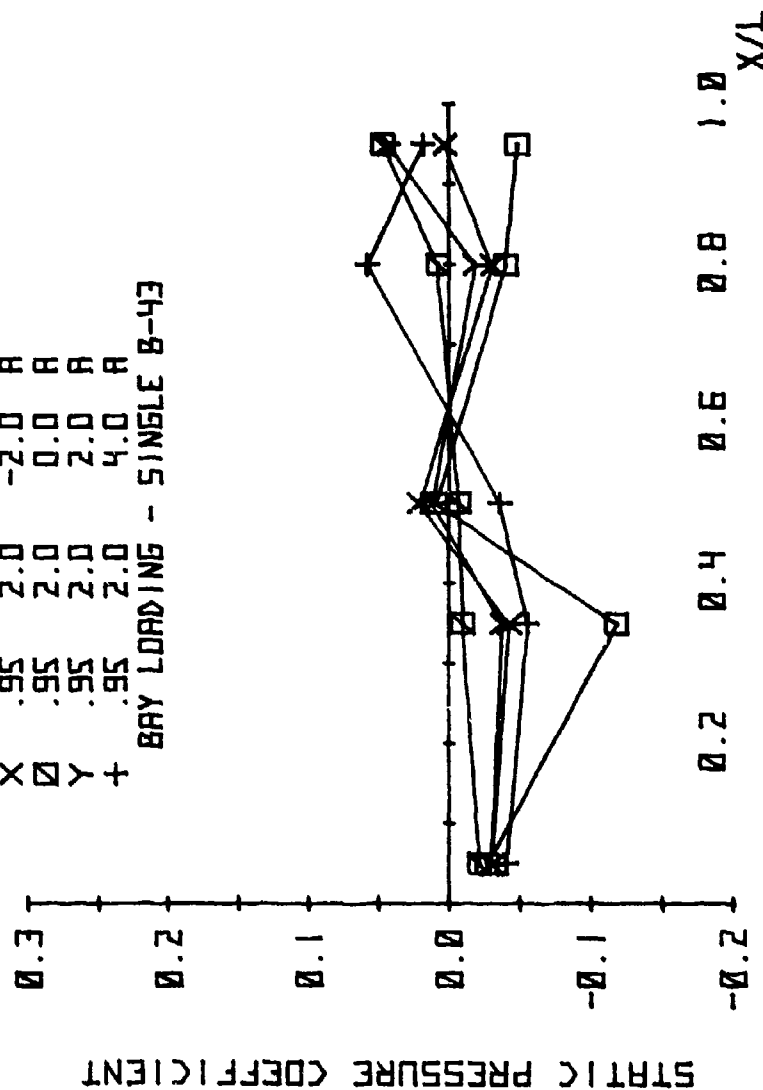


Figure 71b. Effect of Sideslip on Left Wall Static Pressure Distribution with Suppressor A Installed at Mach .95

# SYM MACH ALPHA BETA SUPPR

□	1.3	2.0	-4.0	A
X	1.3	2.0	-2.0	A
○	1.3	2.0	0.0	A
Y	1.3	2.0	2.0	A
+	1.3	2.0	4.0	A

BAY LOADING - SINGLE B-43

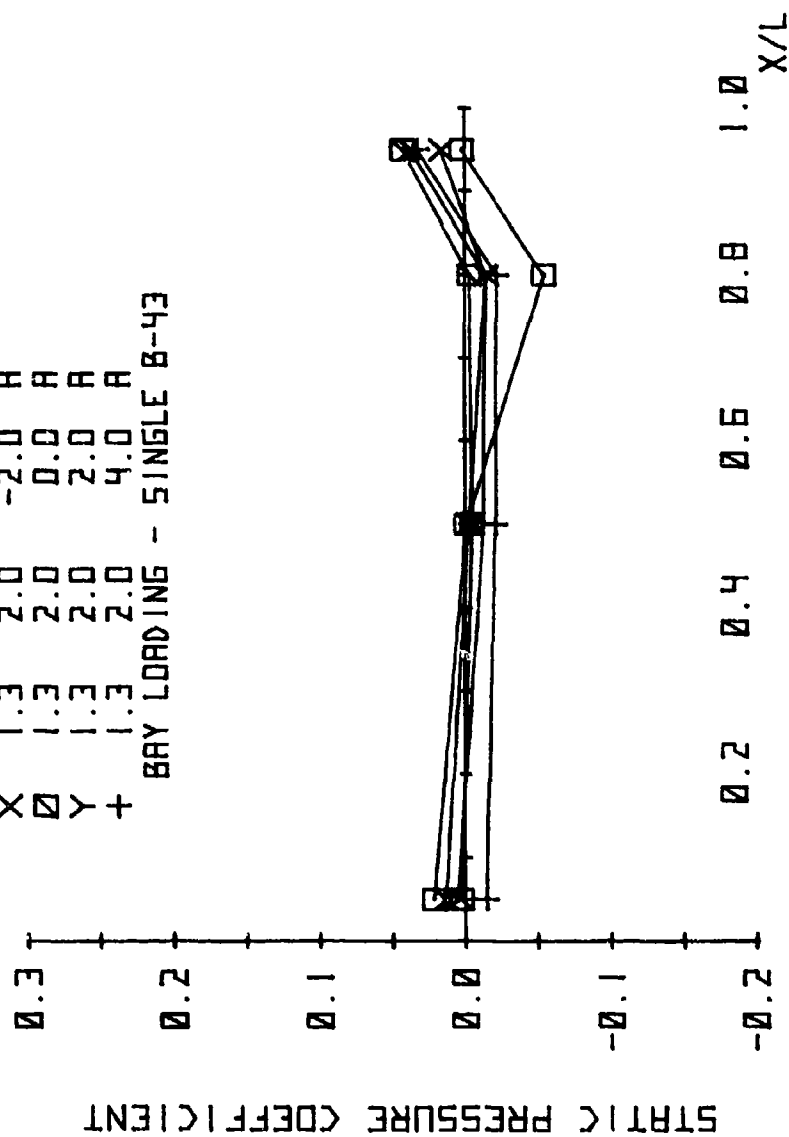


Figure 72a. Effect of Sideslip on Centerline Static Pressure Distribution with Suppressor A Installed at Mach 1.3



Figure 72 presents sideslip data at Mach 1.3 with Suppressor A installed. Sideslip produces an insignificant effect on the centerline and relatively small changes along the left wall. Due to the relatively small effects of sideslip, the following comparisons of the four suppression devices will be made at the zero sideslip condition.

The pressure distributions with and without the suppression devices at Mach .95 and 1.3 are presented in Figures 73 and 74. The shorter devices A and AII generally reduce the static pressure levels less than the two taller devices. At Mach 1.3, the distributions along the left wall clearly show the effects of spoiler height. These data represent only an indirect airloads distribution on the store; therefore, no definitive conclusions can be stated relative to the significance of the changes in steady pressures to the store structural loads.

# SYM MACH ALPHA BETA SUPPR

□	1.3	2.0	-4.0	A
X	1.3	2.0	-2.0	A
□	1.3	2.0	0.0	A
Y	1.3	2.0	2.0	A
+	1.3	2.0	4.0	A

BAY LOADING - SINGLE B-43

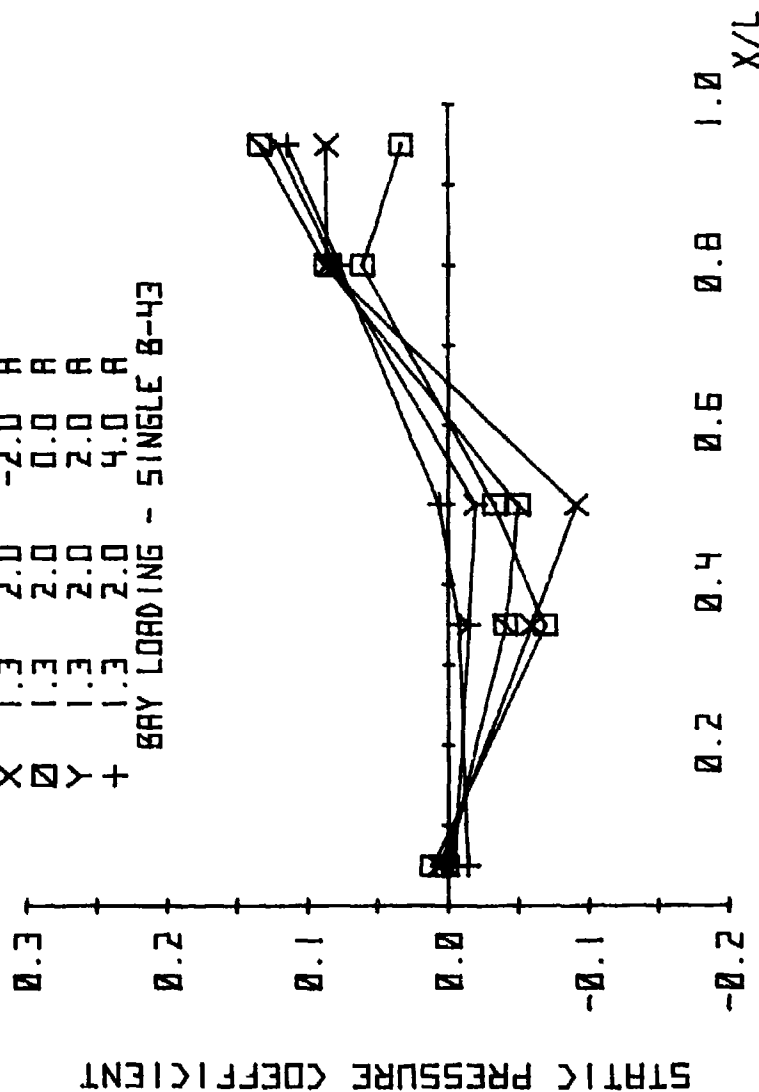


Figure 72b. Effect of Sideslip on Left Wall Static Pressure Distribution with Suppressor A Installed at Mach 1.3

# SYM MACH ALPHA BETA SUPPR

□	.95	2.0	0.0	NONE
X	.95	2.0	0.0	A
Y	.95	2.0	0.0	A1
+	.95	2.0	0.0	A11
◇	.95	2.0	0.0	A111

BAY LOADING - SINGLE B-43

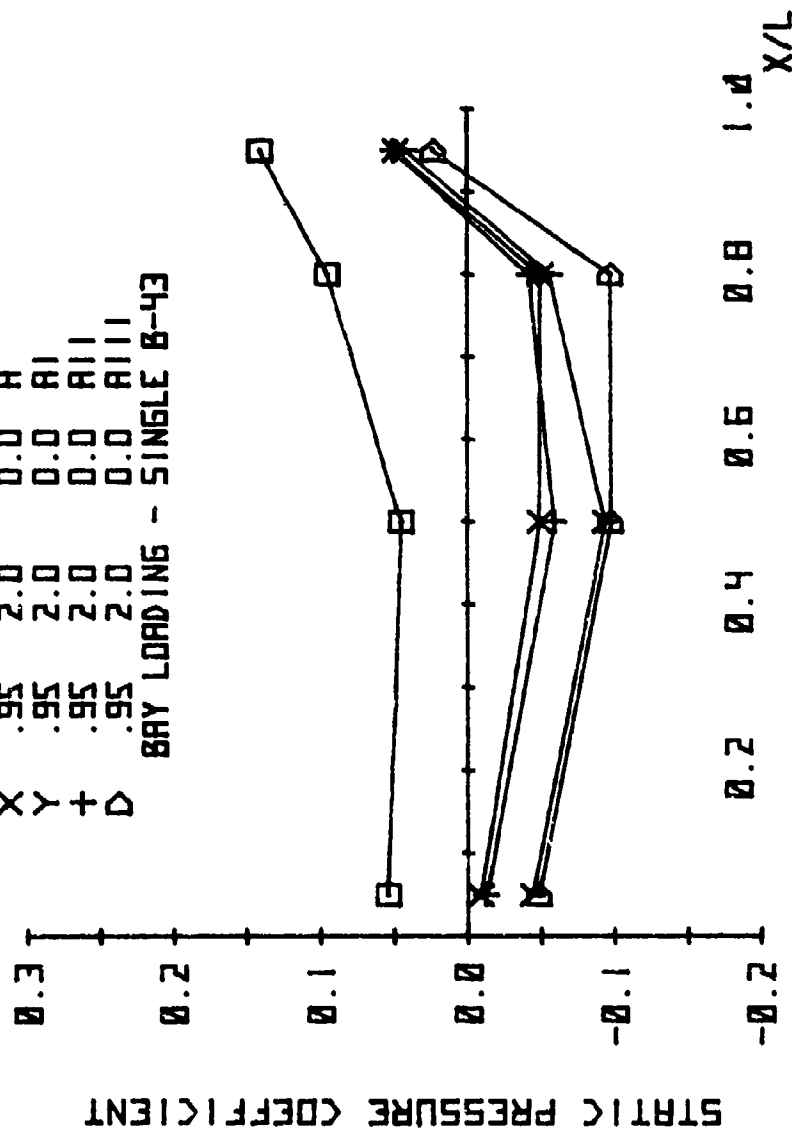


Figure 73a. Comparison of Suppressor Effects on Static Pressure Distributions at Mach .95, Centerline

# SYM MACH ALPHA BETA SUPPR

SYM	MACH	ALPHA	BETA	SUPPR
□	.95	2.0	0.0	NONE
X	.95	2.0	0.0	A
Y	.95	2.0	0.0	AI
+	.95	2.0	0.0	AI1
◇	.95	2.0	0.0	AI11

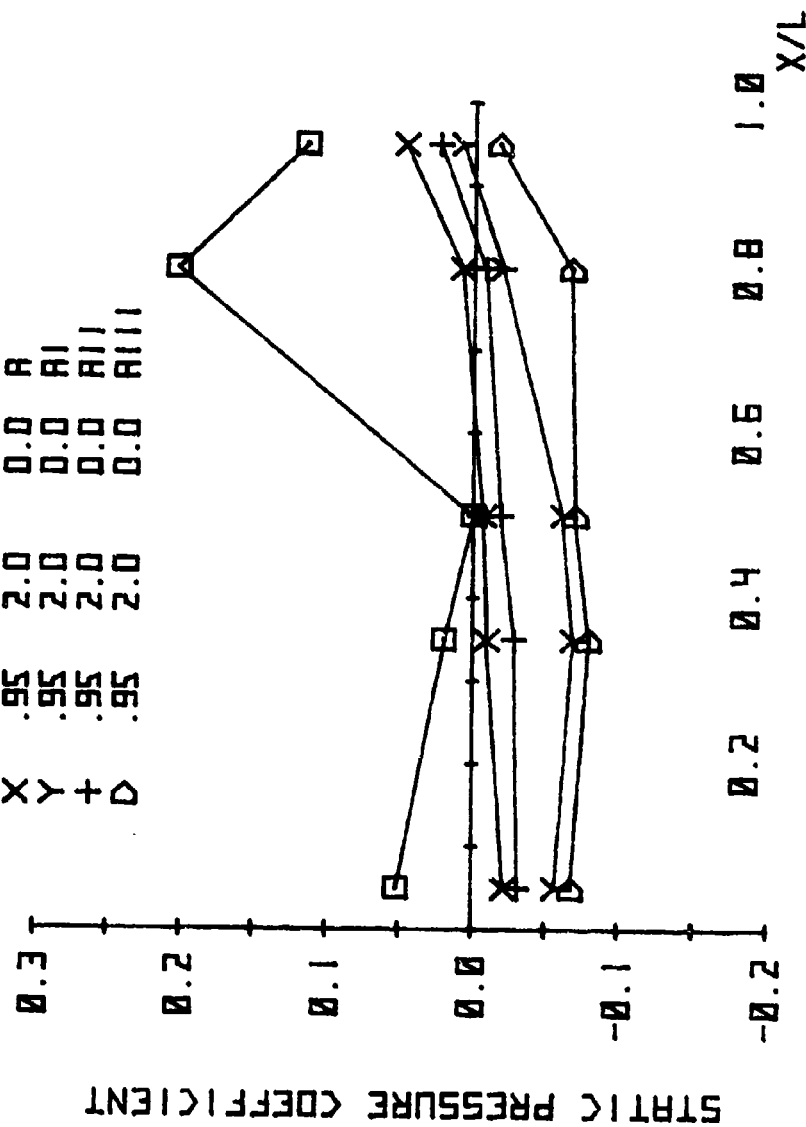


Figure 73b. Comparison of Suppressor Effects on Static Pressure Distributions at Mach .95, Left Wall

# SYM MACH ALPHA BETA SUPPR

□	1.3	2.0	0.0	NONE
X	1.3	2.0	0.0	A
Y	1.3	2.0	0.0	AI
+	1.3	2.0	0.0	AI1
△	1.3	2.0	0.0	AI11

BAY LOADING - SINGLE B-43

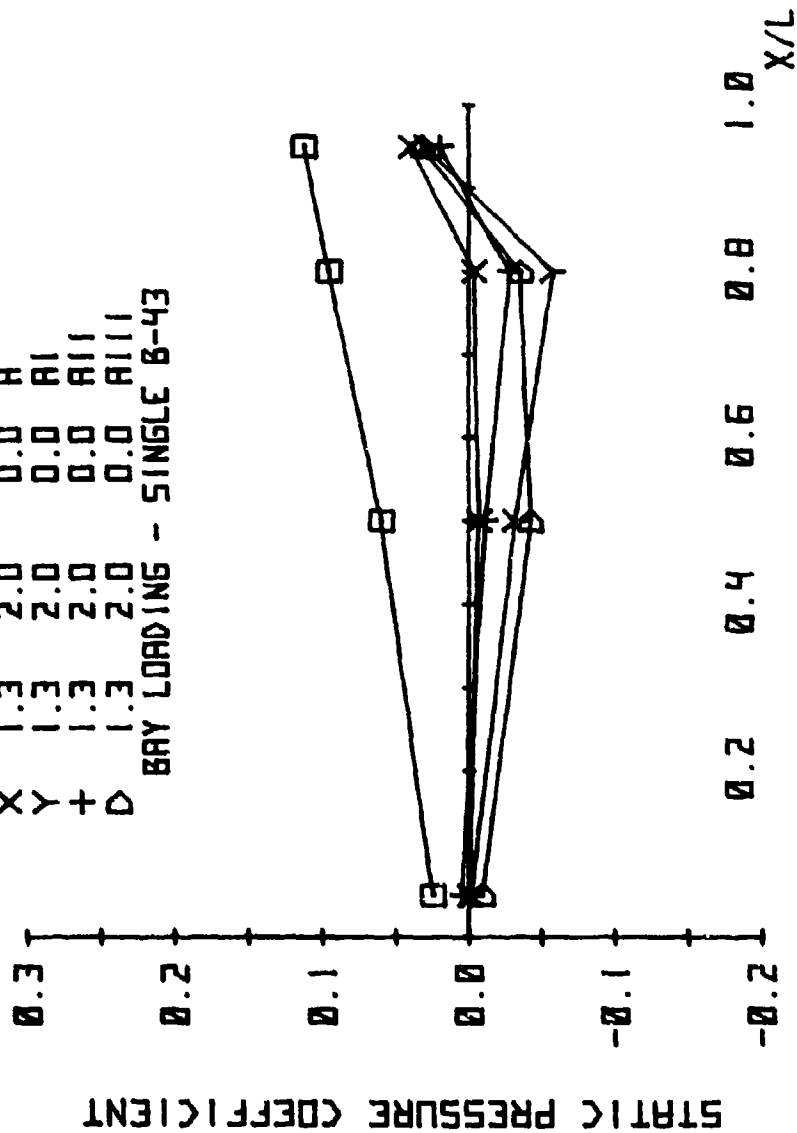


Figure 74a. Comparison of Suppressor Effects on Static Pressure Distributions at Mach 1.3, Centerline

SYM MACH ALPHA BETA SUPPR  
 □ 1.3 2.0 0.0 NONE  
 X 1.3 2.0 0.0 A  
 Y 1.3 2.0 0.0 AI  
 + 1.3 2.0 0.0 AII  
 ◇ 1.3 2.0 0.0 AIII  
 BAY LOADING - SINGLE B-43

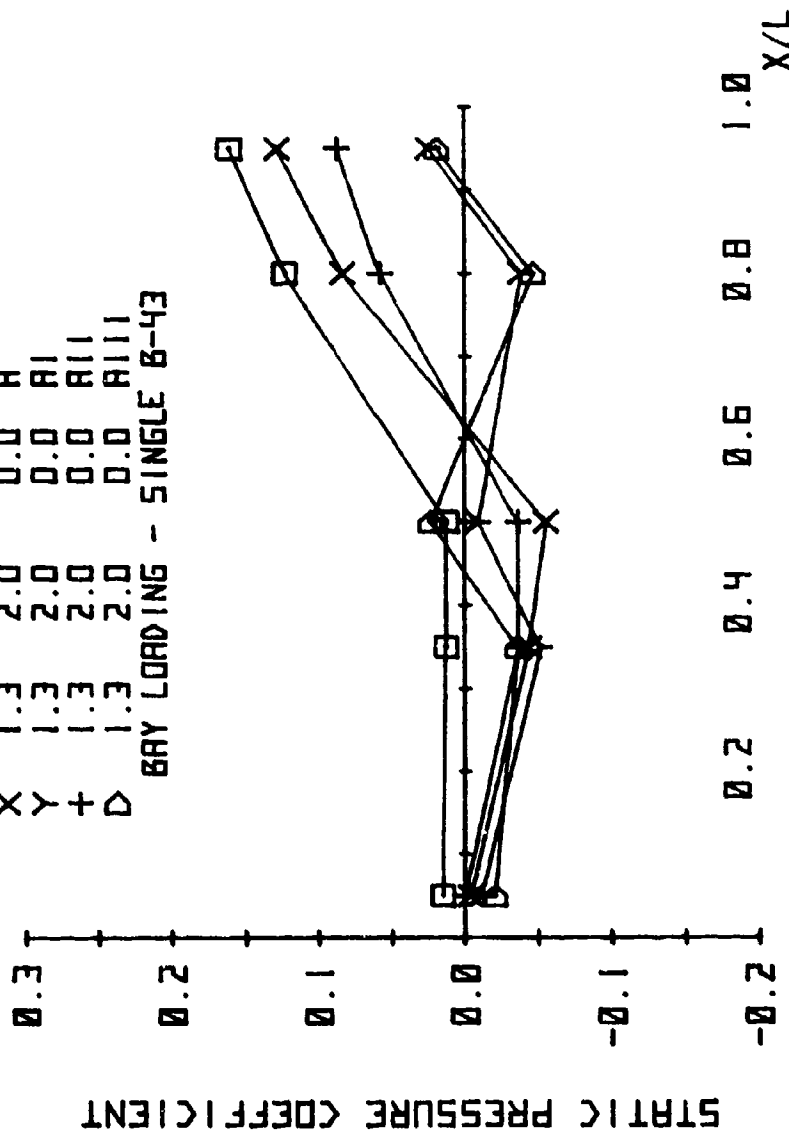


Figure 74b. Comparison of Suppressor Effects on Static Pressure Distributions at Mach 1.3, Left Wall

#### 4.6 Final Assessment and Selection of Suppression Device

Prior to selecting a suppression device for further study and evaluation, criteria were required for the suppressed weapon bay environment in terms of the acoustic energy ( $\text{Prms}/Q$ ). The Mach .95 low altitude separation limit represents the limit environment for the B-43 weapon in the F-111 weapon bay. Therefore, the peak  $\text{Prms}/Q$  levels determined during this program corresponding to Mach .95 and 1000 ft altitude have been defined as the target levels for the suppressed environment at the more severe higher Mach conditions. The left wall adjacent to the store was selected as most representative of the critical store loading because the peak  $\text{Prms}/Q$  levels were observed along this wall. The store extends to approximately 93% of the bay length; therefore, while higher levels were observed on the aft bulkhead, these are not the critical values affecting the store structure.

Figure 75 presents the comparison of the bay environment achieved with Suppressor A to the above criteria scaled to the Mach 1.2, 1000 ft altitude condition. The solid line represents the  $\text{Prms}/Q$  values at Mach .95, 1000 ft reduced by a factor of 37%, which results from the full scale ratio of the dynamic pressure at these two test conditions. The suppressor does achieve a satisfactory environment at all locations forward of approximately the 90% X/L location. A small area of the left wall adjacent to the extreme aft portion of the store (Figure 11) exceeds the criteria; however, the average loading in the critical region between the .5 and .95 instrumentation locations is significantly lower than the above suppression criteria.

# SYM MACH ALPHA BETA SUPPR LOADING

- (1) 2.0 0.0 NONE ONE B-43  
 X 1.2 2.0 0.0 A ONE B-43  
 (1) MACH .95 LEVEL; EQUIVALENT DYNAMIC  
 PRESSURE SCALED TO MACH 1.2.

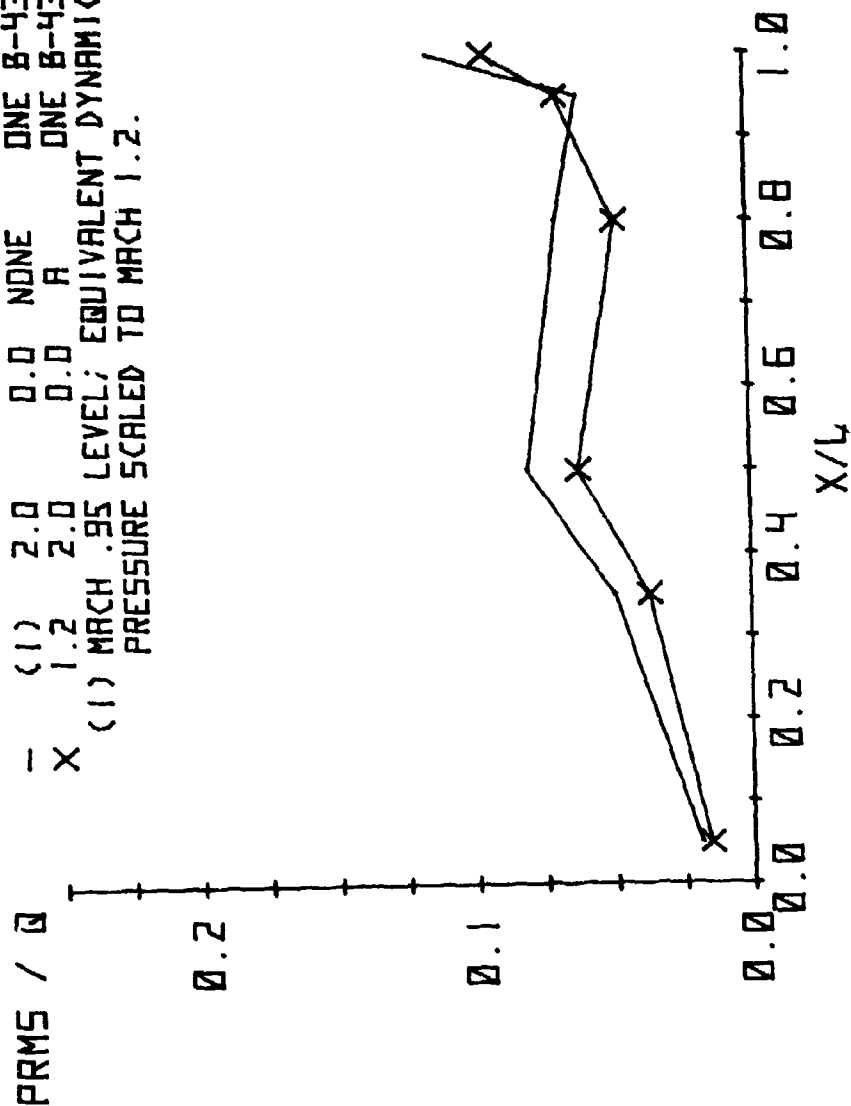


Figure 75. Comparison of Bay Environment Achieved with Suppressor A to Target Environment at Mach 1.2 and 1000 ft Altitude



Figure 76 presents similar results at Mach 1.3 and 4000 ft altitude. Here the required reduction factor is approximately 40%. Almost identical results are achieved indicating that the smallest suppressor does in fact provide acceptable environmental conditions in the bay based upon the criteria established.

Based upon the above results, the full scale flight test suppressor would have the following dimensions:

Width ——— 38 inches  
Height ——— 2.45 inches (70% of full scale boundary layer height)

This full scale device is considered the optimum size to achieve the desired environmental improvement in the open bay while producing the minimum installation penalties. Full scale flight tests will be required to verify and validate the wind tunnel test results presented.

#### 4.6.1 Bay Mounted Gun Installation

Installation of the gun on the right side of the bay moderates the environment in the bay based upon the results acquired during this program. A modified Suppressor A was evaluated during Phase 1 with the gun and with an ECM Pod. (The results of drop tests are discussed in paragraph 4.3.) The modified suppression device (Figure 37) is reduced in width to eliminate gun blast effects or interference. The data in Figure 77 at Mach 1.3 shows a small improvement in the bay environment with the suppressor. This improvement may not be significant from the aero-acoustic viewpoint; however, the beneficial effects on separation characteristics of the B-43 reported above may be significant.

# SYM MACH ALPHA BETA SUPPR LOADING

PRMS / Q

- (1) 2.0 0.0 NONE ONE B-43  
 X 1.3 2.0 0.0 A ONE B-43  
 (1) MACH .95 LEVEL; EQUIVALENT DYNAMIC  
 PRESSURE SCALED TO MACH 1.3.

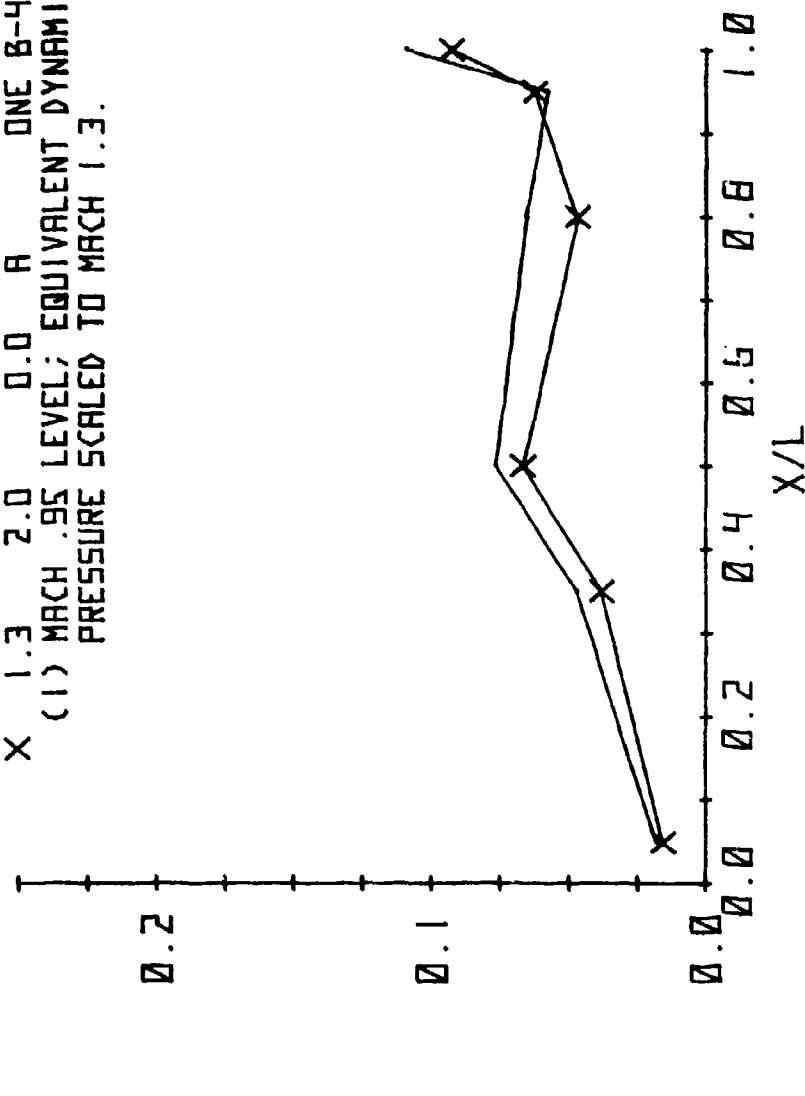


Figure 76. Comparison of Bay Environment Achieved with Suppressor A to Target Environment at Mach 1.3 and 4000 ft Altitude

# SYM MACH ALPHA SUPPR

PRMS / Q

□ 1.3 2.0 NONE  
 X 1.3 2.0 A(MODIFIED)

GUN INSTALLED ON RIGHT SIDE OF BAY  
 SINGLE B-43 ON LEFT SIDE OF BAY.

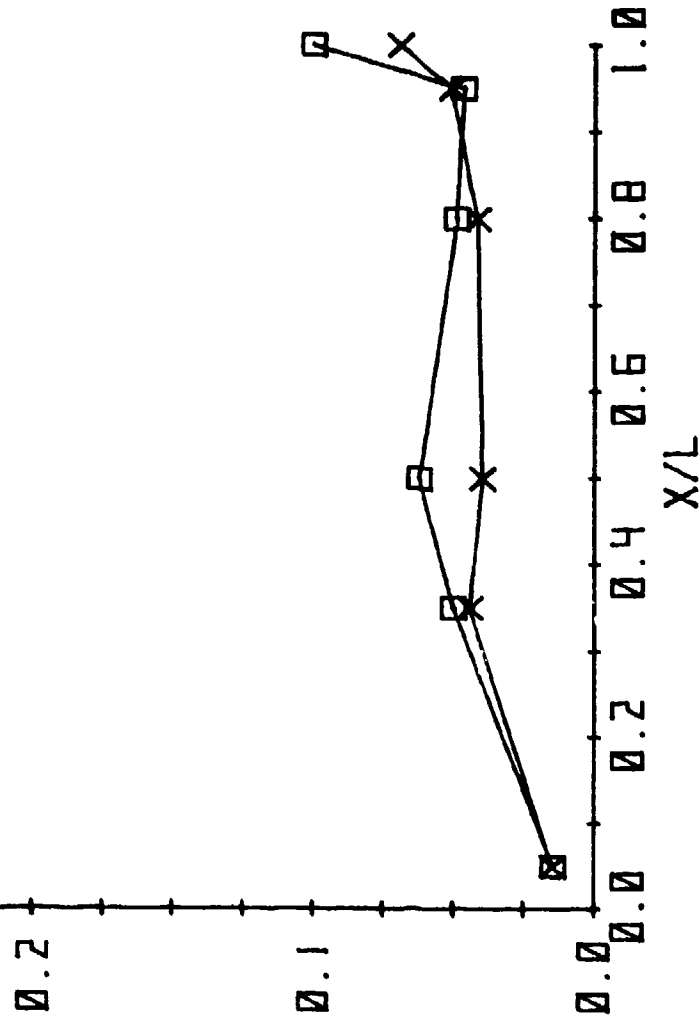


Figure 77. Effect of Modified Suppressor A on Bay Environment with Gun Installed

## SECTION V

### CONCLUSIONS

5.1 Suppression of the turbulent environment within the open weapon bay of the F-111 aircraft has been successfully demonstrated in the wind tunnel by installation of a relatively small saw tooth type suppression device.

5.2 Installation of the suppression device of the type developed during this program can produce favorable effects on the separation characteristics of weapons separated from the internal weapon bay of an F-111 aircraft.

5.3 Flow into the engine inlets of the F-111 aircraft may be adversely affected by the suppression device during sideslip flight conditions.

5.4 Flight tests of the suppression device developed during this program will be required to confirm the effectiveness of the device and to investigate the above adverse effects on inlet flow.

5.5 The available data from this and other research programs clearly demonstrate that future internal weapon bay equipped aircraft must consider the aero-acoustic environment produced by the open cavity during the design phase.

## REFERENCES

1. R.L. Clark, Weapons Bay Turbulence Reduction Techniques, Air Force Flight Dynamics Laboratory, Wright-Patterson AFB, Ohio, 45433, AFFDL-TM-75-147-FXM, December 1975.
2. D.B. Benepe and R.T. Richtman, Study of Weapon Bay Environment Suppression Devices for F-111 Aircraft, FZM-12-13919, General Dynamics, Fort Worth, Texas, August 1976.
3. Test Facilities Handbook (Tenth Edition), Arnold Engineering Development Center, May 1974.
4. Kukainis, Janis, Freedrop Trajectory Characteristics of Bluff-Shaped Bombs Released from the F-111 Aircraft Weapons Bay at Mach Numbers from 0.70 to 1.30, Arnold Engineering Development Center, AEDC-TR-71-103, May 1971.